Space Sci Rev (2011) 161:63–148
DOI 10.1007/s11214-011-9818-4

Review of Pi2 Models

Andreas Keiling · Kazue Takahashi

Received: 16 September 2010 / Accepted: 6 July 2011 / Published online: 21 October 2011

Abstract More than half a century after the discovery of Pi2 pulsations, Pi2 research is still vigorous and evolving. Especially in the last decade, new results have provided supporting evidence for some Pi2 models, challenged earlier interpretations, and led to entirely new models. We have gone beyond the inner magnetosphere and have explored the outer magnetosphere, where Pi2 pulsations have been observed in unexpected places. The new Pi2 models cover virtually all magnetotail regions and their coupling, from the reconnection site via the lobes and plasma sheet to the ionosphere.

In addition to understanding the Pi2 phenomenon in itself, it has also been important to study Pi2 pulsations in their role as transient manifestations of the coupling between the magnetosphere and the ionosphere. The transient Pi2 is an integral part of the substorm phenomenon, especially during substorm onset. Key questions about the workings of magnetospheric substorms are still awaiting answers, and research on Pi2 pulsations can help with those answers. Furthermore, the role of Pi2 pulsations in association with other dynamic magnetospheric modes has been explored in the last decade. Thus, the application of Pi2 research has expanded over the years, assuring that Pi2 research will remain active in this decade and beyond.

Here we review recent advances, which have given us a new understanding of Pi2 pulsations generated at various places in the magnetosphere during different magnetospheric modes. We review seven Pi2 models found in the literature and show how they are supported by observations from spacecraft and ground observatories as well as numerical simulations. The models have different degrees of maturity; while some enjoy wide acceptance, others are still speculative.

Keywords ULF wave · Pi2 pulsation · Magnetosphere · Substorm

A. Keiling (✉)
Space Sciences Laboratory, University of California-Berkeley, Berkeley, CA, USA
e-mail: keiling@ssl.berkeley.edu

K. Takahashi
Applied Physics Laboratory, Johns Hopkins University, Laurel, MD, USA

Glossary

BBF	Bursty bulk flow
BBF-Pi2	Bursty bulk flow Pi2
BM-Pi2	Ballooning mode Pi2
CPS	Central plasma sheet
EIC	Equivalent ionospheric current
FAC	Field-aligned current
FLR	Field line resonance
IC	Inertia current
KAW	Kinetic Alfvén wave
KBI	Kinetic ballooning instability
KHI	Kelvin-Helmholtz instability
LEO	Low Earth orbit
MHD	Magnetohydrodynamics
PBI	Poleward boundary intensification
PCR	Plasmaspheric cavity resonance
PCR-Pi2	Plasmaspheric cavity resonance Pi2
PSBL	Plasma sheet boundary layer
PSM	Plasmaspheric surface mode
PSM-Pi2	Plasmapause surface mode Pi2
PVR	Plasmaspheric virtual resonance
PVR-Pi2	Plasmaspheric virtual resonance Pi2
RX-Pi2	Pulsed reconnection Pi2
SCW	Substorm current wedge
TR	Transient response
TR-Pi2	Transient response Pi2
ULF	Ultra-low frequency
WTS	Westward traveling surge

Contents

1 Introduction

1.1 Scope of Review

In the broadest sense, Pi2 pulsations are short-duration (10–15 min), periodic (40–150 s)[1] ultra-low frequency (ULF) pulsations excited by a source in the nightside magnetosphere. The source provides a mechanism that converts a broadband or non-periodic signal into a periodic signal with a frequency in the Pi2 range. The initial energy for Pi2 pulsations enters the magnetosphere from the solar wind and propagates via the magnetotail towards the ionosphere and the ground. Where along this path, which constitutes a sequence of energy transfer processes, and by what mechanism the energy is converted into a periodic Pi2 signal are the two main questions reviewed in this paper.

By the end of the last century, Pi2 research appeared to converge towards a "unified theory", expressed by Olson (1999) as follows: "What the data reveal is that the Pi2 pulsation is really a class of pulsations and that all of the members of the class are generated by the same event: the onset of field-aligned currents and compressional waves in near-Earth plasma sheet associated with substorm onset". Such a scenario is illustrated in Fig. 1, which shows a west-east current (labeled "source current") as initiator. In the last decade, however, new directions in Pi2 research have expanded upon the limitations of this statement. Whereas early on, Pi2 pulsations were exclusively thought of as a substorm phenomenon and were considered an ideal substorm identifier because they were fairly easily identifiable in ground magnetometer data (Saito 1961; Saito et al. 1976), nowadays the term Pi2 is also applied to pulsations during non-substorm times, if they meet the two simple Pi2 criteria defined above (period and duration). As a result, additional Pi2 generation mechanisms not associated with substorm onset have been proposed. Moreover, there is in fact no consensus yet on the generation mechanism (or mechanisms) of substorm-related Pi2 pulsations, and new models have emerged, challenging more established ones.

Even though Pi2 research has a long history (over half a century), it is still a vigorously pursued field of magnetospheric physics that is of great interest to many, particularly the ULF and substorm communities. While it is obvious that this ULF wave phenomenon is studied by ULF wave researchers, it has also been important to study Pi2 pulsations as transient manifestations of the coupling between the magnetosphere and the ionosphere (Southwood and Hughes 1983; Baumjohann and Glassmeier 1984). The transient Pi2 is an integral part of the substorm phenomenon, especially during substorm onset. Key questions about the workings of magnetospheric substorms are still awaiting answers, and research on Pi2 pulsations can help with those answers. In addition, the role of Pi2 pulsations in association with other dynamic magnetospheric modes has been recognized and explored in the last decade. Thus, the application of Pi2 research has expanded over the years, assuring that Pi2 research will remain active in the current decade and beyond.

[1] Pi2 pulsations can, however, have periods that lie outside this range.

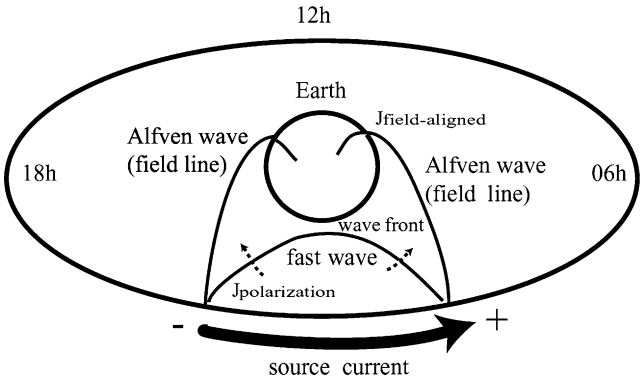

Fig. 1 (From Fujita et al. 2002) Illustration of a Pi2 generation mechanism

The first review of Pi2 pulsations can be found in the comprehensive overview of ULF waves by Saito (1969) and the most recent by Olson (1999). Another review that focused on the transient response model for the generation of Pi2 pulsations was provided by Baumjohann and Glassmeier (1984), while a review that focused on low-latitude Pi2 pulsations was provided by Yumoto (1986). These reviews focused on ground-based observations. However, the recent advances in Pi2 research have come from studies utilizing spacecraft observations from missions, such as AMPTE/CCE, Akebono, GOES, CRRES, Geotail, DE-1, Polar, Cluster, CHAMP, Ørsted, and THEMIS. These new data have not only helped to refine existing Pi2 models, but they have also shown a need for new Pi2 models, completely different from the existing ones. We have gone beyond the inner magnetosphere as the region for Pi2 sources and explored the outer magnetosphere where Pi2 pulsations have been observed in unexpected places such as the tail lobe and the central plasma sheet. Furthermore, spacecraft observations confirmed for the first time their existence in the dayside plasmasphere at middle latitude, and they gave evidence for Pi2-like oscillations in non-magnetic-field quantities, which correlated one-to-one with ground Pi2 pulsations. New spacecraft missions also brought advances in instrumentation, some of which have provided 3-D measurements of the electric field that allowed unambiguous determination of propagation modes and Poynting flux, yielding an assessment of Pi2 energetics. In addition, advances have been made in Pi2 simulation work. In spite of these advances, the Pi2 field remains controversial, and consensus has not yet been reached. Hence, an updated review of the body of knowledge regarding Pi2 models is needed.

This review attempts to clarify the complex and sometimes confusing field of Pi2 research. We refer the reader to Fig. 59 of Sect. 5 for a preview of this complexity. For the purpose of this review, the following five points should be agreed upon:

(a) Pi2 pulsations are not a single phenomenon but several phenomena that create similar oscillations which we collectively call *Pi2 pulsations*.
(b) Pi2 pulsations are global phenomena in the sense that the initial Pi2 signal propagates from the source to remote places in the magnetosphere and to the ground via several paths simultaneously, causing ground Pi2 at multiple places.
(c) The term *Pi2* is not only reserved for magnetic pulsations on the ground, but it has also been used for magnetic field oscillations in space. Although Pi2-like oscillations also occur in other physical quantities, such as plasma flows and particle fluxes, those have not been called Pi2 pulsations.

(d) We must define what we mean by *Pi2 source* (see below). The loose and—in our opinion—sometimes wrong usage of this term has led to some confusion.
(e) We must define what we mean by *Pi2 model* (see below).

What Is a Pi2 Source?

A possible definition is the location in space and the mechanism that generates the characteristic Pi2 frequency in the *geomagnetic field*. However, this definition does not necessarily capture the initial location and source mechanism that controls the Pi2 frequency, which is its most defining feature. That is to say, the first signal with Pi2-like temporal modulations may not appear in the geomagnetic field but in other physical quantities. Therefore, we define the Pi2 source as the location and mechanism that generates the characteristic Pi2 frequency, regardless of the form in which the Pi2 signal first appears. It is also important to distinguish the Pi2 source from the Pi2 energy source, a distinction not always made in the literature. For example, although in one Pi2 scenario a single impulsive flow burst in the magnetotail has been "loosely" considered the Pi2 source of the plasmaspheric cavity resonance, according to our definition this flow burst is not the Pi2 source because it does not control the Pi2 frequency. Instead, it would be more appropriate to speak of the Pi2 energy source.

What Constitutes a Pi2 Model?

Foremost, a Pi2 model must describe the Pi2 source, that is, where and how the characteristic Pi2 frequency is created in the magnetosphere. Second, a Pi2 model should explain the short duration of Pi2 pulsations of approximately 10–15 min, which is equivalent to only several wave cycles. This property distinguishes the "irregular" Pi2 pulsations from the more "continuous" pulsations, which have been coined Pc pulsations. Third, a Pi2 model should ideally provide a propagation model. That is, once the characteristic Pi2 frequency has been established in a physical quantity, how does the periodic signal (or periodic energy) travel through the magnetosphere to the ground? In other words, it should describe the energy transfer processes and energy carriers along the way, realizing that the Pi2 energy appears not only in magnetic field oscillations along the way but in other physical quantities as well. We note that the Pi2 signal could travel to other remote regions of the magnetosphere and eventually dissipate without ever reaching the ground. For the purpose of this review, however, we do not require that the Pi2 models reviewed here provide information on these three aspects; the reason being that some of the more recent models have in fact not matured enough to provide answers to all of them.

In this review, the Pi2 models have been divided into two groups according to the region where the Pi2 source lies: inner magnetosphere (Sect. 2) and outer magnetosphere (Sect. 3). For the purpose of this review, we define the inner magnetosphere as the region Earthward of the inner edge of the plasma sheet, containing the plasmatrough and the plasmasphere with the plasmapause as the transition region between them. The outer magnetosphere is the region located tailward of the inner magnetosphere, containing the central plasma sheet, the plasma sheet boundary layer (PSBL), the tail lobes, and the reconnection region, which contains the X-line. Figure 2 schematically shows these plasma regions together with potential Pi2 source regions (colored), each of which will be addressed in this review. In Sect. 5 this figure will be explained in more detail (i.e., after we have reviewed all Pi2 models).

Seven models with various degrees of support are reviewed here: plasmaspheric cavity resonance (Sect. 2.1), plasmaspheric virtual resonance (Sect. 2.2), plasmapause surface

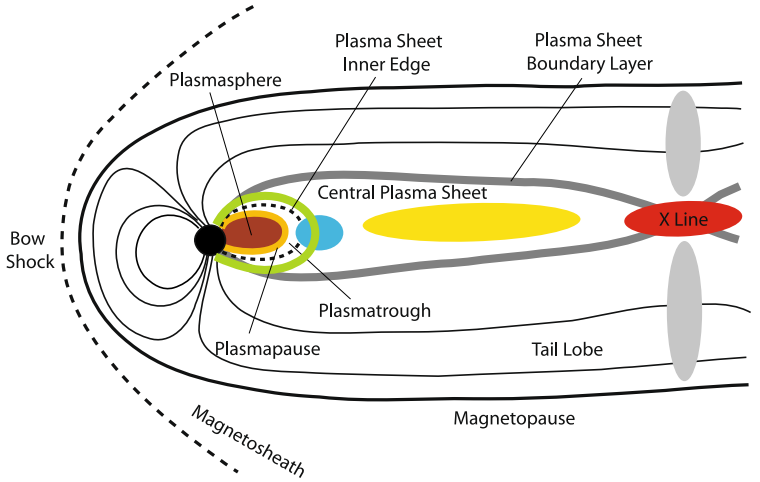

Fig. 2 Locations of potential Pi2 source regions (colored *brown*, *orange*, *green*, *blue*, *yellow*, *red*, and *gray*) inside the Earth's magnetosphere. A source region is the place where a physical mechanism operates that establishes the Pi2 frequency

wave (Sect. 2.3), transient response (Sect. 3.1), plasma instability-driven (Sect. 3.2), BBF-driven (Sect. 3.3), and reconnection-driven (Sect. 3.4). For each model we give observational evidence, as reported in the literature, and point out unresolved or conflicting issues. In Sect. 4, we review propagation modes that are not already reviewed in Sects. 2 and 3. We finish in Sect. 5 by summarizing and by suggesting what needs to be done to bring closure to the investigation of the Pi2 phenomenon. In the following subsections, we briefly review magnetospheric modes during which Pi2 pulsations can occur (Sect. 1.2) and some of the main Pi2 properties (Sect. 1.3).

1.2 Magnetospheric Modes

Although Pi2 pulsations are best known for their association with substorm onset, they also occur during other dynamic magnetospheric modes, such as pseudo-breakups, poleward boundary intensifications (PBIs), and sawtooth injection events. For example, Liou et al. (2000) showed in a statistical study that a significant fraction of Pi2 pulsations are not associated with auroral breakup (i.e., substorm). It was the recognition that some non-substorm-related pulsations resembled substorm-related Pi2 pulsations (i.e., same periodicity and short duration) to call them *Pi2 pulsations* as well. Whether or not they are caused by the same mechanism is still being investigated and current results will be reviewed in Sects. 2 and 3.

After briefly defining each magnetospheric mode, we give examples of Pi2 pulsations associated with some of these modes. For additional information on the various magnetospheric modes, the reader is referred to the review by McPherron et al. (2008).

Substorm and Intensification

A substorm is a collection of phenomena, including a magnetic bay (*H* bay), a substorm current wedge (SCW), particle injections in the near-Earth plasma sheet, and an auroral breakup to name but a few. Early on in substorm research, Saito (1969) recognized that Pi2

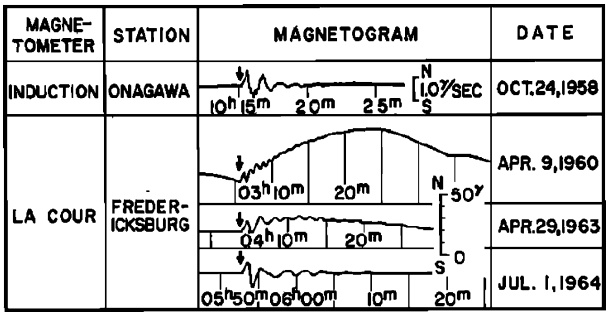

Fig. 3 (From Saito and Matsushita 1968) Early examples of Pi2 pulsations on four different days recorded by induction and La Cour fluxgate magnetometers at low- and mid-latitude ground stations

pulsations are also part of the substorm phenomenon. Coinciding with substorm onset, they are superimposed on the sudden deflection of the substorm magnetic bay, the so-called expansion phase, which can be positive or negative, depending on the latitude of observations. Figure 3 shows an early example of such a superposition. Most Pi2 events reported in the literature are associated with substorms.

Some substorm onsets are followed by additional intensifications in the optical and magnetic signatures. Most of the intensifications are accompanied by a Pi2 (Rostoker et al. 1980). Hence, a substorm can consist of several Pi2 pulsations with no obvious feature distinguishing one from another.

Pseudo-breakup

Pseudo-breakups begin like substorms, at least phenomenologically, but they do not reach the same intensity and global scale as full substorms (e.g., Voronkov et al. 2003). They are either isolated events or occur shortly before substorm onset. Although considered a substorm growth phase phenomenon (McPherron 1991), pseudo-breakups have also been observed during magnetically quiet times (Berkey and Kamide 1976). The physical relationship between pseudo-breakups and substorms has not been determined conclusively, but a common phenomenon of both is a Pi2 at onset.

Poleward Boundary Intensification

Poleward boundary intensifications (PBIs) are auroral intensifications at the poleward boundary of the auroral oval (Lyons et al. 1999) while coinciding with other magnetospheric modes, such as substorms, sawtooth events, and quiet times. PBIs can be accompanied by Pi2 pulsations or Pi2-band activity (Fig. 4). Although defined by their optical signature, small bay-like perturbations in the H component of ground magnetometer data also occur in concert with PBIs. Superimposed on these small H bays are Pi2 pulsations (Sutcliffe 1998; Sutcliffe and Lyons 2002), as can be seen in Fig. 5.

There is now much interest in PBI-associated Pi2 pulsations because they are likely of a different origin than substorm-associated Pi2 pulsations (see Sect. 3.4).

Sawtooth Injection Events

Sawtooth injection events are quasi-periodic, intense energy releases accompanied by sawtooth-shaped energetic particle fluxes at geosynchronous orbit (e.g., Henderson et al. 2006). Although they typically occur during storm intervals, the phenomena associated with

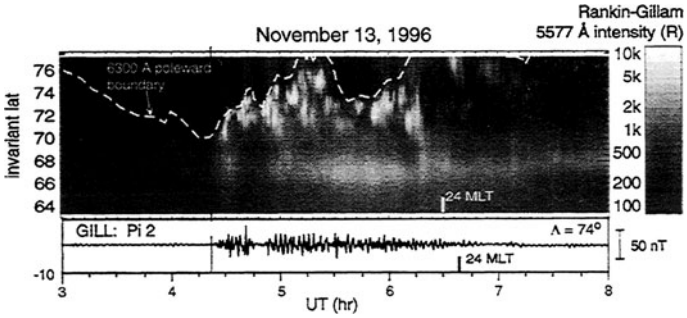

Fig. 4 (From Lyons et al. 1999) Pi2 pulsations recorded on the ground (*lower panel*) in concert with PBIs seen in the optical keogram (*upper panel*)

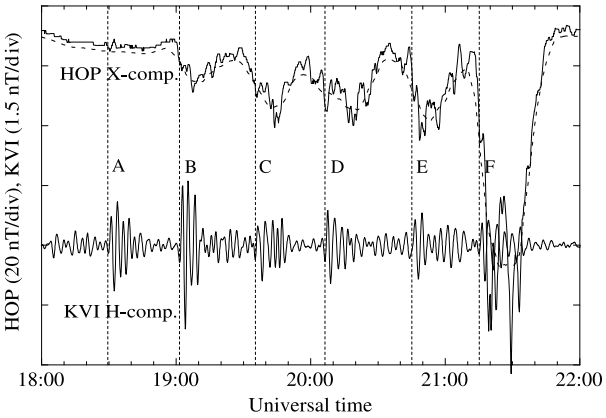

Fig. 5 (From Kim et al. 2005a) Unfiltered and filtered (4–10 mHz) magnetometer data (*H* component) from two high-latitude ground stations showing small bay-like perturbations and simultaneous Pi2 pulsations

a single injection event are similar to those of a substorm; for example, Pi2 pulsations superimposed on *H* bays (Fig. 6). Because of this similarity and the lack of a systematic investigation of these Pi2 pulsations, it is tempting to assume that the associated Pi2 pulsations are generated by the same mechanism (or mechanisms) as those occurring during substorms.

1.3 Pi2 Properties

The Pi2 period range (40–150 s) allows for a large variety of Pi2 pulsations. In addition, other Pi2 properties such as amplitude, frequency spectrum, polarization, duration (number of wave cycles) and repetitions (number of Pi2 events following each other in one active event) can also vary significantly. Although in the beginning of Pi2 research ground properties were only derived from magnetic field data, other quantities such as radar measurements (e.g., Sutcliffe and Nielsen 1990, 1992; Gjerloev et al. 2007) have also been used to characterize Pi2 pulsations (examples can be found in Sect. 2). Ground Pi2 pulsations have corresponding signals in space ("space Pi2"), which oscillate with the same period. These space signals provide important additional information on propagation direction, Poynting flux and plasma environment. Indeed, nowadays most Pi2 studies utilize both ground and space observations to infer the Pi2 generation mechanism.

In this section, we briefly summarize some of the better known Pi2 properties while focusing on ground observations. The associations of these properties with specific Pi2 models

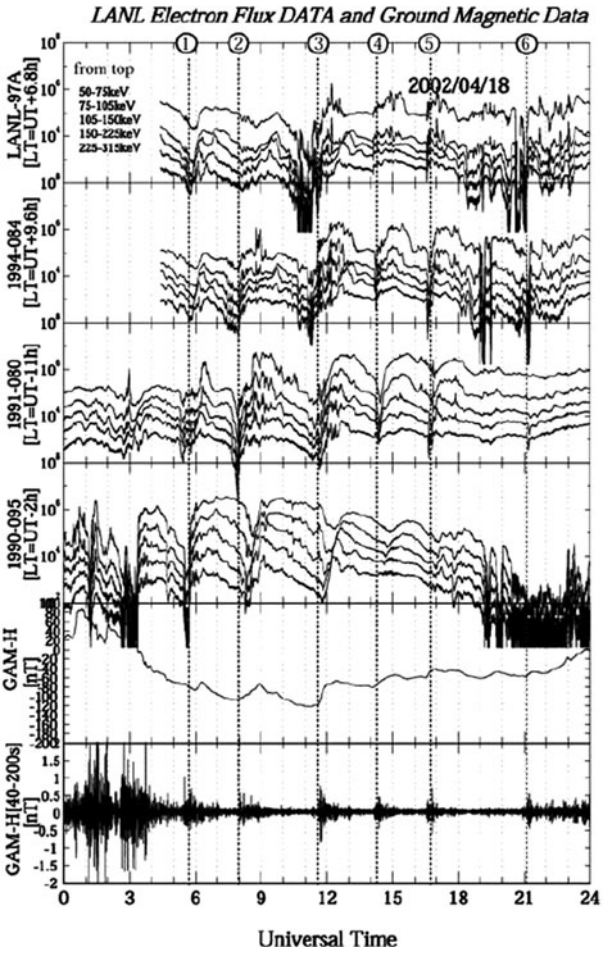

Fig. 6 (From Kitamura et al. 2005) Low-energy electron flux data obtained by four LANL satellites (*top four panels*) and *H* component data from the equatorial station GAM (*bottom two panels*). Six sawtooth injections are identified at times indicated by *vertical dashed lines*. Bandpass-filtered (40–200 s) Pi2 pulsations can be seen in the *last panel*

will be addressed in Sects. 2 and 3. Comprehensive summaries of Pi2 properties, as inferred from ground observations, can be found in the reviews by Saito (1969) and Olson (1999). Since the latter review, no advances have been made in the description of ground Pi2 pulsations. Instead, the main progress has come from spacecraft observations, which will be reviewed in Sects. 2 and 3.

Location

Ground Pi2 pulsations can occur at all longitudes and at latitudes from the dip equator ($L = 1$) up to and even inside the polar cap in the nightside. It is important to note that Pi2 occurrence at specific latitudes depends on the longitude (or equivalently, magnetic local time). At low latitudes, Pi2 pulsations have been recorded at all longitudes, including the dayside (Sutcliffe and Yumoto 1989; Li et al. 1999). At middle latitudes they occur over most of the nightside (e.g., Yeoman et al. 1994), and at high latitudes they occur within a few hours of local time from the center of the SCW (e.g., Singer et al. 1983; Gelpi et al. 1985). More recent reports show that they exist in the nightside polar cap, as well (e.g., Uozumi et al. 2004).

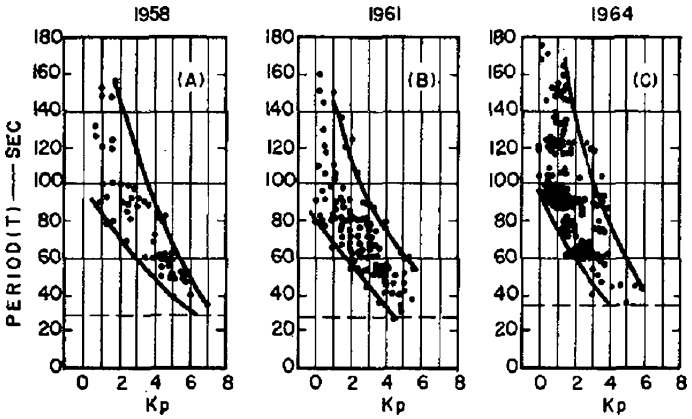

Fig. 7 (From Saito 1969) Relationship between Pi2 period and K_p index for different years

Here it should be mentioned that the classification scheme: low latitude, middle latitude, and high latitude is ambiguous. For example, a popular classification scheme, based only on ground observations, divides Pi2 pulsations into low latitude ($L < 2$), middle latitude ($2 < L < 5$), and high latitude ($L > 5$). Variations such as $2 < L < 4$ (mid-latitude) and $L > 4$ (high latitude) can be found, as well (e.g., Sutcliffe and Yumoto 1989). These classification schemes resulted from the early understanding that Pi2 pulsations can be divided into those that are generated by the SCW and those that are generated by a cavity-type resonance. The emergence of proposals for new Pi2 models in the last decade has made these classification schemes less useful, and they can even be misleading since Pi2 models can account for Pi2 pulsations covering more than one L range. Thus, we caution the reader not to equate each L range with a different Pi2 type, as will become clear in this review.

An alternative classification based on physical properties was made by Samson (1982), who defined high latitude as any region influenced by magnetic fields from the ionospheric substorm electrojet. The region located latitudinally below would be considered middle latitude. This definition is much preferred, allowing for latitudinal motion of the electrojet with geomagnetic conditions (also compare our definition of inner and outer magnetosphere in Sect. 1.1). Another useful latitudinal division of ground Pi2 pulsations (e.g., Yeoman and Orr 1989) is auroral (zone) Pi2 and subauroral (zone) Pi2, where auroral zone could refer to the definition given by Samson (1982), and subauroral zone refers to the region equatorward of the auroral zone. With this definition, the auroral zone is conjugate to plasma sheet field lines, and the subauroral zone is conjugate to the plasmatrough and perhaps part of the plasmasphere. In both schemes low latitudes can still be defined as $L < 2$ so as to acknowledge Pi2 pulsations observed in this range at both dayside and nightside.

Period

For many decades, it has been known that the Pi2 period varies with geomagnetic activity as measured by the *AE* and K_P indices (Saito and Matsushita 1968). Increased activity corresponds to shorter period (Fig. 7). However, we have also learned that the Pi2 period can vary with latitude and longitude during the same time interval. This is one indicator telling us that more than one Pi2 mechanism operate simultaneously in the magnetosphere.

Typically, Pi2 periods are longer (90–120 s) at high latitude than at middle and low latitudes (closer to 50 s) (e.g., Olson and Rostoker 1975). However, Pi2 events can also

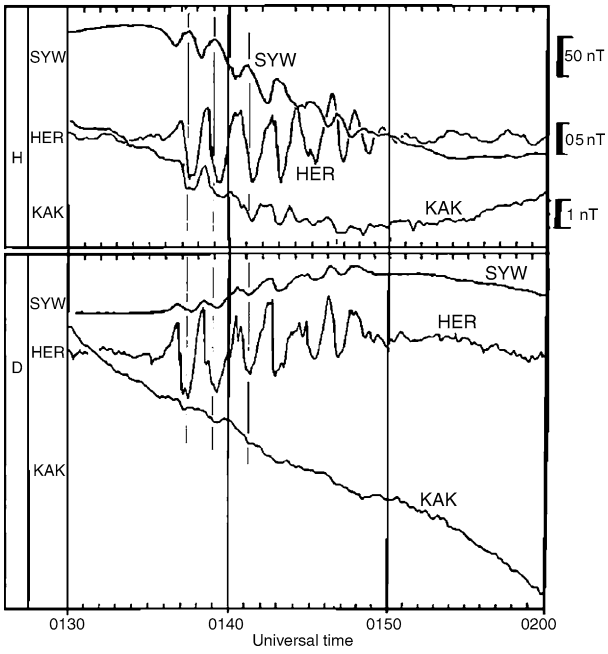

Fig. 8 (From Yumoto et al. 1990) Pi2 pulsations concurrently detected on the ground at high-latitude (SYW, $L = 6.15$) and low-latitude (HER, $L = 1.88$) stations on the nightside and at a low-latitude station (KAK, $L = 1.23$) on the dayside

have a common period spanning low to high latitudes (Fig. 8). A surprising fact is that low-latitude Pi2 pulsations can have the same period in the nightside and dayside, spanning many hours of local time (Sutcliffe and Yumoto 1989). In contrast, longitudinally separated high-latitude Pi2 pulsations can show variations from one station to the next (Kim et al. 2005a).

High-latitude Pi2 pulsations associated with substorms typically have complicated frequency spectra (Samson 1982) that have been attributed to additional field-aligned currents and electrojets. Multiple spectral peaks (up to four) have been reported in a single event (e.g., Stuart et al. 1979; Lin et al. 1991). At low and middle latitudes, on the other hand, Pi2 pulsations are more sinusoidal (i.e., monochromatic).

Amplitude

A characteristic Pi2 feature is amplitude variation with latitude and longitude. The amplitude can range from less than 1 nT at low latitudes to over 100 nT at high latitudes (auroral zone) where it reaches its maximum (e.g., Jacobs and Sinno 1960; Saito 1969; Rostoker and Samson 1981). The largest Pi2 pulsations are found near magnetic midnight at high latitudes. Other local amplitude maxima have been identified at nightside middle latitudes, the so-called secondary amplitude maximum (Stuart 1974; Fukunishi 1975), and near the dayside dip equator (Yanagihara and Shimizu 1966; Stuart and Barsczus 1980; Sastry et al. 1983). Figure 9 shows an example of a dayside equatorial amplitude maximum, recorded at the ground station POH, located at the dip equator. At this station the amplitude was about three times that at stations located from 20–46° magnetic latitude and with phase lags of ∼30°.

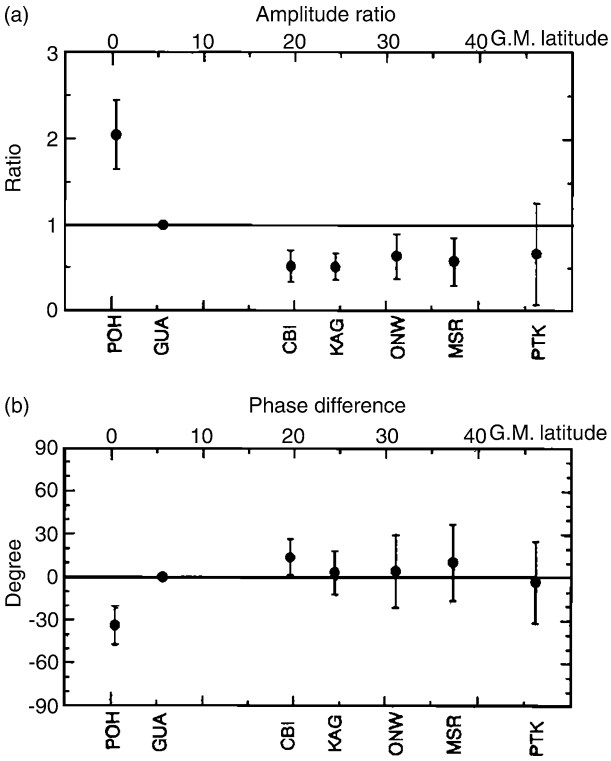

Fig. 9 (From Shinohara et al. 1997) Amplitude (*top*) and phase (*bottom*) of dayside Pi2 pulsations relative to the Pi2 pulsation signal at GUA. The stations cover $L = 1.0$–2.1

Polarization

The polarization pattern of ground Pi2 pulsations is rather complex, and a division of the pattern according to latitude has been attempted. At high latitude near the westward traveling surge (WTS), Samson and Rostoker (1983) described a double polarization change in the latitudinal direction (Fig. 10). They suggested that the equatorward and poleward reversals were associated with ionospheric and field-aligned currents, respectively. Although this polarization pattern has been observed by several authors (e.g., Samson and Rostoker 1983; Lester et al. 1985; Samson 1985), other patterns surrounding the head of the WTS have also been described (e.g., Pashin et al. 1982).

At middle latitudes, Pi2 polarization has a characteristic longitudinal pattern. In Fig. 11 each arrow shows the direction of the horizontal polarization ellipse of the local Pi2 pulsation. Notably, the arrows between 40° and 55° point toward a common location. Lester et al. (1983) noted that this pattern is longitudinally fixed with respect to the field-aligned currents of the SCW (see also Sect. 3.1). In addition, at middle latitudes of approximately $L = 4$, a polarization reversal associated with the secondary amplitude maximum occurs (see above under 'Amplitude').

At low latitudes, the H component is in phase in both hemispheres and 180° out of phase in the D component (e.g., Li et al. 1998). Li et al. (1998) also reported a longitudinal polarization pattern similar to that observed at middle latitudes, whereas others (e.g., Sutcliffe 1981) have reported a low-latitude polarization pattern that differs from that seen at middle latitudes.

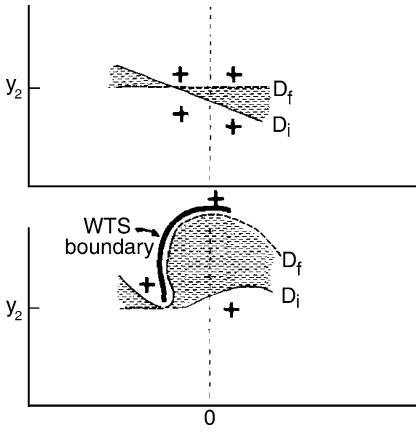

Fig. 10 (From Samson and Rostoker 1983) Polarization diagrams in the vicinity of the auroral bulge and the WTS. The symbol (+) denotes counterclockwise polarization (H-D plane) and the *shaded areas* denote clockwise polarization. D_f indicates a reversal due to field-aligned currents and D_i denotes a reversal due to ionospheric currents

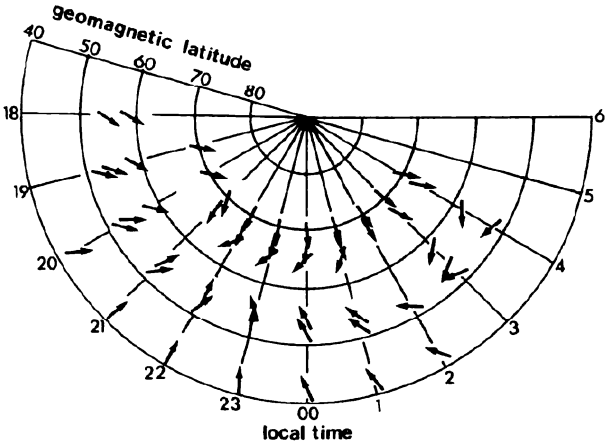

Fig. 11 (From Björnsson et al. 1971) Directions of Pi2 polarization ellipses in the H-D plane

Duration and Repetition

One of the defining Pi2 criteria is their short lifetime, which can range from two wave cycles to ten or more (approximately 10–15 min). Typically, low- and mid-latitude Pi2 pulsations have more wave cycles than high-latitude Pi2 pulsations (Webster et al. 1989; Li et al. 1998).

Furthermore, Pi2 pulsations often occur successively within the same substorm event (e.g., Fig. 12). Hsu and McPherron (2007) reported that a substorm can be associated with up to six Pi2 pulsations, but the most probable number is two. Saka et al. (2002) even showed eight Pi2 pulsations closely following each other within one hour. The time between individual Pi2 pulsations ranges from 5 to 50 min, with 20 min being the mean separation (Hsu and McPherron 2007)

Propagation

Longitudinal and latitudinal phase (time) delays are common for Pi2 pulsations. Although westward propagation dominates at all latitudes, eastward propagation also occurs (e.g., Baranskiy et al. 1980; Lester et al. 1983; Li et al. 1998). At high latitudes eastward and westward propagation can exceed 20 km s^{-1} (e.g., Webster et al. 1989).

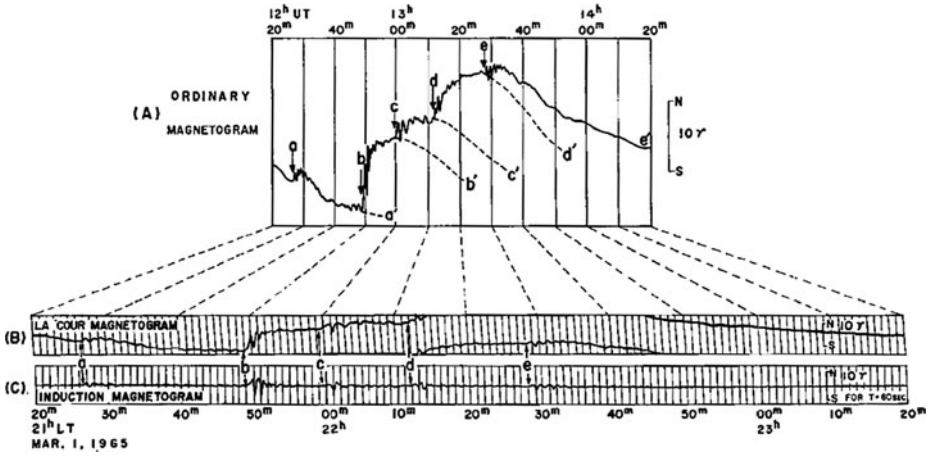

Fig. 12 (From Saito 1969) Example of a large H bay (b–e′) showing several individual magnetic bays and Pi2 pulsations (b, c, d, and e)

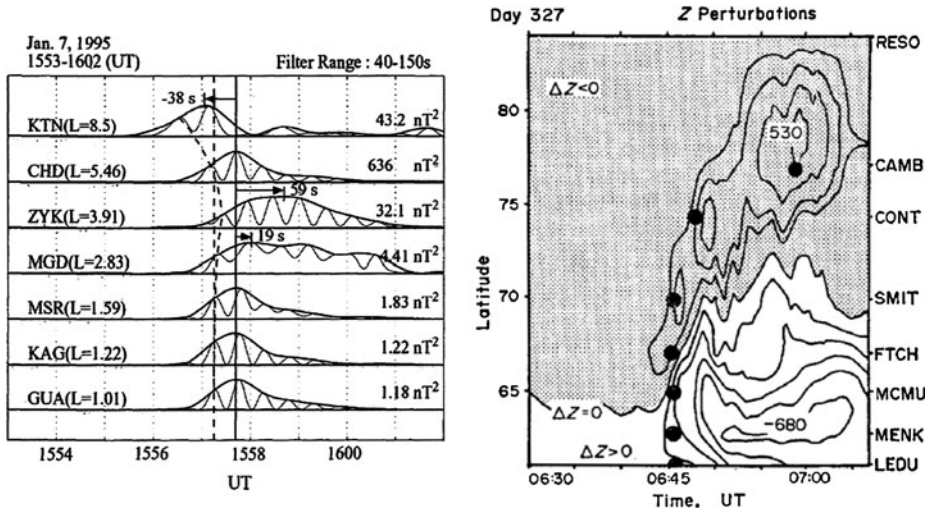

Fig. 13 Arrival of Pi2 signals in relation to latitude. (*Left*) (From Uozumi et al. 2000) Pi2 is first recorded at $L = 8.5$ followed by lower L-value stations. (*Right*) (From Olson and Rostoker 1975) Contour plot of the vertical (Z component) perturbations along the Alberta meridian magnetometer chain plotted as a function of latitude and time. *Dots* show Pi2 onsets at different latitudes, illustrating northward propagation

Although north-south time delays are common at high latitudes, they can also be found at low and middle latitudes. For example, Uozumi et al. (2000) showed in a statistical study that Pi2 pulsations were first observed in the polar cap region, albeit with smaller amplitude than those closer to the simultaneously occurring aurora, followed by mid- and low-latitude Pi2 pulsations (Fig. 13). This appears to be in conflict to earlier reports of high-latitude Pi2 pulsations (Olson and Rostoker 1975) that move poleward, apparently together with the poleward motion of the electrojet (Fig. 13). However, a resolution to this discrepancy might be that two different Pi2 generation mechanisms operated for the reported events.

2 Inner-Magnetospheric Models

For the purpose of discussing Pi2 properties of inner-magnetospheric models, we define the inner magnetosphere as the region Earthward of the inner edge of the plasma sheet, containing the plasmasphere and the plasmatrough. Whereas the plasma sheet is populated with hot plasma ($T > 1$ keV), the plasmatrough is usually dominated by ionospheric cold plasma on open drift orbits and the plasmasphere is populated by ionospheric cold ions drifting on closed orbits around the Earth. With this definition the inner magnetosphere is a passive region as regarding ULF waves, where cold plasma magnetohydrodynamics (MHD) is a good approximation and the wave properties are determined by the background plasma, magnetic field configuration, and the boundary conditions prescribed on the inner boundary (i.e., ionosphere) and the outer boundary. By contrast, the outer magnetosphere is an active region where hot plasma contributes to energy conversion/release processes related to substorms and phenomena that map to the auroral zone. Part of the energy in the substorm-time plasma sheet is converted to ULF waves in the inner magnetosphere. Although highly dependent on the geomagnetic activity level, the radial distance of the plasma sheet inner edge is close to geosynchronous orbit (Elphic et al. 1999), and we consider $L < 6$ (magnetic latitude $\sim 66°$) as a practical definition of average inner magnetosphere. Ground observations made within the inner magnetosphere are often classified into low latitude ($L < 2$) and middle latitude ($2 < L < 5$), although these are somewhat arbitrary (see additional discussion in Sect. 1.3).

An important feature of the inner magnetosphere is the plasmapause which is the transition region between the plasmasphere and the plasmatrough. Since the plasmaspheric ions reside on the same flux tube for a long time while the ionosphere keeps feeding ions, the density in the plasmasphere is much higher than in the plasmatrough. The plasma density changes by a factor of 10 or more across the plasmapause corresponding to a change in the Alfvén velocity by a factor of 3 or more (assuming that the ion composition stays the same across the plasmapause, which may not be the case (e.g., Fraser et al. 2005)). This velocity change affects the spatial structure and spectral contents of MHD waves propagating in the inner magnetosphere. The plasmapause moves from $L \sim 2$ during highly disturbed periods (e.g., major storms) to $L \sim 7$ during geomagnetic quiescence (Nishida 1966; Chappell et al. 1970; Carpenter and Anderson 1992; Laakso et al. 2002; Goldstein et al. 2003; O'Brien and Moldwin 2003). Accordingly, the properties of MHD waves in the inner magnetosphere should strongly depend on geomagnetic activity.

Pi2 pulsations in the inner magnetosphere can be discussed mostly in terms of the poloidal and toroidal modes that date back to the work of Dungey (1954). In the cold plasma MHD theory an axisymmetric magnetosphere sustains two decoupled MHD eigenmode-oscillations if the azimuthal wavenumber (m) is taken to be zero: axisymmetric toroidal mode and axisymmetric poloidal mode. The toroidal mode is an azimuthal oscillation of field lines with L-dependent frequencies, while the poloidal mode is a radial oscillation of field lines with an L-independent frequency. In the real magnetosphere any MHD disturbance has a finite azimuthal extent or wavelength, which means that m is finite and the poloidal and toroidal modes are coupled. Therefore, observational reference to the poloidal or toroidal mode is usually based on the relative strength of the two polarization modes. Also, an axisymmetric magnetosphere is merely a theoretical simplification. The real magnetosphere has a strong day-night asymmetry and the radius of the plasmasphere varies with local time. This asymmetry can become important when modeling the longitudinal structure of Pi2 pulsations.

Inner-magnetospheric models, which have the generation of the Pi2 frequency inside the inner magnetosphere, can be classified into three types (Fig. 14): plasmaspheric

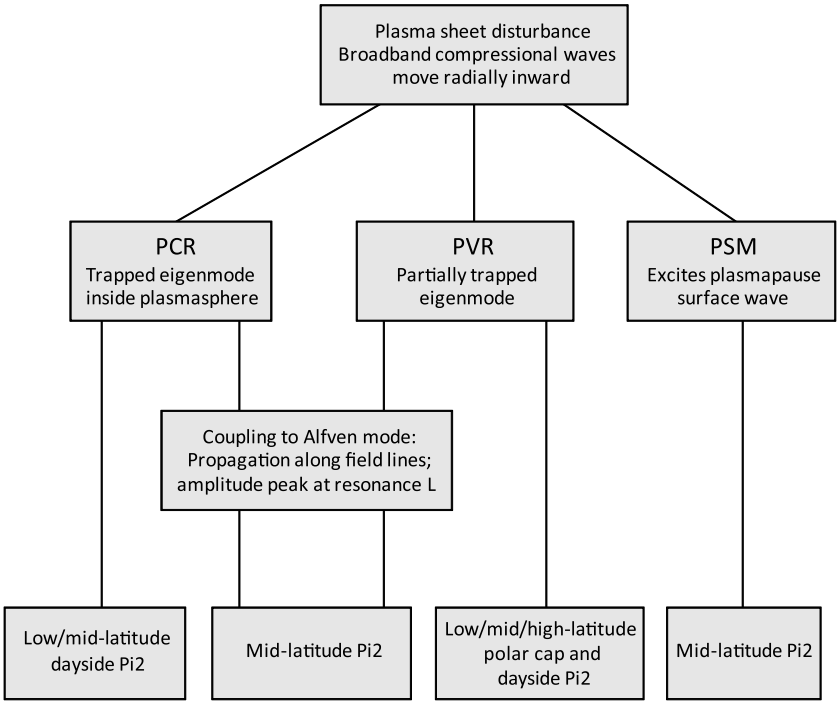

Fig. 14 Block diagram illustrating possible Pi2 sources and propagation mechanisms in the inner magnetosphere

cavity resonance (PCR), its generalization, the plasmaspheric virtual resonance (PVR), and plasmapause surface mode (PSM). The first two modes (illustrated in the first two branches on the left) are predominantly poloidal waves with a strong compressional (fast mode) component and small m that fill a large volume of the inner magnetosphere. The surface mode (illustrated in the third branch) is by definition localized to the plasmapause and is also expected to exhibit poloidal polarization but with large m as formulated by Chen and Hasegawa (1974b). In a popular scenario PCR, PVR, or PSM are excited by an externally applied impulsive (or equivalently, broadband) disturbance. The impulse propagates deep into the inner magnetosphere as fast mode waves and excites compressional global MHD eigenmodes or the surface eigenmode. In the case of the global modes, once they have selected a dominant frequency or frequencies from the impulse, standing Alfvén waves (toroidal modes) of the same frequency can be excited on a thin L shell through the field line resonance mechanism (Chen and Hasegawa 1974a; Southwood 1974). It is important to note that inner-magnetospheric models not only account for low- and mid-latitude Pi2 pulsations, but also high-latitude Pi2 pulsations and, more surprisingly, polar cap Pi2 pulsations.

What happens if the external disturbance has an intrinsic periodicity is an interesting question (cf. Sect. 3). Conceptually, the inner magnetosphere can resonate with such input if the driving disturbance has frequencies that match the compressional eigenmode frequencies, in which case the input waves will be resonantly amplified at the matching frequencies. If the frequencies do not match, the input waves will still be detected unless they are completely reflected at a turning point. This phenomenon can be classified as forced oscillations.

In reality, however, the external source is neither purely impulsive nor purely periodic. For example, even relatively well-defined flow burst oscillations will have a finite bandwidth, and as a consequence the global mode resonance (or surface mode) may occur at frequencies within the bandwidth of the external disturbances but not exactly at the same frequencies of the spectral peaks of the input. Evaluating the efficiency or quality factor of the resonance requires simultaneous spectral measurements of the input (BBFs) and response (inner magnetosphere compressional waves) for a wide range of input frequencies. Such an analysis has not been conducted and our review will be limited to observations within the inner magnetosphere that can be compared with the models of the inner magnetosphere eigenmodes.

The remainder of this section reviews the basic theoretical concepts and the observational evidence of the plasmaspheric cavity resonance, the plasmaspheric virtual resonance, and the plasmapause surface mode.

2.1 Plasmaspheric Cavity Resonance

2.1.1 Model

Cavity resonance is defined to be a fast mode eigenmode in a magnetospheric cavity. The resonance is characterized by discrete frequencies and spatial eigenmodes that are determined by the cavity geometry and the spatial variation of the MHD wave velocity (e.g., Alfvén velocity, V_A) inside the cavity (we will consider a cold plasma which sustains only the fast mode and Alfvén mode). In early theoretical studies of cavity resonance the magnetopause was assumed to be the outer boundary (e.g., Kivelson et al. 1984; Allan et al. 1986a; Lee and Lysak 1989). This is not realistic in the nightside magnetosphere where the stretched magnetotail allows fast mode energy to escape tailward, although some reflection at the plasma sheet inner edge might occur. Therefore, the plasmapause is the more likely outer boundary for the cavity that sustains Pi2 pulsations. Note that even in numerical studies, assuming a perfectly reflecting magnetopause, compressional modes localized to the plasmasphere exist (Allan et al. 1986b; Zhu and Kivelson 1989) in support of the concept of PCR. PCR is closely related to PVR, sharing common physical properties such as polarization and nodal structures. The main difference is how the plasmapause boundary condition is treated for fast mode waves that have wavelengths comparable to the dimension of the plasmasphere. In our definition PCR corresponds to cases where the plasmapause is treated as a perfect reflector. Our review of PVR studies is given in Sect. 2.2. Another concept closely related to cavity resonance is the waveguide mode (Samson et al. 1992), which also has a radially standing structure but azimuthal propagation is its key property. Since the waveguide mode is usually employed in discussing wave propagation along the magnetopause we will not make specific references to this mode.

Figure 15 illustrates magnetic field perturbations associated with the simplest possible cavity resonance in a model box magnetosphere. The fundamental mode is shown here since it is likely the most powerful harmonic similar to other resonances occurring in nature. Figure 15a illustrates the magnetic field configuration of the mode in a magnetic meridian (the x-z plane) at two epochs separated by half a wave period. In both panels the outer boundary is the plasmapause ($L = L_{pp}$), and the inner boundary ($L = 1$) corresponds to the ionosphere at low latitudes. The upper (lower) boundary is the northern (southern) ionosphere at high latitudes, where the field lines are tied to the ionosphere. In the real magnetosphere the magnetic field inclination relative to the Earth's surface changes smoothly from zero at the magnetic equator to 90° at the pole. This transition has not been fully incorporated even in simulations that use a dipole magnetic field (e.g., Lee and Lysak 1989; Fujita and

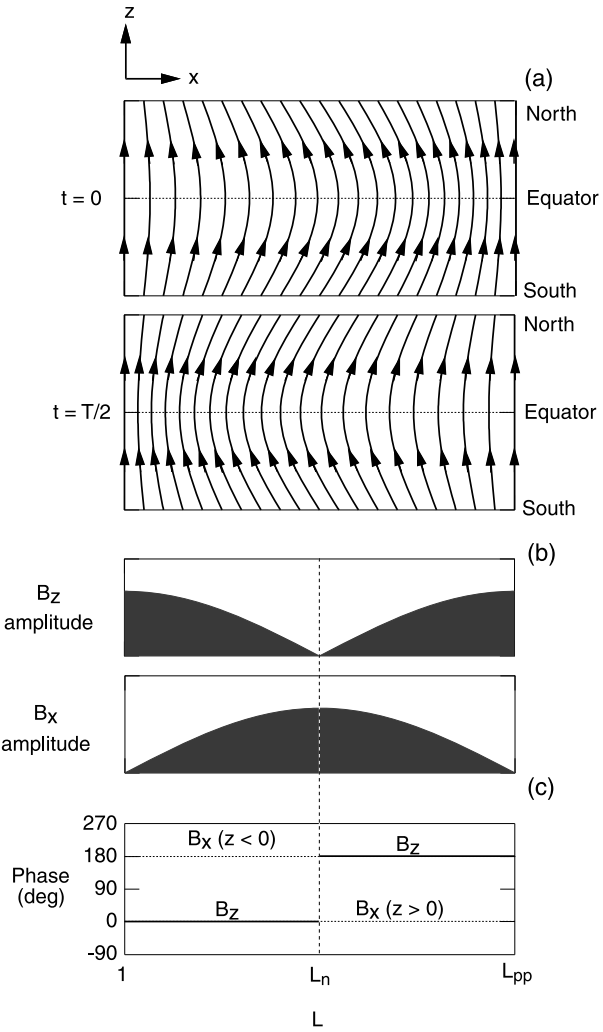

Fig. 15 (Adopted from Takahashi et al. 1995) Illustration of magnetic field oscillations associated with simple plasmaspheric cavity resonance. (**a**) Snapshots of the magnetic field configuration in the meridian plane for a fundamental cavity resonance mode in a box magnetosphere. (**b**) The radial profile of the amplitude of the magnetic field poloidal components. L_n is the node of the B_z component. (**c**) The radial profile of the phase of the poloidal components. The B_z phase changes by 180° across L_n

Patel 1992) and remains a major area for improvement in quantitative models of ULF wave propagation near the ionosphere.

Although highly simplified, Fig. 15 shows a few important features of the mode that can be compared with observation. First, the resonance mode has half a wavelength between the radial boundaries (as well as between the northern and southern ionospheric boundaries). Consequently, the period of the mode, T_{PCR}, is given by the fast mode bounce time between the radial boundaries:

$$T_{PCR} = 2R_E \int_1^{L_{pp}} dL / V_{Aeq} \tag{1}$$

where V_{Aeq} is the equatorial Alfvén velocity. If V_{Aeq} is taken to be a constant, we obtain $T_{PCR} = 2R_E L_{pp} / V_{Aeq}$. As representative values we adopt $V_{Aeq} \sim 700$ km/s and $L_{pp} \sim 4$ (e.g., Takahashi and Anderson, 1992) and get $T_{PCR} \sim 70$ s, which indeed falls into the traditional Pi2 period range (40–150 s). When the frequency is numerically obtained for a realistic L

dependence of V_{Aeq}, the node of B_z (L_{n} in Fig. 15) is shifted toward L_{pp} (plasmapause) and the higher harmonics occur at frequencies that are not integral multiples of the fundamental frequency (Yeoman and Orr 1989; Lin et al. 1991; Itonaga et al. 1992; Cheng et al. 2000; Denton et al. 2002).

Second, the model describes the magnetic field polarization (Fig. 15a). The PCR mode is characterized by poloidal motion of the field line, so the radial (B_x) and magnetic-field-aligned (B_z) components oscillate (we will use local right-handed x-y-z coordinates for the field components in the radial, azimuthal, and magnetic field aligned directions). The field line displacement is symmetric about the magnetic equator (i.e., the harmonic mode is also "fundamental" along the field line), which means $B_x = 0$ and $B_z \neq 0$ there. On a given field line, field line bending increases from the equator to the ionosphere, resulting in an increasingly strong appearance of the B_x component farther away from the equator. At the higher-latitude ionosphere (upper and lower boundaries) the magnetic field line oscillation is purely transverse if the field lines are strictly tied to the conducting ionosphere. However, at the lower-latitude ionosphere (inner boundary) the field perturbation is purely compressional. Note that as stated above, this distinction of the lower-latitude and higher-latitude ionospheres is an artifact of the box model. In the real magnetosphere the magnetic field perturbation will contain both the B_x and B_z components at all latitudes except at the equator and the pole. The electric field polarization corresponding to the magnetic field oscillation can be found from Faraday's law $\partial \mathbf{B}/\partial t = -\nabla \times \mathbf{E}$. This equation shows that the electric field perturbation for the field line oscillation shown in Fig. 15 is directed along the y (azimuthal) axis and is $\pm 90°$ out of phase with respect to the magnetic field perturbation.

Third, the model predicts the radial structure of the amplitude and phase (Fig. 15b). The B_z component has a node at $L = L_{\mathrm{n}}$ across which the B_z phase changes by 180°. By contrast, the B_x component has an antinode at $L = L_{\mathrm{n}}$ and its phase remains constant on a given (north or south) side of the equator. In order to define the phase at a single spacecraft that can be anywhere in the box, we can use the ground H component of the low-latitude Pi2 signal as the reference, since H maps to the B_z component at the equatorial region (Allan et al. 1996). Also, the amplitude ratio and phase shift (Fig. 15c) between B_x an B_z is a useful parameters in detecting cavity resonance modes.

Until now we have ignored the azimuthal structure of the PCR mode. The strictly meridional magnetic field oscillation illustrated in Fig. 15 is possible only when $m = 0$, which is equivalent to decoupling of the poloidal and toroidal modes. In the real magnetosphere, m is always finite and there is a finite amount of coupling between the two polarization modes. Furthermore, the energy source for Pi2 is localized near midnight, which causes high-latitude Pi2 pulsations to show much stronger longitudinal localization. This is very important when one tries to understand the transition from mid-latitude to low-latitude Pi2 pulsations and the local time variation of Pi2 properties (see review by Yumoto 1986).

So far, we have discussed the PCR model assuming a lossless plasmasphere, but in reality the plasmasphere is far from an ideal cavity. In fact a Pi2 pulsation typically lasts only about 10–15 minutes, or several cycles, implying substantial damping. Possible damping mechanisms are energy escape into the magnetotail (Lee et al. 2004; Fujita et al. 2001) and mode conversion to the shear Alfvén mode, which is damped through Joule dissipation at the ionosphere (Osaki et al. 1998; Newton et al. 1978).

2.1.2 Observations

Next we present an observational evaluation of the model, organized by period (or frequency), harmonics, damping time scale, polarization, and radial and azimuthal mode structures.

Period

The cavity resonance model for the mid- and low-latitude Pi2 was first suggested by Saito and Matsushita (1968), based on the analysis of more than 6000 Pi2 events detected at $L \sim 1.3$ and $L \sim 2.4$ over a complete solar cycle. A key signature of the cavity mode was the common frequency that was observed at the different latitudes. Another key signature was the variation of the Pi2 period with geomagnetic activity: the period was shorter for higher geomagnetic activity as inferred from K_p (Fig. 7 in Sect. 1.3). In computing the Pi2 period using (1), Saito and Matsushita (1968) assumed a radially smooth density variation and an outer boundary at the transition region between open and closed field lines. They attributed the variation of the Pi2 period to the change of the radial distance of the outer boundary; namely, for stronger geomagnetic activity the radial distance becomes smaller, resulting in a shorter Pi2 period.

The qualitatively same result can be obtained by assuming the outer boundary to be the plasmapause. The plasmapause distance is typically in the range from 2 to 7 R_E, with smaller values associated with higher geomagnetic activity (Chappell et al. 1970; Laakso et al. 2002; O'Brien and Moldwin 2003). Studies assuming the plasmapause to be the outer boundary found reasonable agreement between observed and modeled cavity mode Pi2 frequencies (Yeoman and Orr 1989; Lin et al. 1991; Cheng et al. 2000; Denton et al. 2002; Takahashi et al. 2003a). The PCR model also explains why the frequency of Pi2 pulsations observed during very quiet time tends to be very low (Sutcliffe 1998).

In case-by-case studies, the PCR model has been questioned on the basis of the difference between the observed and predicted Pi2 frequencies. For example, Kim et al. (2005b) reported a significant mismatch between the frequency of an observed Pi2 (11 mHz) and the PCR frequency (28 mHz) estimated using (1) for a realistic V_{Aeq} profile in the magnetosphere derived by Denton et al. (2006). Even with the assumption of a larger radial distance of the effective outer boundary in consideration of a possible extension of the mode beyond the plasmasphere (the PVR effect, Sect. 2.2), the model frequency was higher than the observed frequency. Although Kim et al. (2005b) favored a BBF model for their particular Pi2 event (see Sect. 3.3 for more discussion on the BBF-driven mechanism), caution is in order regarding the mass density estimates employed by the model (see below for additional comments).

Another observational aspect of low-latitude Pi2 pulsations that differs from the simple PCR model is the spatial variation of the Pi2 frequency within the plasmasphere, both with longitude (Kosaka et al. 2002; Han et al. 2003) and latitude (Kim et al. 2005a). The variation contradicts the simple PCR model, which predicts a mode that oscillates at the same frequency anywhere in the plasmasphere (note that there are other studies indicating that the Pi2 frequency does not depend on longitude, e.g., Sutcliffe and Yumoto (1989) and Nosé et al. (2006)). However, a numerical simulation study by Fujita and Itonaga (2003) offers an explanation for the longitudinal variation within the framework of the PCR model. The key ingredient in this simulation is the local time variation of the Alfvén velocity, which mimicked the velocity decrease near the plasmasphere bulge at dusk. It was found that the plasmaspheric eigenoscillation consisted of a number of longitudinal harmonic modes with different frequencies and that the superposition of the modes resulted in a local time dependence of the frequency of the cavity resonance mode.

In estimating the PCR frequencies, one should note that existing plasmasphere models are usually derived from observed electron number densities (e.g., Carpenter and Anderson 1992; Laakso et al. 2002; O'Brien and Moldwin 2003). The radial profile of the mass density, which controls MHD wave speed, can differ significantly from that of electrons (Fraser

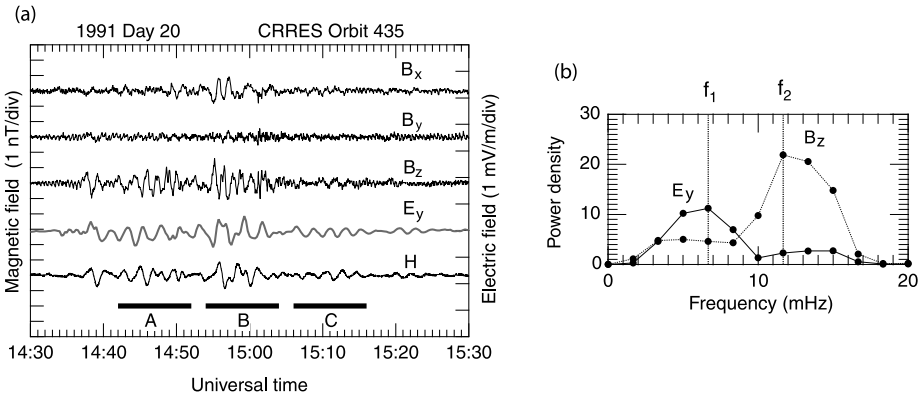

Fig. 16 (From Takahashi et al. 2003b) Multiharmonic Pi2 pulsations observed near midnight in the equatorial plasmasphere with CRRES and on the ground at Kakioka. (**a**) Time series plots of the measured field components (B_x, B_y, B_z: magnetic field components at CRRES; E_y: azimuthal component of the electric field at CRRES; H: magnetic field horizontal component at Kakioka. (**b**) Power spectra of the E_y and B_z components for time interval B

et al. 2005). Constructed using various ground and satellite observations near the time of the Pi2 event, the mass density model adopted by Kim et al. (2005b) was far more realistic than statistically derived plasmasphere models. Still, the mass density was estimated from toroidal wave frequencies that were measured away from midnight, which implies a considerable uncertainty in the mass density at the Pi2 generation region.

Harmonics

There is no reason why only the fundamental PCR is excited. In fact, there is observational evidence for the higher harmonics both in terms of frequency and nodal structure. As for the frequency, spectral analyses of ground Pi2 pulsations reported multiple (up to four) spectral peaks (Stuart et al. 1979) and these have been attributed to PCR harmonics (Lin et al. 1991; Nosé 1999; Cheng et al. 2000). Multi-frequency Pi2 pulsations detected by spacecraft have also been attributed to the PCR model (Denton et al. 2002).

Both observational and theoretical studies report a second to fundamental frequency ratio (f_2/f_1) between 1.4 and 2.0 for the PCR mode with the most likely value around 1.7 (Denton et al. 2002). Since the ratio is quite different from the ratio ∼2.7 for toroidal standing Alfvén waves (Takahashi et al. 2004), one could argue that field line resonance does not play a role in frequency selection process for low-latitude Pi2 pulsations.

Spacecraft observation of the nodal structure for a single Pi2 is difficult, but a CRRES case study reported detection of a node and an antinode of multi-harmonic Pi2 pulsations. For the pulsation event, reported by Takahashi et al. (2003b) and illustrated in Fig. 16, the spacecraft was located at midnight, on the magnetic equator, and Earthward of the plasmapause that was identified from the electron number density measured at CRRES (using a plasma wave experiment). The Kakioka ground station ($L = 1.3$), from which the H-component data are taken, was also located at midnight. The time series plots (Fig. 16a) shows that at CRRES the pulsations are strongly compressional (B_z) with little sign of an azimuthal (B_y) oscillation; the azimuthal electric field (E_y) shows strong oscillations as expected for a poloidal mode, but their frequency f_1 (∼7 mHz: fundamental) is much lower than the B_z frequency f_2 (∼12 mHz: second harmonic). Meanwhile, the spectrum of the

ground H component exhibited a peak at both f_1 and f_2. Since an Earthward-propagating fast mode wave does not have spatially stationary node or antinode, peaks in the E_ϕ and B_z spectra for a propagating wave should occur at the same frequencies at all radial distances. The fact that E_y and B_z each had a single spectral peak but at a different frequency (Fig. 16b) is convincing evidence for a multiharmonic standing fast mode wave. When the CRRES events are interpreted in term of the PCR model, the spacecraft was located at L_n point in Fig. 15 where the fundamental mode ($f = f_1$) had a B_z node and E_y had an antinode. For the second harmonic ($f = f_2$), the node and antinode designation reverses, so only the B_z oscillation was visible. The frequency ratio f_2/f_1 for the event is ∼1.7 close to that predicted by numerical models.

Damping Time Scale

Pi2 pulsations typically last 10 minutes corresponding to several oscillation cycles. Unless there is periodic forcing this implies that the plasmaspheric cavity has a reasonably high Q value. Numerical simulations indeed produce fairly robust cavity mode Pi2 pulsations even when strong damping is incorporated from ionospheric Joule dissipation and energy escape into the tail and solar wind (e.g., Fujita et al. 2002; Lee et al. 2004; Lee and Takahashi 2006) (see Fig. 20 in Sect. 2.2).

According to an energy loss rate evaluation based on spacecraft measurements, however, the damping time scale of the PCR mode can be much shorter. Osaki et al. (1998) studied two Pi2 pulsations detected by the Akebono satellite as it passed through the nightside plasmasphere. The pulsations accompanied a shear Alfvén wave, which propagated toward the ionosphere. The Poynting flux (in the direction of the ambient magnetic field) of the Alfvén wave was such that the compressional mode energy is lost in a time scale (∼10 s) shorter than the period of the Pi2 pulsations. This result favored an external driving mechanism (Itonaga et al. 1997b) such as periodically generated BBFs.

In view of the numerical simulations mentioned above, the damping mechanism warrants further investigation since the energy budget calculation by Osaki et al. (1998) was based on simplifying assumptions on the size of the region of compressional mode as well as on the spatial variation of pulsation amplitude. It will be interesting to compute the field-aligned Poynting flux of simulated Pi2 pulsations and evaluate whether the energy loss via propagating Alfvén wave occurs globally or at limited L. If the domain of strong Alfvén waves is limited, the damping of the compressional mode may not be as severe as Osaki et al. estimated.

Polarization

Spacecraft observations are essential in determining the polarization mode of Pi2 pulsations because the ionospheric screening effect can modify the polarization of magnetospheric MHD waves propagating to the ground (e.g. Kivelson and Southwood 1988). There is strong evidence for poloidal oscillations in magnetic field data from equatorial satellites. Lin and Cahill (1975) made the first spacecraft (Explorer 45) observation of magnetic Pi2 pulsations in the inner magnetosphere ($L \sim 5$) in the evening sector. The seven Pi2 pulsations reported in their study were in fact all compressional and occurred simultaneously with ground Pi2 pulsations. When CCE magnetometer data were surveyed over a wider range of L and local time, numerous similar poloidal events were found which exhibited high coherence with ground Pi2 pulsations (Takahashi et al. 1992 1995). In addition, low altitude (<1000 km) magnetic field observations by the UARS (Takahashi et al. 1999), CHAMP (Sutcliffe and

Lühr 2003), and Ørsted (Han et al. 2004) satellites indicated similar polarization of magnetic pulsations that were unambiguously associated with ground low-latitude Pi2 pulsations. In these spacecraft observations the toroidal component (B_y) also exhibited oscillations, but they had low coherence with ground Pi2 pulsations compared to the poloidal components (B_x and B_z).

Not all Pi2 pulsations observed in space are strongly compressional. Kim et al. (2005a) reported that magnetic field Pi2 pulsation observed in the plasmasphere by the Polar spacecraft was transverse (see also Osaki et al. 1998). A PCR mode would have produced a compressional oscillation. Although it is possible that these observations are indeed the manifestation of a mechanism different from the PCR model (e.g., time modulated BBFs), it is also possible to explain them by some properties of the PCR model. Regarding the transverse polarization, one could argue that the Polar spacecraft did not detect compressional oscillations because it was located ∼30° away from the magnetic equator. Lee (1996) showed that fast mode waves in the dipole magnetosphere tend to be localized to the equatorial region owing to the variation of Alfvén velocity along the field line. An equatorially confined PCR can couple to Alfvén waves (see Sect. 4) and produce substantial transverse magnetic field oscillations if the mode structure is symmetric about the magnetic equator as illustrated in Fig. 15.

Radial Mode Structure

Early studies inferred the Pi2 radial mode structure using latitudinal arrays of ground magnetometers. Observations on the nightside revealed that Pi2 oscillations are highly coherent below $L \sim 4$, although oscillations with the same frequency can be detected at higher latitudes (Björnsson et al. 1971; Yeoman and Orr 1989; Osaki et al. 1996; Shinohara et al. 1997; Li et al. 1998). Some of these observations (e.g., Björnsson et al. 1971; Yeoman and Orr 1989) also found amplitude and phase structure of the H component that can be attributed to a PCR.

Figure 17 shows an example of the latitudinal structure of a Pi2 pulsation taken from Björnsson et al. (1971), which have been confirmed in later studies (e.g., Lester and Orr 1983; Yeoman and Orr 1989). In the H-component time series plots, ordered by magnetic latitude (Fig. 17a), the amplitude tends to increase with latitude. Interestingly though, a closer inspection reveals that the amplitude became smaller from WN to ENK before becoming larger from HMA to ASE. Equally interesting is the switch of the sign of the perturbation (180° phase shift) occurring between ENK and HAM. The amplitude and phase for this event are plotted in Fig. 17b as a function of magnetic latitude (open circles). Notice that the magnetometers were densely distributed so that one can be sure that the phase shift occurred at the location (magnetic latitude ∼61°, $L \sim 4.3$) of the amplitude minimum (i.e., the node of H). This latitudinal structure differs from that of field line resonance (Chen and Hasegawa 1974a; Southwood 1974), which predicts an amplitude peak accompanied by a 180° phase shift. Field line resonance effect has been observed both on the dayside (e.g., Samson et al. 1971) for Pc4-5 pulsations and on the nightside (Keiling et al. 2001) for Pi2 pulsations (see Sect. 4.1). Confirming a much earlier study (Jacobs and Sinno 1960) an amplitude maximum occurred somewhere between 50° ($L = 2.4$) and 60° ($L = 4.0$), a latitude lower than the H-component minimum. This amplitude maximum was not accompanied by a 180° phase shift either. These observations led Yeoman and Orr (1989) to propose the PCR model as the generation mechanism of Pi2 pulsations observed below $L \sim 4$.

One needs to take a statistical approach to the Pi2 mode structure when using satellite data, since it is impossible to have numerous spacecraft distributed along L for a given Pi2

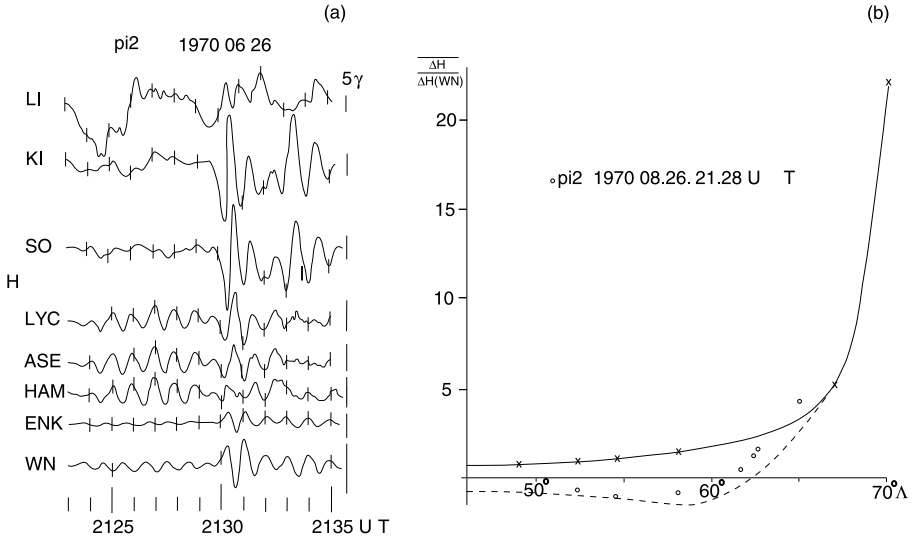

Fig. 17 (From Björnsson et al. 1971) A Pi2 pulsation observed with a ground magnetometer array. (**a**) H-component time series. (**b**) The *open circles* show the amplitude for the event shown in (**a**) as a function of magnetic latitude. The amplitude is normalized to that at Wingst (WN) and its sign is positive if in phase with high-latitude oscillation, negative if ∼180° out of phase. The *solid curve* is statistically obtained amplitude with no phase information. The *dashed curve* is statistically obtained amplitude with the phase information included as with the *open circles*

event. In early studies that employed this approach, Takahashi et al. (1992, 1995) examined magnetic field data from the AMPTE/CCE spacecraft and inferred that a node of the B_z component existed near $L = 4$. They also noted that the B_x-B_z cross phase showed an L and magnetic latitude dependence that is predicted in Fig. 15c. Due to lack of plasma density measurements, however, the CCE studies were unable to discuss the radial mode structure in reference to the plasmapause location. A more complete statistical construction of the radial mode structure and its relation to the plasmapause was possible with more recent spacecraft such as CRRES and Polar. The CRRES results will be described in Sect. 2.2 in relation to the PVR model.

Longitudinal Structure

Cavity modes having an m value on the order of one should be observed at all local times. However, spacecraft observations of Pi2 pulsations in the dayside magnetosphere is challenging because they are easily masked by Pc4 pulsations driven by the solar wind pressure variations (Takahashi et al. 2005) or by transmission of upstream waves into the magnetosphere (Heilig et al. 2007). Only on rare occasions dayside Pi2 pulsations have been reported from spacecraft observations in the magnetosphere: at $L \sim 6$ in the equatorial magnetosphere (Nosé et al. 2003) and at a LEO satellite (Han et al. 2004). In a systematic survey of AMPTE/CCE magnetic field data or CRRES electric field data Takahashi et al. (1995, 2003a) were unable to find Pi2 pulsations in the dayside equatorial magnetosphere at $2 < L < 6$ except for a few events near dawn.

The Nosé et al. (2003) event was detected with the ETS-VI satellite when it was at $L \sim 6.3$ near ∼0700 MLT. The electron number density measured at the EXOS-D (Akebono) satellite on essentially the same meridian indicated the plasmapause at $L = 6.8$. The

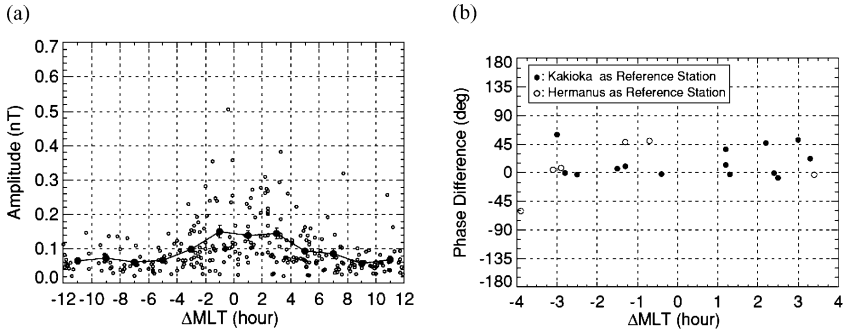

Fig. 18 (From Nosé et al. 2006) Longitudinal properties of low-latitude Pi2 pulsations. (**a**) Local time dependence of Pi2 amplitude in the H-component at Kakioka ($L \sim 1.3$) (**b**) Phase delay between Kakioka and Hermanus ($L \sim 1.5$), which are longitudinally separated by ∼120°

Pi2 pulsation had strong poloidal components B_x and B_z, which oscillated ∼180° out of phase. The B_z component was in phase with the ground H component at low latitude. These properties are the same as those of the nightside Pi2 pulsation (e.g., Takahashi et al. 1995) and support the PCR model.

If Pi2 pulsations propagate to the dayside as a cavity mode, there is no reason that a cavity mode excited on the dayside cannot propagated to the nightside. In fact, there is observational evidence for a dayside plasmaspheric cavity mode (Takahashi et al. 2009) and its propagation to the night side (Takahashi et al. 2005). Studies of such events could shed light on the role the plasmasphere commonly plays in trapping fast mode waves.

On the ground, dayside Pi2 pulsations are abundant, although their detection is usually limited to $L < 2$, a region sparsely covered by spacecraft except for those in LEO orbits. Specific Pi2 properties consistent with the PCR model include the day-night matching of waveform and the small phase shift over a large longitudinal distance. Early reports of dayside Pi2 pulsations include those by Yanagihara and Shimizu (1966) and Stuart and Barsczus (1980). Sutcliffe and Yumoto (1991) proposed that the PCR is the reason for such a global property of low-latitude Pi2 pulsations.

In an comprehensive study in which a sudden increase in the brightness of Polar UVI images was used as a requirement in selecting Pi2 events, Nosé et al. (2006) confirmed that Pi2 pulsations at $L \sim 1.3$ are detected at all local times. As shown in Fig. 18a the amplitude of these events were higher on the nightside than on the dayside by a factor of ∼2, which is certainly not what one expects for longitudinally uniform PCR modes. However, the symmetry can be explained by localization of the Pi2 energy source on the nightside (Pekrides et al. 1997; Fujita et al. 2002; Lee and Takahashi 2006). The high timing accuracy at both stations used (Kakioka and Hermanus) allowed Nosé et al. (2006) to determine the phase delay between the two stations and the corresponding m number. The phase difference was in general small (<60°) and about a half of the events had a phase delay very close to zero, or $m \sim 0$, (Fig. 18b), confirming earlier observations by Kitamura et al. (1988). Other studies using longitudinally separated stations reported $m < 3$ (e.g., Li et al. 1998). With such a small m-number, the PCR model is certainly a better model than the plasmapause surface mode model (Sect. 2.3).

2.2 Plasmaspheric Virtual Resonance

2.2.1 Model

The idealized PCR model assumes perfect reflection of fast waves at the inner and outer boundaries of the plasmasphere. Whereas it is more easily envisioned that the ionosphere is a (near) perfect reflector under certain conditions, there is no a priori reason, why the plasmasphere should behave as a perfect reflector. Consequently, the effectiveness of plasmasphere in trapping fast mode waves needs to be examined numerically without imposing specific boundary condition at the plasmapause. Such simulations have been conducted and they confirmed that plasmaspheric compressional eigenmodes are indeed excited under a variety of assumptions on the plasmapause density gradient, boundary condition on the magnetopause and at the ionosphere, and the degree of energy loss by fast mode propagation into the tail (Allan et al. 1986b; Zhu and Kivelson 1989; Lee 1996; Pekrides et al. 1997; Itonaga et al. 1997a; Lee and Lysak 1999; Fujita et al. 2000, 2001, 2002; Fujita and Itonaga 2003; Lee and Takahashi 2006). Lee and coworkers pointed out that, analogous to quantum physics, the plasmaspheric compressional eigenmodes are classified as a virtual resonance rather than as an idealized cavity mode resonance (Lee 1998; Lee and Kim 1999; Lee and Lysak 1999). The PVR mode has its energy mostly confined in the plasmasphere but has finite energy beyond the plasmapause.

The radial profile of PVR, obtained in a dipole simulation (Lee and Lysak 1999) and evaluated slightly above the magnetic equator is shown in Fig. 19. The features that differ from the PCR model are: (a) oscillations of E_y and B_z extend beyond the plasmapause (L_{pp}); (b) a node (labeled L_n) of B_z and the corresponding antinode of E_y are located just inward of the plasmapause; and (c) the phase difference between E_y and B_z is still $\sim$90° outside the plasmasphere, which means that the fast mode is still trapped there. Note that the concept of a simple PCR is valid in qualitatively organizing the observations within the plasmasphere as far as the radial mode structure and the mode frequency are concerned.

Simulation studies have addressed the local time dependence of PVR (Pekrides et al. 1997; Fujita et al. 2002; Lee and Takahashi 2006). Figure 20 shows an example that incorporated day-night asymmetry (Fujita et al. 2002). In this simulation the magnetosphere had a dipole magnetic field and the plasmapause was located midway ($L \sim 5.6$) between the inner and outer boundaries of the simulation domain, the ionosphere had finite Pedersen conductivity, the outer boundary allowed escape of fast mode waves, and the energy source was an impulse representing the cross-tail portion of the SCW with a local time extent of $\pm$2 hours around midnight. The initial impulse applied on the nightside boundary propagates inward, and once it reaches the inner boundary a global coherent oscillation is established (Fig. 20a). The electric field time series shows much larger amplitude on the night side compared to the dayside.

Another aspect of Pi2 pulsation that simulation studies addressed is the local time dependence of the orientation of the major axis of polarization ellipse reported from ground observation. At middle latitude ($L \sim 3$) the axis is directed northeast before midnight and northwest after midnight (e.g., Baranskiy et al. 1970; Lester et al. 1983; Singer et al. 1985). Lester et al. (1983) explained the polarization by oscillatory currents superposed on the three-dimensional SCW. Simulation shows that the polarization pattern can alternatively be explained in terms of MHD wave propagation in the inhomogeneous magnetosphere (Pekrides et al. 1997; Fujita et al. 2002). Pekrides et al. (1997) investigated the local time dependence of the polarization axis by adopting a longitudinally localized impulse to stimulate pulsations in a hemicylindrical magnetosphere with a plasmasphere

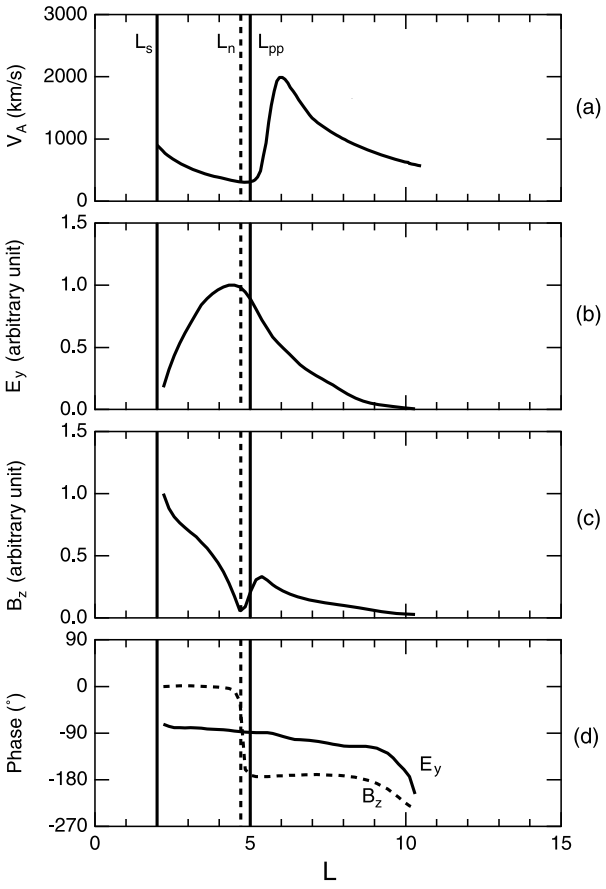

Fig. 19 (From Takahashi et al. 2003a) Radial structure of the fundamental virtual resonance obtained in a dipole MHD simulation. The field perturbations are evaluated near the equator. (**a**) Alfvén velocity at the equator used in the simulation. (**b**) Electric field amplitude E_y. (**c**) Magnetic field amplitude B_z. (**d**) The E_y-B_z cross phase

imbedded. Plots of the polarization axis as a function of local time (Fig. 21) demonstrates that the axis orientation near the plasmapause exhibit a strong local time dependence that is qualitatively the same as the observations. This phenomenon has been attributed to strong poloidal-toroidal mode coupling near the plasmapause. Below the plasmapause the axis lies in the north-south direction, indicating the dominance of (trapped) poloidal mode.

2.2.2 Observations

Spacecraft Observations Near the Magnetic Equator

In situ measurements of the electric and magnetic fields of Pi2 pulsations along with the background plasma density is a viable method to test the PVR model. Note that the mass density remote sensing technique using ground magnetometer arrays (Waters et al. 1991) does not work on the nightside due to lack of toroidal wave activity. In-situ density measurements by satellites or global imaging of the plasmasphere (Sandel et al. 2003) is essential in establishing the background plasma structure. We commented in Sect. 2.1 on results of satellite magnetic field analysis that did not make specific reference to the plasmapause.

Figure 22 shows the radial profile of Pi2 pulsations constructed by plotting individual measurements (dots) made on CRRES as a function of the satellite distance relative to the

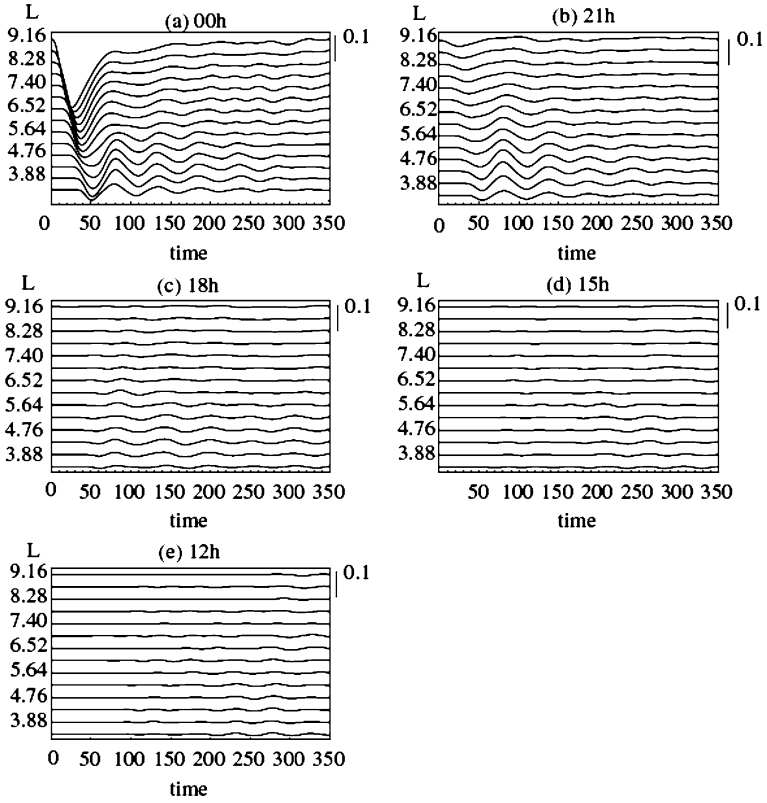

Fig. 20 (From Fujita et al. 2002) Time series plots of the azimuthal component of the equatorial electric field, corresponding to the poloidal mode, at five local times obtained in a simulation study of plasmaspheric virtual resonance

plasmapause (Takahashi et al. 2003a). The azimuthal electric field (E_y) power normalized to ground H power (Fig. 22a) shows that the electric field oscillation is spread over the plasmasphere with an indication of a mild peak inward of the plasmapause, just as illustrated in Fig. 19b. The field components E_y and B_z oscillate $\sim\pm 90°$ out of phase, a property of radially standing MHD wave. A similar phase delay occurred in two successive Pi2 pulsations observed by the Polar satellite as it moved from $L = 4.1$ to 3.7 and MLAT $= 14°$ to 10° (Keiling et al. 2001). Although the plasmapause location was not determined on the Polar orbit, it was considered likely that the satellite was outside the plasmasphere, based on the high geomagnetic activity ($K_p > 5$) and the plasma density inferred from a particle experiment covering the 12 eV–18 keV energy range.

Spacecraft Observations in the Polar Cap

A rather surprising recent discovery on low-latitude Pi2 pulsations, which is well beyond the prediction of the PCR model but is consistent with the PVR model, is their extension to the plasma sheet and polar cap as observed by the Polar (Keiling et al. 2001; Kim et al. 2005c) and DE-1 (Teramoto et al. 2008) satellites. As before, these studies selected events on the basis of high satellite-ground coherence to ensure that the satellites detected the same wave mode that produced low-latitude Pi2. The sample waveform plot in

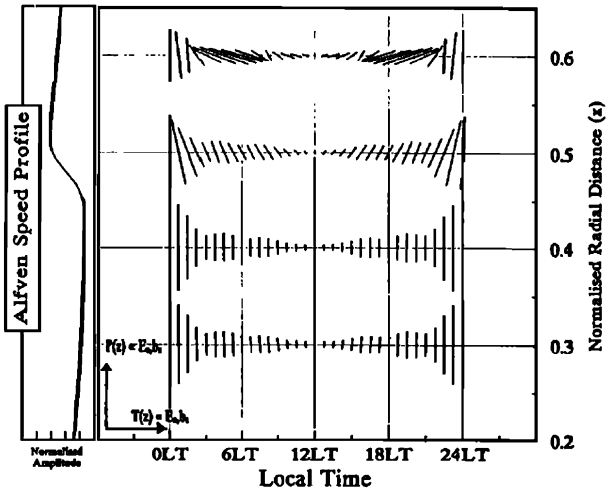

Fig. 21 (From Pekrides et al. 1997) Major axis of polarization of simulated Pi2 pulsation as a function of local time plotted at selected latitudes. The length of the line is proportional to the amplitude. The Alfvén speed profile is also shown on the left

Fig. 23a provides compelling evidence that the same oscillation was detected on the ground ($L \sim 1.3$) and in the polar cap, in this case at a geocentric distance of ~4.5 R_E and at a magnetic latitude of 85°. The B_z component was the most dominant in space but its amplitude (~0.1 nT) was much smaller than on the ground (~1 nT). A statistical summary of the Polar observations at lower magnetic latitudes (~20° to ~60°) shows (Fig. 23b) that the Pi2 pulsation appeared in the plasma sheet or in the tail lobe and had the following characteristics: The B_z/H amplitude ratio was of the order of 0.1 and decreased with outward distance from the plasmapause (top panel); and the B_z-to-H cross phase was close to 180° (middle panel). These observations fit the numerical PVR model illustrated in Fig. 19.

2.3 Plasmapause Surface Mode

2.3.1 Model

The MHD wave equation applied to a thin transition region in Alfvén velocity yields a solution termed surface eigenmode (Chen and Hasegawa 1974b). The plasmapause is a primary candidate to sustain such mode and the plasmapause surface mode (PSM) has been suggested to be a source mechanism for Pi2 pulsations in the inner magnetosphere. Similar to the PCR and PVR modes, the surface mode can be excited by impulsive disturbances applied to the plasmasphere, such as current disruption and braking of impulsive BBF in the near-Earth magnetotail.

If we label the magnetic field intensity B and the mass density across a plasmapause by the subscripts 1 (plasmasphere side) and 2 (plasmatrough side), the period of the surface mode, T_{PSM}, is gives as

$$T_{PSM} = \left(\frac{k_z^2(B_1^2 + B_2^2)}{\mu_0(\rho_1 + \rho_2)}\right)^{-1/2} \sim \left(\frac{2k_z^2 B_1^2}{\mu_0 \rho_1}\right)^{-1/2} = T_{A1}/\sqrt{2} \tag{2}$$

where k_z is the wave number parallel to the ambient magnetic field and takes discrete values because of the boundary condition at the ionosphere (Yeoman and Orr 1989). The final expression is obtained assuming $B_1 \sim B_2$ (magnetic field is continuous across the plasmapause) and $\rho_1 \gg \rho_2$ (plasma density is much higher in the plasmasphere than in the plasmatrough) and the field line eigenfrequency at the inner edge of the plasmapause (we assume a

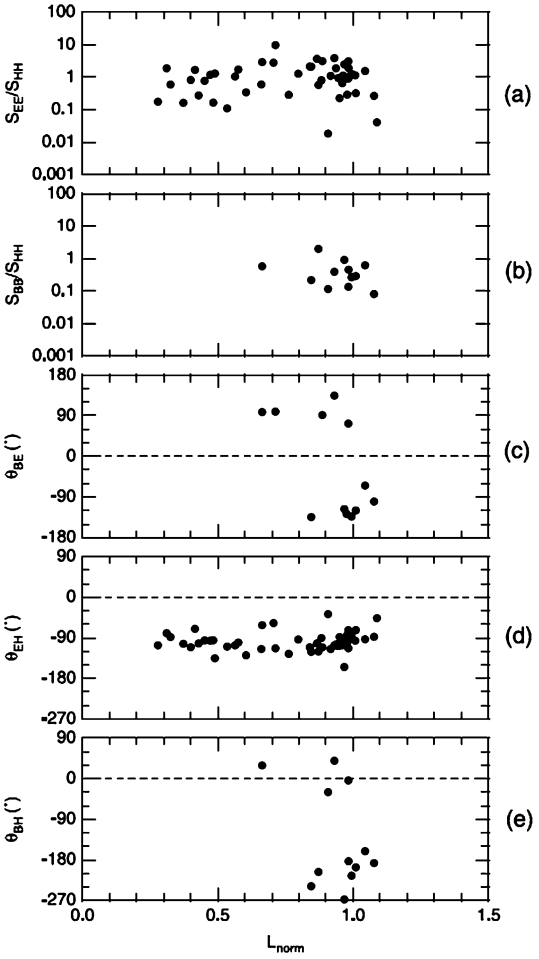

Fig. 22 (From Takahashi et al. 2003a) Spectral parameters of Pi2 pulsations observed by CRRES and plotted as a function of distance normalized to the distance of the plasmapause that was encountered on the orbit associated with each Pi2. All spectral parameters were evaluated at the frequency of the Pi2 pulsations. (**a**) Power density in the E_y component (S_{EE}) divided by the power density in the H component at Kakioka (S_{HH}). (**b**) Same as (**a**) except for S_{BB} (power density of B_z). (**c**) E_y-B_z cross phase. (**d**) E_y-H cross phase. (**e**) B_z-H cross phase

fundamental mode), T_{A1}, is given by

$$T_{\mathrm{A1}} \approx 2 \int_{\mathrm{South}}^{\mathrm{North}} ds / V_{\mathrm{A}} \tag{3}$$

where the integral is taken along the magnetic field line from the southern ionospheric footprint to the northern footprint at the inner edge of the plasmapause. For a large azimuthal wave number the field line motion is meridional and T_{A1} corresponds to the fundamental guided poloidal mode (Radoski 1967).

In analytical theory the surface wave solution is obtained by assuming a large azimuthal wave number (compared to the wave number along the field line) (Chen and Hasegawa 1974a). With large m, the mode resembles the guided poloidal mode (solution for $m = \infty$, see Sect. 2.3), so it is possible to have different frequencies at longitudes separated by many wave numbers.

The most distinctive observable feature of PSM would be the amplitude variation with distance from the plasmapause. The amplitude is peaked at the plasmapause and decreases exponentially with distance from the plasmapause. Therefore, if there is a means to deter-

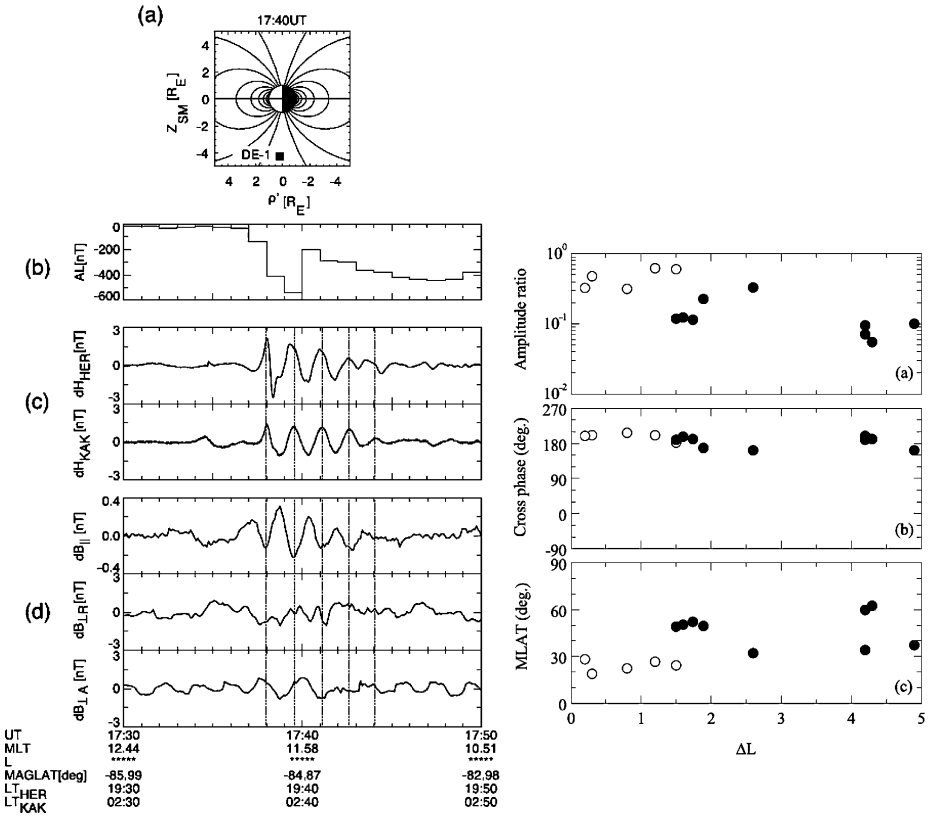

Fig. 23 (*Left*) Comparison of magnetic field data from Kakioka and DE-1 (polar cap) for a Pi2 event (Teramoto et al. 2008). Projection of the satellite position and dipole field lines on the noon-midnight meridian is shown at the top. (*Right*) Summary of Polar-Kakioka high-coherence Pi2 events (Kim et al. 2005c). The *open* and *filled circles* indicate Polar observations in the plasma sheet and the tail lobe, respectively. (*Top*) B_z (*Polar*) to H (Kakioka) amplitude ratio; (*middle*) B_z-H cross phase; and (*bottom*) magnetic latitude as a function of ΔL, the distance from the plasmapause

mine the location of the plasmapause, it should be straightforward to find PSM using ground magnetometer arrays or elliptically orbiting satellites. A well observed feature in ground magnetometer data is the appearance of a second amplitude maximum at latitudes below the larger auroral Pi2 maximum. This secondary maximum has been much debated in the literature, and the plasmapause surface wave has been considered one candidate (Sutcliffe 1975) for its generation in addition to a cavity mode (e.g., Yeoman and Orr 1989) and FLR (e.g., Fukunishi 1975).

2.3.2 *Observations*

The observed global extent (both in longitude and in L) and small m-values of Pi2 pulsations in the plasma make PSM generally an unsuitable mechanism for low-latitude ($L < 2$) Pi2. Arguments for PSM should be valid only for pulsations at middle latitude ($L \sim 4$) that have a maximum power in the close vicinity of the plasmapause. In support of the PSM model, Lester and Orr (1983) reported such pulsation events using magnetometer data from ground

magnetometer arrays and electron density data from the GEOS-1 satellite. However, the PSM is not the only model that can explain the latitudinally localized pulsations. As we will discuss in Sect. 4, coupling of a PCR/PVR mode with standing Alfvén waves (field line resonance) near the plasmapause offers an alternative explanation.

Other studies used (2) as the basis to support the PSM model. Sutcliffe (1975) confirmed early studies (e.g., Rostoker 1967) of the positive correlation between the Pi2 frequency and geomagnetic activity level (i.e., K_p) and suggested that larger plasmasphere (thus longer field line length along the plasmapause) leads to lower Pi2 frequency. Unfortunately, it may be difficult to distinguish compressional eigenmodes (PCR/PVR) from the surface mode solely based on the statistical behavior of Pi2 frequency. The reason is that both the PCR period (1) and the PSM period (2) depend on the plasmapause size (field line length for (3) is proportional to the plasmapause distance), that is, the period is longer for larger plasmasphere. Accordingly, a negative correlation between Pi2 period and geomagnetic activity level is not a unique feature of PSM.

In related studies, Kosaka et al. (2002) and Han et al. (2003) used five longitudinally distributed, low-latitude magnetometers ($L = 1.2$–1.6) to show that the frequency of individual Pi2 pulsations can vary with local time. These authors considered the PSM as a possible mechanism for the longitudinal variation, but the local time dependence could also be explained within the concept of the PCR/PVR (Fujita and Itonaga 2003), as described in Sect. 2.1.

2.4 Summary

We have defined the inner magnetosphere as a region where ULF wave physics is governed by cold plasma MHD without an energy source for Pi2 pulsations. This makes it much easier to build theoretical models of Pi2 pulsations in the inner magnetosphere than in the outer magnetosphere where both the Pi2 source and the Pi2 energy source reside (see Sect. 1.1 on how we defined Pi2 source and Pi2 energy source). In principle, we should be able to understand the spatial and temporal structures of the inner magnetosphere Pi2, if we can prescribe the behavior of the pulsations on the boundaries: the plasma sheet inner edge, the ionosphere, and the magnetopause.

Much progress has been made on inner magnetosphere Pi2 pulsations in the past decade, owing to coordinated observations from the ground and space as well as numerical simulations. Major areas of interest included: the role of the plasmasphere in trapping compressional (fast mode) waves; longitudinal structure; coupling of compressional waves to shear Alfvén waves; and ionospheric effects (the last two will be summarized in Sect. 4). Numerical simulation proved to be a powerful tool in modeling wave trapping in the plasmasphere. Virtually all simulations show that cavity mode (or virtual resonance) is excited if the outer boundary of the simulated domain, usually some distances outward of the plasmasphere, is subjected to an impulsive disturbance. Simulated Pi2 properties that are confirmed by satellite observations include dominance of the poloidal components E_y and B_z, radial amplitude and phase structure of these field components, and the frequencies of the harmonics.

Properties of compressional waves that are beyond a simple cavity mode are also found in the simulations. One important realization is that the plasmaspheric mode is not strictly confined in the plasmasphere and thus can be detected outside the plasmapause. This feature, which is not predicted from the idealized cavity mode, has given an adequate explanation to the surprising observation of Pi2 pulsations in the polar cap that are identical to low-latitude Pi2 pulsations. In addition, simulations that included a realistic azimuthal structure of the excitation region (the SCW), plasma mass density (plasmasphere dusk bulge), and energy

loss rate were able to explain local time dependence of Pi2 amplitude, frequency (alternatively attributed to plasmaspheric surface mode) and polarization (alternatively attributed to the oscillating SCW).

The response of the inner magnetosphere to periodic external disturbances (e.g., BBFs; see Sect. 3) remains to be understood. Numerical simulations have not incorporated such a scenario, although it will be a fairly straightforward implementation to make (see Lee and Lysak 1991). Periodic driving and cavity mode resonance are not mutually exclusive processes. If the applied disturbance is impulsive (broadband spectrum), the plasmasphere will respond by establishing eigen-oscillations at discrete frequencies. If the applied disturbance is monochromatic (narrowband), the plasmasphere will amplify the input wave only when the resonance frequency matches the driving frequency. Ideally, observational determination of the frequency dependence of the plasmasphere gain factor (amplitude of plasmaspheric wave/amplitude of the driving wave) will resolve the issue.

The third inner-magnetospheric Pi2 model reviewed here is the least likely to occur. Evidence of surface waves has been searched for in numerically simulated Pi2 pulsations. Simulations that assumed a realistic V_A profile across the plasmapause and a realistic azimuthal wave number ($m < 10$) found no evidence of wave modes localized to the plasmapause (Allan et al. 1986b; Zhu and Kivelson 1989; Lee 1996). It thus appears that a surface wave Pi2 is possible only when the m number is unusually large or the plasmapause is unusually thin. There is also some spacecraft evidence that the secondary amplitude maximum is not caused by these surface waves but rather by FLR (see Sect. 4).

3 Outer-Magnetospheric Models

In the previous section we reviewed models in which the Pi2 frequency first appeared in the inner magnetosphere. In this section, we review models with an outer-magnetospheric frequency source (Pi2 source). Here the outer magnetosphere is defined as the plasma sheet (central plasma sheet and plasma sheet boundary layer), the tail reconnection region, and the tail lobes. The plasma sheet is an active region where hot ($T > 1$ keV) plasma contributes to energy conversion/release processes related to phenomena that map to the auroral zone in addition to MHD waves, which are the dominant mechanism in the inner magnetosphere. Plasma density and plasma energy are significantly lower in the lobe than in the plasma sheet. The lobes are generally considered to be passive regions during convective particle transport from the solar wind, through the magnetopause and into the plasma sheet. Plasma sheet disturbances, such as reconnection and fast plasma flows, affect the lobes' dynamics via the transfer of ULF wave energy.

The block diagram in Fig. 24 illustrates possible Pi2 sources in the outer magnetosphere and associated propagation paths. The two models illustrated on the left have their source regions in the nightside somewhere in the range from $\sim$9 to $\sim$13 R_E geocentric distance (although deviations of this range are possible), i.e., in the presumed current disruption region where the SCW is initiated. The most-widely accepted outer-magnetospheric model (first branch on the left) is the transient response (TR) model of substorm-related Pi2 pulsations. In this model, the initial Alfvén wave that carries the transient field-aligned current of the SCW is partially reflected from the upper ionosphere followed by several bounces between opposite ionospheres. This bouncing creates a Pi2 signal at high latitudes (auroral zone) on the ground. An alternative scenario (second branch) for high-latitude, auroral zone Pi2 pulsations is based on plasma instabilities in the near-Earth plasma sheet. It has been suggested that propagating and non-propagating periodic oscillations of ballooning modes can generate ground Pi2 pulsations.

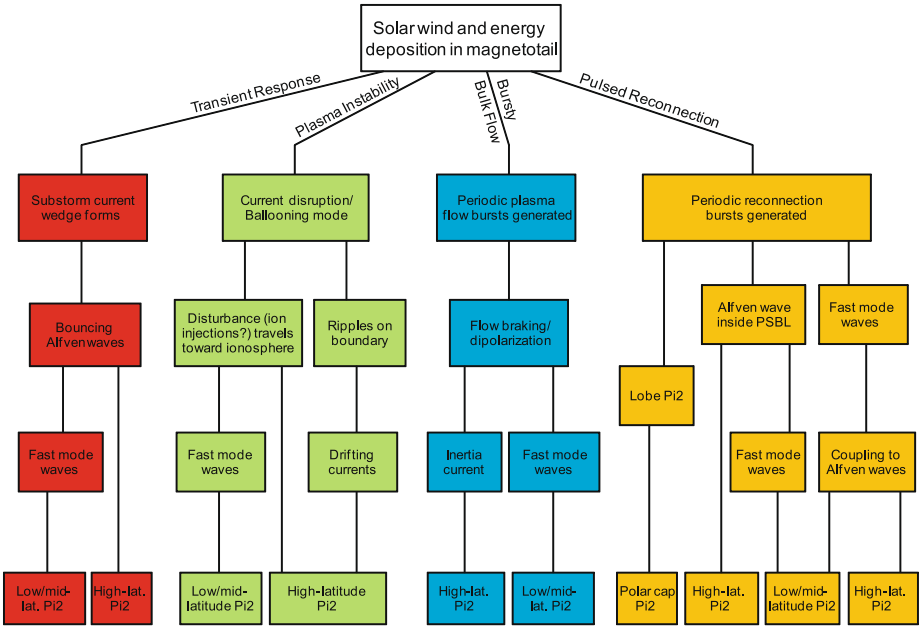

Fig. 24 Block diagram illustrating possible Pi2 sources in the outer magnetosphere and associated propagation paths to the ground

In the last decade ground Pi2 pulsations have been associated with periodic signals in the outer magnetosphere at distances ($>15\ R_E$) beyond the location where the SCW is initiated. Since the Pi2 signals propagated Earthward, the source region was inferred to be the midtail to distant tail. Different observations have resulted in two models, illustrated in the last two branches of Fig. 24. In one model (third branch) the braking of modulated, Earthward-propagating plasma flows in the near-Earth plasma sheet launch periodic compressional waves and inertia currents that eventually reach the ionosphere, causing ground Pi2. Importantly, in this scenario the flow properties determine the properties of the associated ground Pi2. In the other model (fourth branch), the Pi2 source is located at the reconnection site. Initially, correlations of traveling compression regions (TCRs) in the tail lobes with ground Pi2 pulsations suggested pulsed reconnection events that directly control the Pi2 frequency observed on the ground. Additional observations have led to several scenarios for the coupling of the Pi2 signal from the reconnection site to the ground.

It is important to note that although the Pi2 sources of outer-magnetospheric models lie on high-latitude, auroral zone magnetic field lines (approximately $L > 6$), they have been employed to explain ground Pi2 pulsations located not only on high latitudes but also on middle and low latitudes, which can be explained by the propagation properties of the magnetospheric Pi2 signals. Several outer-magnetospheric models have also been associated with low-latitude Pi2 pulsations on the dayside. A non-MHD process might contribute to this propagation path. In this process Pi2 electric field disturbances applied to the high-latitude (auroral) region on the nightside propagate to the dayside through the ionosphere-ground waveguide and drive ionospheric currents in the equatorial region. These oscillating currents then produce measurable magnetic field oscillations on the ground. This propagation path is further reviewed in Sect. 4.

For many decades, the TR model had been the only successful outer-magnetospheric model. The reason for the emergence of new outer-magnetospheric Pi2 models in the last decade is two-fold. First, they provide alternative explanations for Pi2 pulsations typically attributed to inner-magnetospheric models, and second, they provide explanations for some ground Pi2 pulsations that are neither explained by inner-magnetospheric models nor by the TR model (for example, PBI-related Pi2 pulsations and some lobe Pi2 pulsations). With the exception of the TR model, there are not yet as many observational studies for outer-magnetospheric Pi2 models as there are for inner-magnetospheric models. Because the Pi2 signals have to travel greater distances from the source and travel through additional plasma regimes before they reach ground than Pi2 pulsations generated in the inner magnetosphere, there are more potential propagation paths available. Providing observational evidence requires simultaneous measurements from several spacecraft along the propagation paths; however, the limited number of spacecraft in the magnetotail makes it difficult to identify definite paths, and it remains a major area for improvement. Nevertheless, it is the outer-magnetospheric models that have brought the largest advances in Pi2 research in the last decade.

The remainder of this section reviews the basic theoretical concepts and the observational and numerical evidence of the outer-magnetospheric models.

3.1 Transient Response

3.1.1 Model

The magnetotail periodically undergoes reconfigurations (e.g., Hones 1979). One of its most dramatic changes, the dipolarization from its stretched configuration, is associated with the development of the SCW (Clauer and McPherron 1974), which electrically connects the near-Earth plasma sheet with the ionosphere (Fig. 25). The formation of this current system starts out as a transient Alfvén wave that propagates toward the ionosphere (e.g., Baumjohann and Glassmeier 1984). A mismatch of conductance between Alfvén wave and ionosphere leads to partial reflection of the Alfvén wave (e.g., Mallinckrodt and Carlson 1978). Assuming a continued supply of current, the main current then carries a tailward-traveling Alfvén wave. Trapped between northern and southern ionospheres, the wave bounces back and forth until a quasi-steady, field-aligned current system is established. This bouncing Alfvén wave causes the ground Pi2 pulsations. Therefore, the Pi2 period in this so-called transient response (TR) model is the result of the Alfvén wave travel time along the entire length of the field line and back:

$$T_{\mathrm{TR}} \approx 4 \int_{ion}^{eq} dl_{\parallel} / V_{\mathrm{A}}(l_{\parallel}) \tag{4}$$

where V_{A} is the Alfvén velocity and the integration is along the magnetic field line from the ionosphere to the current generator region in the equatorial plasma sheet. With a travel time of 30–40 s from the near-Earth plasma sheet to the ionosphere, we obtain periods of 120–160 s, which cover the upper range of the Pi2 band (40–150 s).

The wave dissipation that causes the short duration of the Pi2 pulsations has three possible contributions. In most cases wave reflection from the ionosphere is only partial, and the part that penetrates the ionosphere is dissipated via Joule heating (e.g., Osaki et al. 1998). Even before the Alfvén wave reaches the ionosphere, part of its electromagnetic energy can be converted into kinetic particle energy. For example, at substorm onset the optical intensification of the aurora is caused by electrons that have been energized by kinetic Alfvén waves

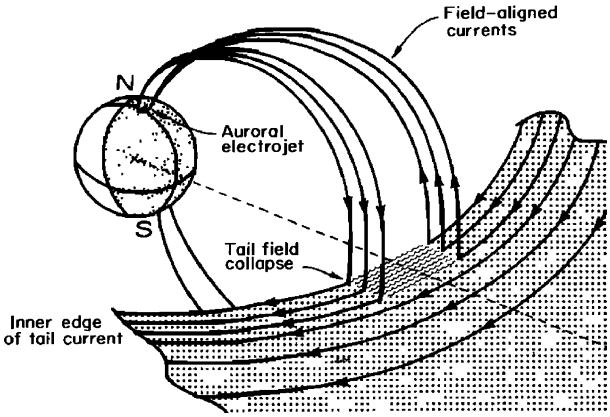

Fig. 25 (From Clauer and McPherron 1974) Schematic illustration of a substorm current wedge

(KAW) of the SCW (Mende et al. 2003). It has been argued that the KAWs, having small perpendicular scales, are generated by larger-scale shear Alfvén waves via phase mixing at density gradients and other mechanisms (Seyler 1990; Genot et al. 2004; Streltsov and Lotko 2004; Singh et al. 2007; Wright and Allan 2008). Furthermore, since the current-carrying Alfvén waves of the SCW are azimuthally localized, they couple to fast mode waves that radiate energy away (Southwood and Hughes 1983).

The mechanism of Alfvén wave initiation, which occurs somewhere between 9 and 13 R_E, is not specified in the TR model. Several mechanisms such as plasma flow braking/diversion and magnetic pileup (Shiokawa et al. 1997; Birn et al. 1999), cross-field current instability (Lui et al. 1991; Lui 1996), and ballooning instabilities of various types (e.g., Voronkov et al. 1997; Bhattacharjee et al. 1998) have been proposed. If we take the different trigger mechanisms into account, the TR model stands for a class of Pi2 scenarios (Webster et al. 1989), each with the same underlying mechanism of creating the characteristic Pi2 frequency, namely Alfvén wave bouncing. We note that the same trigger mechanisms have also been invoked for Pi2 pulsations associated with cavity-type Pi2 models (PCR/PVR), by launching transient fast mode waves into the inner magnetosphere (see Sects. 2.1 and 2.2).

The TR model applies to Pi2 pulsations that occur during substorms and subsequent auroral intensifications, which follows from results that show a relationship between the westward traveling surge (WTS) and Pi2 pulsations during substorm onsets (e.g., Rostoker and Samson 1981; Pashin et al. 1982; Singer et al. 1983; Lester et al. 1984). However, the onset of any field-aligned current that connects to the ionosphere could lead to bouncing Alfvén waves under appropriate ionospheric conditions and could thus cause ground Pi2 pulsations in accordance with the TR model. Hence, the TR mechanism may also apply to Pi2 pulsations related to pseudo-breakups and sawtooth events (Sect. 1.2), because it is to be expected that field-aligned currents develop during these modes as well.

Based on the idea that bouncing Alfvén waves generate Pi2 pulsations, Pilipenko et al. (2005) proposed a scenario in which the onset of anomalous resistivity on auroral field lines leads to an Alfvénic pulse that bounces back and forth between the ionosphere and the anomalous resistive layer, generating ground Pi2. The ionospheric Alfvénic resonator (Polyakov and Rapoport 1981) is another example of transient, bouncing Alfvén waves, although the frequency in this case is not in the Pi2 range. Variations of the TR model based on Alfvén wave pulses (wavelets) that do not bounce but are individually launched and absorbed have been proposed (Samson et al. 1985; Webster et al. 1989; Solovyev et al. 2000). However, because the Pi2 frequency is not created by Alfvén wave bouncing—an

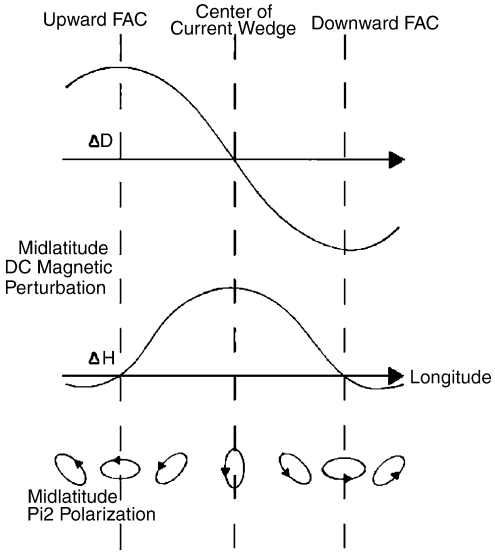

Fig. 26 (From Lester et al. 1984) (*Top*) Schematic representation of longitudinal variations in the magnetic H and D components resulting from the substorm current wedge. The *bottom panel* shows the predicted Pi2 azimuth pattern

essential component of the TR mechanism—but by some mechanism in the magnetotail that periodically launches the wavelets towards Earth, we put these scenarios into the categories of plasma-instability-driven or BBF-driven Pi2 models (as described in Sects. 3.2 and 3.3, respectively).

Uncertainties remain regarding the spatial extent of TR-Pi2 pulsations on the ground. The scenario of bouncing Alfvén waves applies only to high-latitude, auroral zone Pi2 pulsations; it does not describe how the Pi2 pulsations propagate from the source in the plasma sheet to lower latitudes (Yumoto et al. 1989). Nevertheless, it is widely believed that one type of mid-latitude, subauroral Pi2 pulsations is caused by the TR mechanism (Baumjohann and Glassmeier 1984), and in some event studies it has been suggested that even low-latitude Pi2 pulsations are caused by this mechanism (e.g., Li et al. 1998). Although coupling between Alfvén waves and compressional waves, which would be capable of crossing magnetic field lines to reach lower latitudes, is a popular coupling scenario, recent simulation results argue against such a coupling as the source of lower-latitude TR-Pi2 pulsations (Fujita et al. 2002). Therefore, it is an ongoing effort to investigate the propagation modes of the TR model.

3.1.2 Observations

Although ground-based evidence for the TR model is plentiful, space evidence is very limited. Since nearly three decades ago when Baumjohann and Glassmeier (1984) pointed out that surprisingly few reports using spacecraft data exist to show the TR mechanism in operation, the situation is essentially unchanged today. For the well documented ground-based evidence of the TR model, in particular for high-latitude Pi2 pulsations, we refer the reader to the reviews by Baumjohann and Glassmeier (1984) and Olson (1999). Essentially, no new ground-based results have been reported since then. Hence we focus on a spacecraft-based and numerical evaluation of the TR model, organized by the following topics: polarization, spectral content, substorm current wedge, and bouncing Alfvén waves.

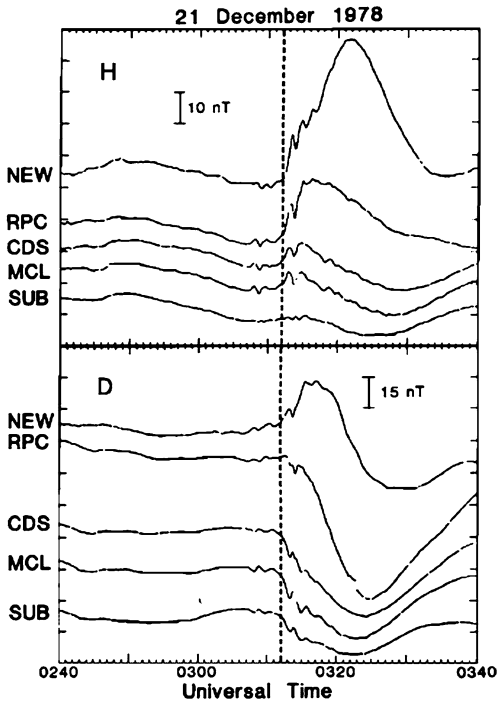

Fig. 27 (From Gelpi et al. 1987) (*Top*) Pi2 pulsations superposed on mid-latitude, positive H bays. (*Bottom*) Corresponding perturbations of the D component

Polarization

Characteristic polarization signatures of mid- and high-latitude ground Pi2s associated with the TR model are the following. A pair of FACs, being part of the SCW, manifests in longitudinal variations of the ground magnetic field components H and D (Fig. 26). At individual ground stations, the variations show as positive and negative H bays superposed by Pi2 pulsations. The Pi2 that rides positive (negative) H bays is typically referred to as mid-latitude (high-latitude) Pi2 (Fig. 27). The mid-latitude Pi2 has a smaller magnetic field amplitude than the high-latitude Pi2. The orientation of the polarization ellipse of mid-latitude Pi2 pulsations rotates (bottom of Fig. 26) in relation to the large-scale upward and downward FAC current system (Lester et al. 1983, 1984). Gelpi et al. (1987) recognized that the center of the longitudinal polarization pattern is in fact farther to the west (i.e., closer to the head of the WTS) than is indicated in Fig. 26. In contrast, the polarization pattern at high latitudes is more complicated. For example, Samson and Rostoker (1983) investigated the influence of the WTS on the polarization of ground Pi2 pulsations and identified distinct regions surrounding the WTS (see Fig. 10 of Sect. 1).

The rotation of polarization ellipses, typically observed at middle latitudes, has also been observed for Pi2 pulsations at low latitudes (Lanzerotti and Medford 1984; Li et al. 1998; Takahashi and Liou 2004), which suggests that low-latitude Pi2 pulsations might also be associated with the TR mechanism. However, contradictory reports, showing different patterns at low latitudes, were also reported (e.g., Sutcliffe 1981).

Although the polarization pattern is a cornerstone observation for the TR model, results from simulation studies question its applicability to mid-latitude Pi2 pulsations as a unique identifier. For example, MHD simulations employing an initially purely compressional, broadband signal in response to a sudden change in the near-Earth plasma sheet,

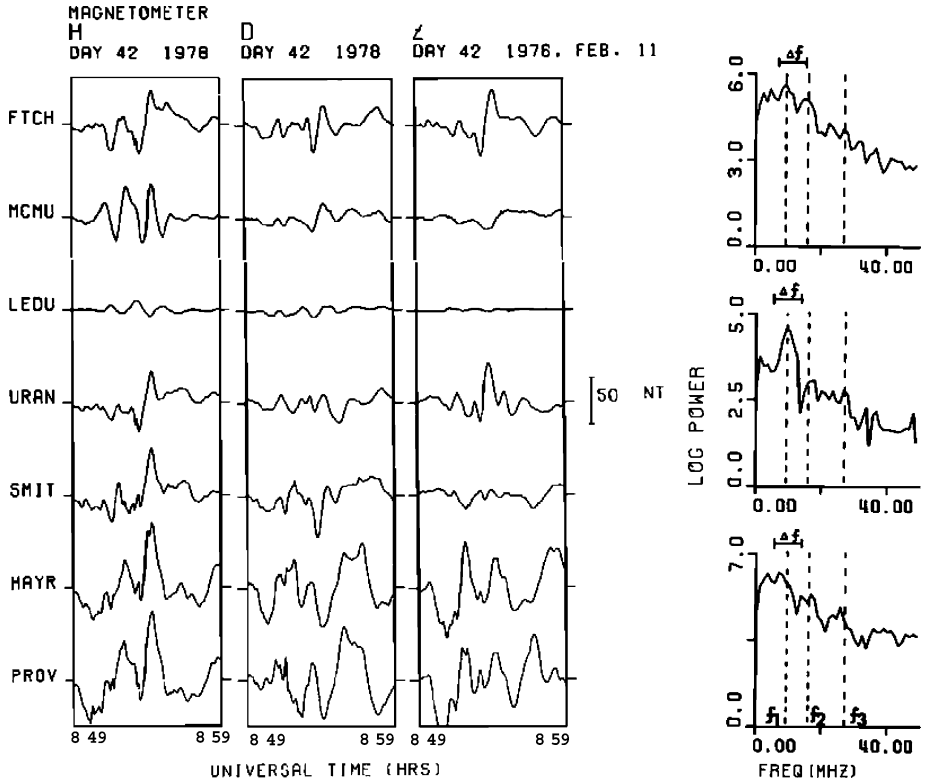

Fig. 28 (From Samson and Harrold 1983) (*Left*) Pi2 pulsations over a range of latitudes and (*right*) power spectra (H component) for selected ground stations

such as dipolarization, have shown that mode coupling in a PCR-dominated inner magnetosphere leads to a mixture of poloidal and toroidal modes at middle latitudes with the same longitudinal variations of the polarization ellipses as those ascribed to the TR model (Pekrides et al. 1997; see Fig. 21 of Sect. 2.2). Similar simulation results were obtained by Allan et al. (1996) (see also Fujita et al. 2002 and Takahashi and Liou 2004).

Spectral Content

Although mid- and high-latitude Pi2 pulsations at substorm onset have been associated with the TR model, their magnetic field power spectra differ significantly. Whereas at middle latitudes the power spectrum tends to be monochromatic, it shows several frequency peaks at high latitudes, i.e., in the vicinity of the substorm electrojet (Samson 1982). One of the high-latitude peaks has been called the Pi2, either because it falls in the Pi2 range or because it is close or identical in frequency to a mid-latitude Pi2. Figure 28 shows an example of spectral variations of Pi2 pulsations at several ground stations, covering middle latitudes (e.g., LEDU) and high latitudes (e.g., PROV). Samson and Harrold (1983) assigned the spectral peak at $f_1 = 9$ mHz to the Pi2. While the peak shows clearly at LEDU and less so at FTCH, there might be a small frequency shift at PROV; however, the authors argued for the same frequency at PROV. In reviewing other case studies of TR-Pi2, it was noted that most studies have only focused on the analysis of the monochromatic mid-latitude

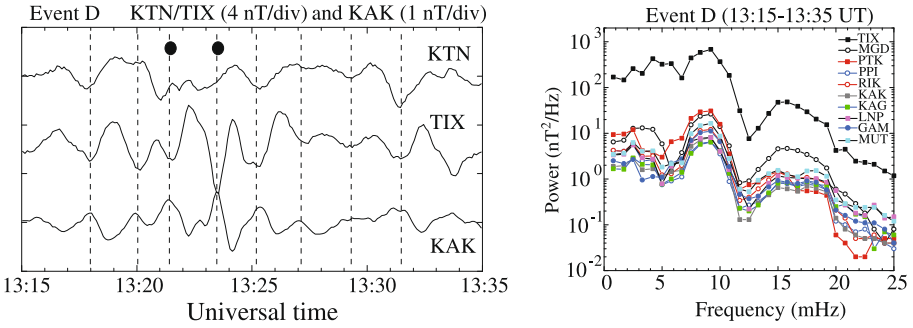

Fig. 29 (From Kim et al. 2010) Ground magnetometer data (H component) for a Pi2 event recorded at high-latitude stations (KTN, TIX) and at a low-latitude station (KAK), together with the power spectra of all investigated stations of the 210° MM network

Pi2; thus, a detailed comparison of the spectral content of mid-latitude and high-latitude Pi2 pulsations is not possible in this review. An exception was the study by Hughes and Singer (1985), who analyzed mid-latitude Pi2 pulsations but also mentioned that concurrent high-latitude Pi2 pulsations had the same period, albeit no high-latitude data were presented.

Low-latitude Pi2 pulsations generally have a higher frequency (>15 mHz) than those at higher latitudes. (Pi2 models that can account for the smaller period are reviewed in Sect. 2). However, in a few event studies, it was reported that low- to high-latitude Pi2 pulsations showed identical periods (Yumoto et al. 1990; Li et al. 1998; Kim et al. 2010). For example, Kim et al. (2010) showed for several events that the frequency content was identical with increasing magnetic field amplitude for higher-latitude pulsations (Fig. 29). Because of larger amplitudes at high latitude, it was suggested that the Pi2 source was in the outer magnetosphere, and that the TR mechanism was a viable generation mechanism for their events. In Sects. 3.2 and 3.4, we review Pi2 case studies that also reported identical pulsation periods at all latitudes, while arguing for different generation mechanisms.

Li et al. (1998) reported the presence of two frequency components, both in the Pi2 range, in low-latitude data with the higher-frequency peak being dominant (Fig. 30). In contrast, at high latitude the high-frequency peak was not present, and the low-frequency peak matched that at low latitude. Therefore, the authors concluded that two separate Pi2 sources operated simultaneously: the TR mechanism, accounting for the low-frequency Pi2; and the PCR mechanism, accounting for the high-frequency Pi2. Moreover, the results suggest that the TR mechanism generated not only the high-latitude Pi2 but also one of the low-latitude Pi2 pulsations.

To gain an understanding of the spectral content of mid-latitude and high-latitude Pi2 pulsations, Fujita et al. (2002) conducted numerical simulations in a 3-D dipole magnetic field model. The dipole geometry, as opposed to a uniform geometry, allowed for coupling between the shear Alfvén mode and fast mode. The energy source was an impulsive disturbance (few tens of second) at approximately 9 R_E in form of a localized azimuthal (dusk-to-dawn) current, limited to ±2 h local time around midnight (see Fig. 1 of Sect. 1.1). Figure 31 shows time series of the radial electric field component, E_v, which represents the toroidal mode (see Sect. 2.2 for results of the poloidal mode), in the equatorial plane for different L values (from 3.44 to 9.16) and various local times (from

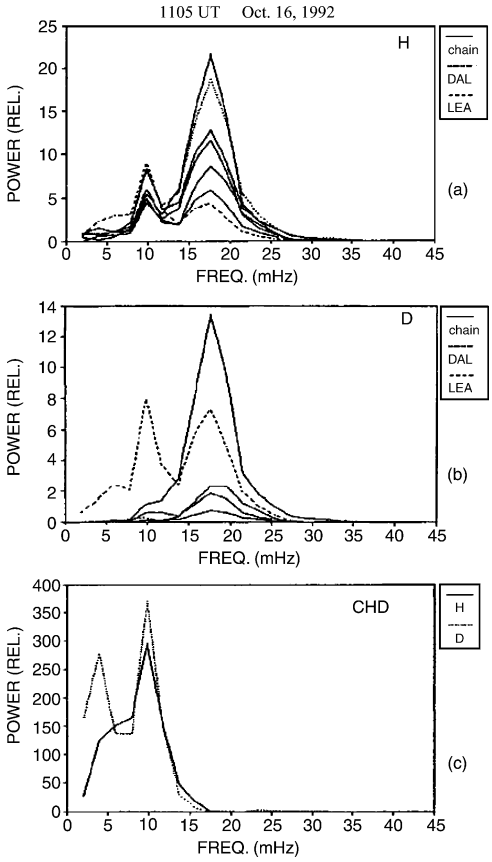

Fig. 30 (From Li et al. 1998) (*Top*, *middle*) The H and D component power spectra of a Pi2 event from low-latitude stations ('chain' refers to the 210°E Magnetic Meridian Chain stations used in the study). (*Bottom*) The H and D component power spectra of the same event at the high-latitude station CHD

midnight to noon). In the simulation several frequency components develop at high latitude ($L = 9.16$), also seen in the power spectra (bottom, right), with maximum amplitude near the source current at 21-h MLT. This agrees with ground observations, which typically show more irregular pulsations composed of several frequency components near the WTS (Samson and Harrold 1983), which would correspond to 21-h MLT in the simulation. The additional peaks have usually been attributed to electrojet noise (Samson 1982), while the simulation results suggest that they are due to the spectral content of the impulsive source current and the bouncing nature of the Alfvén waves on high-latitude field lines.

At lower latitudes ($L \leq 7.4$), i.e., subauroral field lines, the frequency spectrum is different from that at high latitude ($L = 9.16$). At $L = 7.40$ (still outside the plasmasphere in the simulation) there are two frequency peaks (8 and 26 mHz) with the lower one having the larger amplitude. There is only one spectral peak (22 mHz) in the plasmapause region at $L = 5.64$. In the inner plasmasphere at $L = 3.44$, there are two spectral peaks at 14 and 20 mHz. The latter is generated by the PVR mode (Sect. 2.2). Thus, the simulation reproduces the observations of fewer frequency peaks on field lines below the source region ($L = 9.16$). In addition, we emphasize that the oscillations at high latitude ($L = 9.16$) and those at middle latitudes ($L \leq 7.4$) do not have identical frequency peaks. Therefore, different Pi2 mechanisms simultaneously operate at middle and high latitudes in the simulation, even though the Pi2 energy source (the impulsive dusk-to-dawn current) is the

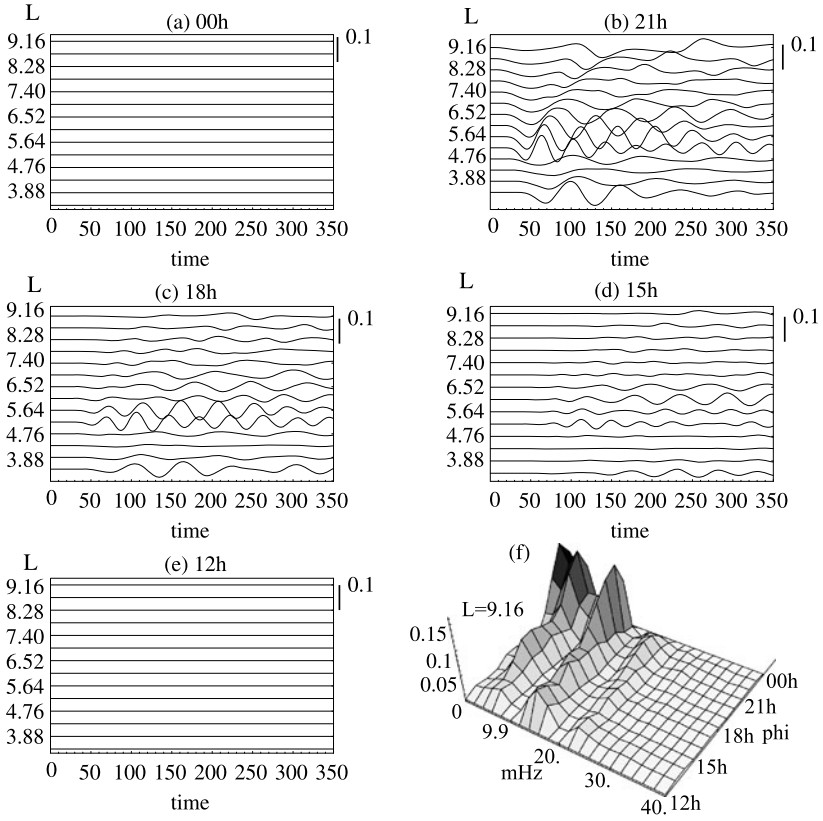

Fig. 31 (Modified from Fujita et al. 2002) Waveforms of the radial electric field, δE_v, in the equatorial plane for $L = 9.16$ to 3.44 at (**a**) 0000, (**b**) 2100, (**c**) 1800, (**d**) 1500, and (**e**) 1200 LT. The plasmapause is located at around $L = 5.64$. The positive deviation in this figure signifies an outward change in δE_v. (**f**) Local time variations of the power spectra for δE_v in the equatorial plane at $L = 9.16$ (source region)

same for all oscillations in the simulation (see Sect. 1.1 for definitions of Pi2 frequency source and Pi2 energy source). Although the simulation results do not support the coupling scenario of high-latitude Pi2, established by the bouncing Alfvén waves, to mid-latitude Pi2, caution is in order because the results are only based on data points at the equatorial plane and do not consider a possible coupling between Alfvén waves and compressional waves away from the equatorial plane, perhaps at lower altitude. On high-latitude source field lines ($L = 9.16$), on the other hand, the results are consistent with the TR model.

The simulation results further demonstrate that the behavior of the toroidal mode depends on latitude. Whereas at high latitude ($L = 9.16$) the Alfvén waves are bouncing waves, they are standing waves along field lines at lower latitudes and their frequencies increase with smaller L values. This L-dependent behavior, reported for Pi2-associated FLR located in the outer magnetosphere during substorms (e.g., Saka et al. 1996; Takahashi et al. 1996; Keiling et al. 2003), is attributed to field line shortening which corresponds to an increase in eigenfrequency of the field line. These FLRs are generated by mode coupling to the broadband compressional wave launched from the initial disturbance (the dusk-to-dawn current) in the simulation, with one exception; inside the plasmasphere an FLR is coupled to

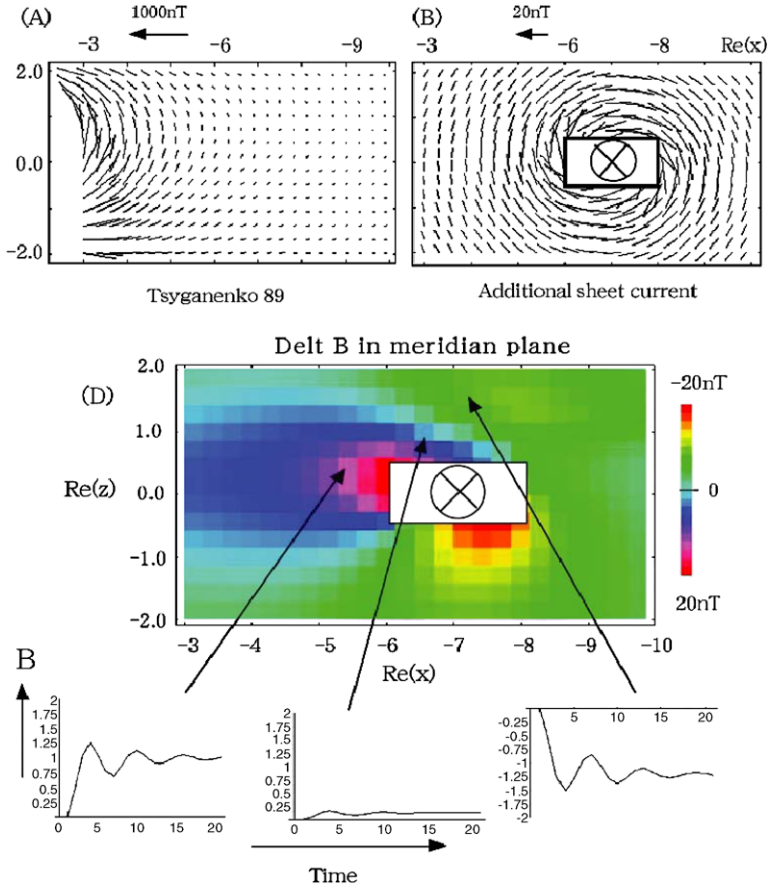

Fig. 32 (From Saka et al. 2004) (*Top*) Background field line vectors in the midnight meridian ($X = 3$–$10\ R_E, Z = -2$–$2\ R_E$) calculated by use of the Tsyganenko 89 model, and field line vectors in the midnight meridian produced by the dusk-to-dawn current sheet (shown by the *rectangle*) located at an L between 6 and 8 in the midnight sector. (*Middle*) Meridional cross section of the changes of the field magnitude B. The current sheet is marked by the *rectangle*. (*Bottom*) Predicted time variation of the field magnitudes caused by the damped modulation of the current intensity is schematically illustrated at three different positions (from left to right): positive B region, demarcation region, and negative B region

a monochromatic PVR that developed in the simulation (see Sect. 4.1 for spacecraft data illustrating this coupling).

Substorm Current Wedge

Early spacecraft-based evidence for a physical connection between the SCW and ground Pi2 pulsations focused on a comparison of the magnetic field deflections of the first Pi2 pulse in space and the main field-aligned current at substorm onset (Sakurai and McPherron 1983). Both were shown to be consistent, suggesting a causal relationship. Using a simple model, the effect of the SCW current for Pi2 pulsations has been revisited more recently by Saka et al. (2004). The model superposes the magnetic field of the Tsyganenko 89 magnetic field model and the magnetic field of an azimuthal (dusk-to-dawn) current sheet at L

values between 6 and 8 with a thickness of 1 R_E (top of Fig. 32). The middle panel shows the deviation (color-coded) of the total magnetic field due to this localized current sheet, showing regions of enhanced and reduced magnetic field. The three time series at the bottom schematically illustrate the predicted variations of the field magnitudes caused by the damped current intensity modulations. The results were compared with a multiple Pi2 event. During a two-hour interval with eight Pi2 pulsations, GOES-6 magnetic field data showed both positive and negative magnetic field intensity deviations correlated with the onsets of the ground Pi2 pulsations, as recorded by a low-latitude ground station (not shown here). It was suggested that GOES-6 moved in and out of the enhanced and reduced magnetic field regions. These observations support the generation of the large-scale current. In addition, fluctuations on the large-scale current were interpreted as SCW oscillations. However, no high-latitude Pi2 was reported for comparison, and the reported low-latitude Pi2 pulsations were not correlated.

The SCW is more confined azimuthally than the high- and mid-latitude Pi2 pulsations (e.g., Gelpi et al. 1985), and mid-latitude Pi2 pulsations spread over many more longitudes than high-latitude Pi2 pulsations (Yeoman et al. 1994), which only occur within a few hours of local time from the center of the SCW (e.g., Singer et al. 1983; Gelpi et al. 1985). Thus, it is inevitable that compressional waves must play a role in the propagation modes of this Pi2 type. The excitation of compressional waves from a point-like source (i.e., the SCW) is consistent with these observations. For example, Saka et al. (2004) (see previous paragraph) suggested that the observed SCW fluctuations in their event may have launched poloidal mode waves that excited the lower-latitude Pi2 pulsations. However, the coupling of the bouncing Alfvén wave to compressional waves that propagate across field lines and lead to the mid-latitude Pi2 with exactly the same period as that of the bouncing Alfvén wave has so far not been shown. Although Lin and Cahill (1975) reported compressional waves in association with Pi2 pulsations, no one-to-one correlation was found.

Bouncing Alfvén Waves

It is generally thought that the formation of the SCW provides the transient Alfvén wave that is responsible for the TR-Pi2 on the ground. Thus, an expected signature of the TR mechanism is Alfvén wave bouncing in association with the SCW. Using the CRRES satellite, Maynard et al. (1996) reported bi-directional variations in the field-aligned Poynting flux in the near-Earth plasma sheet at substorm onset with periods in the Pi2 range, consistent with the transient Alfvén waves. Diamagnetic oscillations of the neutral sheet, also in the Pi2 range, were interpreted by Bauer et al. (1995) as driven responses to bouncing Alfvén waves associated with the SCW. We note that neither of these studies showed direct one-to-one correlation between space and ground Pi2, however. Ground-based evidence for bouncing Alfvén waves is the observation of an equivalent ionospheric current (EIC) vortex that alternated between counter-clockwise and clockwise rotation in the Pi2 frequency range (Pashin et al. 1982). EIC vortices with opposite rotational sense have been associated with downward and upward field-aligned currents.

As suggested by Fujita et al. (2000)'s simulation, the bouncing Alfvén waves do not form field line resonances. Nevertheless, signatures of standing waves could still be possible due to the interference of downward and upward traveling Alfvén waves. If a westward movement of the field-aligned currents is however taken into account, the spatial displacement would prevent such standing wave signatures, and so far a standing wave signature has not been observed in space for TR-Pi2s. (Caution is in order not to confuse this standing

wave signature with FLR which has been observed in association with mode coupling to a PCR/PVR mode (e.g., see Sect. 4).)

It is surprising that there has never been a report on coherent ground and space Pi2 pulsations in association with the TR mechanism. Instead, comparisons have consistently shown different periods between ground and space Pi2 pulsations (e.g., Lin and Cahill 1975; Sakurai and McPherron 1983; Singer et al. 1983; Hughes and Singer 1985; Yumoto et al. 1990; Saka et al. 2004; see also Sect. 4 for comparisons with particle fluxes).

3.2 Plasma Instability

3.2.1 Model

Several features of wave activity in the near-Earth plasma sheet surrounding substorm onset have been identified (see reviews by Lui 1996, and Ohtani 2001). In the late 1980s, it was recognized that substorm onsets are associated with large-amplitude magnetic field fluctuations in the near-Earth plasma sheet (e.g., Takahashi et al. 1987). Lui et al. (1992) interpreted these fluctuations as temporal structures associated with substorm onset, as opposed to the erratic crossing of a spatial structure (e.g., X line). The magnetic fluctuations encompass low- to high-frequency components (e.g., Lui and Najmi 1997). High-frequency components are thought to be associated with the mechanism disrupting the current sheet, while low-frequency components are possibly associated with an MHD instability (e.g., Miura et al. 1989; Roux et al. 1991; Cheng 1991; Ohtani and Tamao 1993; Bhattacharjee et al. 1998; Cheng and Lui 1998) that might pre-condition the current sheet leading to its subsequent disruption. Several studies also reported wave activity in the Pi2 frequency band (e.g. Cheng and Lui 1998; Erickson et al. 2000; Sigsbee et al. 2002; Saito et al. 2008; Liang et al. 2009), but their causal relationship with ground Pi2 pulsations was not investigated. Indeed, caution is in order because Pi2-frequency-band waves are not necessarily related to ground Pi2 pulsations as reviewed here; for one, Pi2-band activity can be more broadband, and for another, they might not have the typical short duration of only a few wave cycles of Pi2 pulsations.

On the basis of ground-based observations only, few studies suggested that wave activity driven by plasma instabilities in the near-Earth plasma sheet—without specifying the instability mode and its coupling to the ionosphere—could cause ground Pi2 pulsations (Solovyev et al. 2000; Yumoto et al. 2001). Recently, coordinated ground-space data comparisons provided evidence for these earlier suggestions (Keiling et al. 2008b, 2011). In both latter studies, it was suggested that ballooning mode/instability was responsible, albeit of different types. Since the early work by Roux et al. (1991), who suggested a causal connection between ballooning mode and the WTS, observational evidence for ballooning mode/instability has only slowly grown (Saito et al. 2008; Keiling et al. 2008c; Liang et al. 2009; Zhu et al. 2009). For example, Saito et al. (2008) and Keiling et al. (2008c), using single-spacecraft and multiple-spacecraft data, respectively, showed supporting observational evidence for the drift ballooning mode. Nonetheless, the properties of the various types of ballooning modes are still not well characterized observationally. Even though spacecraft observations are progressively more confirming their existence, their coupling to the ionosphere is still poorly understood.

In the scenarios reviewed here, it is the periodicity of ballooning mode/instability, rather than the repetitive bouncing of Alfvén waves along field lines of the TR model, that directly controls the Pi2 pulsation. Although mathematical frameworks for various types of ballooning mode/instability exist (e.g., Miura et al. 1989; Cheng 1991; Ohtani and Tamao 1993;

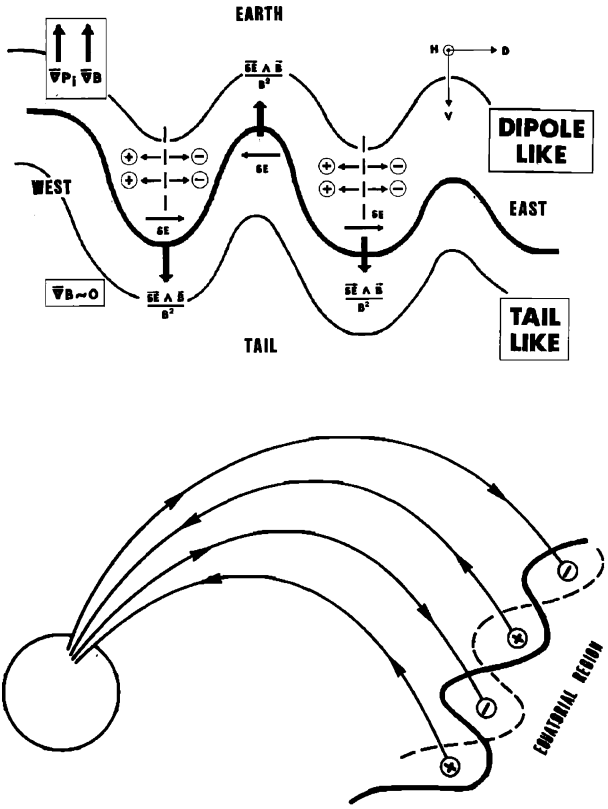

Fig. 33 (From Roux et al. 1991) Sketches of instability (*top*) and field-aligned current structures (*bottom*) associated with the development of an MHD instability

Bhattacharjee et al. 1998), they have typically been associated with Pc5 pulsations and not with Pi2 pulsations. However, several theoretical investigations have also associated them with pulsations in the Pi2 frequency range. While Cheng and Lui (1998) identified a low-frequency kinetic ballooning instability (KBI) with an oscillation period of 50–75 s, which lies at the lower end of the Pi2 range (50–140 s), Crabtree et al. (2003) investigated compressional drift waves and suggested that they might play a role in substorm-associated Pi2 pulsations. Analyzing two types of drift modes, Horton et al. (2001) suggests that nonlinear plasma oscillations can go into chaotic pulsations, not unlike the transition from Pc5 to Pi2 signals, thus providing a synthesis of the two types of pulsations.

An early analysis of ballooning instability (Miura et al. 1989) shows that there are ideal MHD ballooning modes and (non-ideal MHD) drift ballooning modes. The ideal MHD ballooning mode does not propagate. Both stable and unstable ballooning modes are short-wavelength combination of shear Alfvén and slow magnetosonic waves. While the unstable mode does not have a real frequency, the stable mode has a real frequency, which is determined not only by the Alfvén frequency but also by the free energy from inhomogeneities in pressure and curvature (e.g., Hameiri et al. 1991). When the ion diamagnetic drift effect is taken into account, the ballooning mode becomes drift ballooning mode and propagates westward. The drift ballooning mode has a real frequency, which is due to the ion diamagnetic drift (e.g., Miura 2004). The wavelength, being a fundamental property of drift ballooning mode, is controlled by the pressure gradient scale length and the curvature radius. Due to the diamagnetic drift, the ballooning mode perturbations are recorded as oscillations at a fixed point in space. Consequently, the Pi2 period, T_{BM}, associated with this mode is

given by:

$$T_{\mathrm{BM}} = \lambda_{\perp} / V_{\mathrm{ph}}, \tag{5}$$

where $\lambda_{\perp}$ is the perpendicular wavelength of the ballooning mode wave and V_{ph} is its phase velocity. In the non-ideal MHD models, both stable and unstable modes can acquire an additional real frequency associated with other higher order drifts due to finite Larmor radius effects.

Associated with the ballooning modes are frequency-modulated energetic particle fluxes (e.g., Horton et al. 2001) and FACs (e.g., Roux et al. 1991) that can couple to the ionosphere where they might cause the ground Pi2 signature. This coupling can be understood with the qualitative description given by Roux et al. (1991) (Fig. 33). In this scenario, magnetic drifts lead to charge separation in an initially small perturbation near the inner edge of the plasma sheet. The resulting electric field causes the perturbation to grow, causing further charge separation. The excess electrons on one side of the wave crest stream towards the ionosphere, resulting in an upward field-aligned current. In the ionosphere, the current connects to the downward current (the return current) which is connected to the excess positive charge in the wave perturbation in space. If several perturbations are present, a current system with multiple upward and downward FACs can form.

For decades it has proven difficult to observe the substorm instability in the near-Earth plasma region. This difficulty directly translates to this Pi2 model as well, since it has its source in this instability region. It also remains a major challenge to describe the coupling of the outer magnetosphere to the ionosphere, a topic still poorly understood in substorm physics in general. As a result, a paucity of reports makes it difficult to characterize the ground signatures that would allow identifying this mechanism.

The geophysical context for this Pi2 type is a class of substorms that develop from a plasma instability in the near-Earth plasma sheet. If this instability does not lead to a substorm breakup, it could lead to a pseudo-breakup. Hence, it is also likely that some Pi2s associated with pseudo-breakup are caused by the same mechanism.

3.2.2 Observations

Arnoldy (1986) reported successive electron injections with temporal variations in the Pi2 frequency range and simultaneous ground Pi2, which were not one-to-one correlated, however (Fig. 34). Although it was argued that the two phenomena were likely related, it was not commented on how the series of injections coupled to the ground. It appears possible that the plasma-instability-driven mechanism caused the ground Pi2, albeit the authors did not suggest such a scenario. Furthermore, we caution because although particle flux oscillations/modulations in space and their correspondence with ground Pi2 are expected signatures of plasma-instability-driven Pi2 pulsations, such modulations have also been associated with other Pi2 models (e.g., Bauer et al. 1995; Saka et al. 1997; Åsnes et al. 2004). Therefore, this particle signature alone is insufficient evidence for the plasma-instability-driven Pi2 mechanism. For example, in Arnoldy (1986)'s event, periodic flow bursts (Sect. 3.3) could also be envisioned as a source of both electron injections and ground Pi2. Hence, it is clear that additional data would be required to draw firmer conclusions.

Comparing ground magnetometer data from 190°–210° MM network stations to 4-s auroral data from the all-sky TV camera at Tixie station (TIX) during Pi2 events at high latitudes (Fig. 35), Solovyev et al. (2000) argued for a relationship between high-latitude Pi2 pulsations and auroral arc formation based on the following observation. The maximum

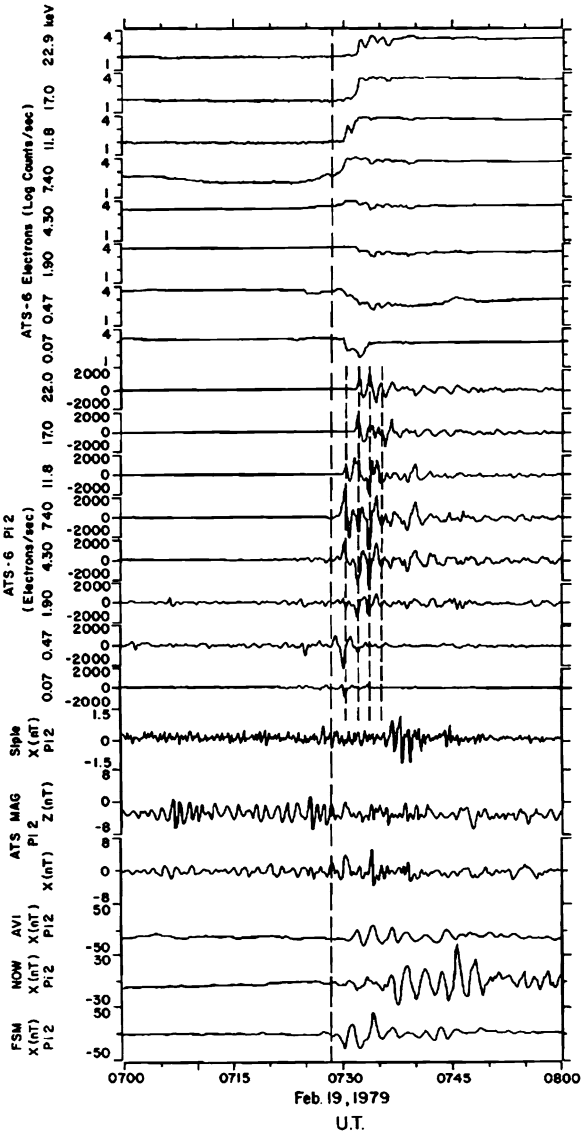

Fig. 34 (From Arnoldy 1986) ATS6 and ground data during a substorm on February 19, 1979. *Top eight panels*: Count rate in different electron energy channels. *Next eight panels*: Band-pass filtered (40–150 s) electron count rates. *Ninth panels*: Ground induction magnetometer data from Siple ($L = 4.2$). *Tenth and eleventh panels*: ATS6 magnetic field. *Bottom three panels*: Filtered (40–150 s) ground magnetometer data from various stations. *Vertical dashed line* marks substorm onset

Pi2 amplitude was observed at the same location as an auroral arc that showed a wave-like structure. It was noted that the arc oscillation period (30–200 s) (i.e., the ratio of the arc wavelength to the wave propagation velocity) was similar to the Pi2 period. The wave-like structure traveled azimuthally with a velocity of about 1 km/s. Further, the polarization patterns were similar to the rotation in the wave-like structures. Hence, it was suggested that Pi2 excitation and spatial arc distortion were due to a common process, namely, the development of a magnetospheric plasma instability, and that temporal Alfvénic wavelets were launched from ripples on the inner plasma sheet boundary. In this scenario, it is assumed that the Pi2 pulsations are a sequence of transient wavelets which reflect only once from the ionosphere. However, although similar periods were reported in the two types of signals (magnetic field

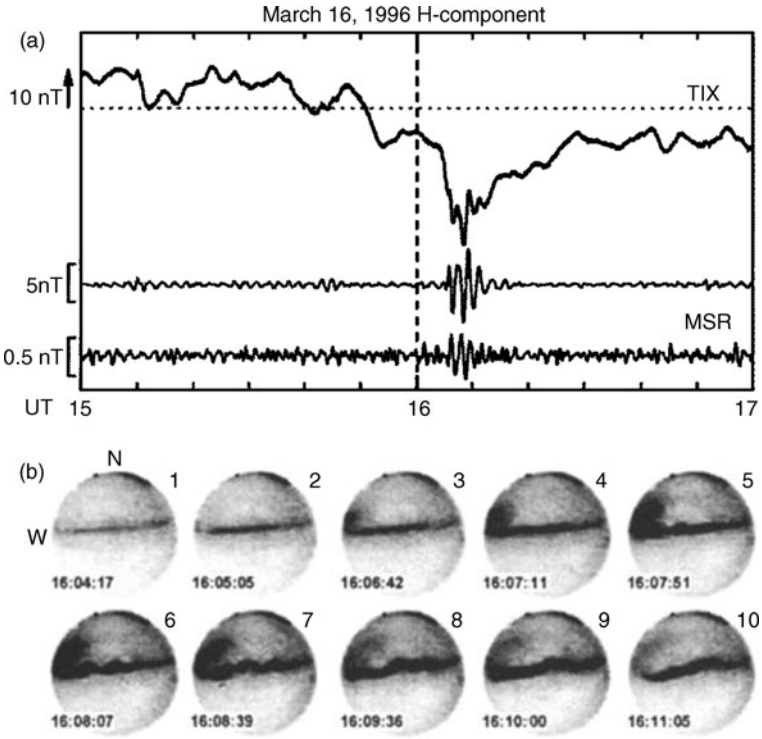

Fig. 35 (From Solovyev et al. 2000) (**a**) Unfiltered H component of the magnetic field at Tixie Bay (TIX) and filtered H component at TIX and MSR. (**b**) All-sky images of an auroral activation at TIX

and optical), they were not shown to correlate one-to-one, and also, no spacecraft data were available to provide evidence of the instability region.

More recently, Keiling et al. (2008b, 2011) investigated two consecutive Pi2 events that showed markedly different properties (panel (f) in Fig. 36). A notable feature was the dual slope in the substorm magnetic bay (H component): a shallower, negative slope followed by a steeper, larger slope associated with auroral intensification and particle injections in space. Both slopes were superposed by Pi2 pulsations. The first Pi2, between 1110 and 1116 UT, with small amplitude occurred before auroral breakup, while the second Pi2, between 1118 and 1126 UT, had extremely large amplitudes ($\sim$100 nT). (Note: Panel (e) shows the onset of a substorm, occurring further east of the Pi2 events described here; see further details in Keiling 2011). In space, particle fluxes were correlated one-to-one with both ground Pi2 events (discussed below). It is interesting to note, however, that for the smaller Pi2 the correlated particle energies were $<$50 keV, whereas for the larger Pi2 the particle energies were $>$100 keV. This energy difference suggests that two mechanisms operated.

The correlated particle and ground magnetic field oscillations of the large-amplitude, global Pi2 had a period of 135 s (right side of Fig. 36). Several different time delays were recorded. While the flux modulations/injections were dispersionless among the different energy channels at THEMIS (not shown here), LANL-97A recorded time delays among its own channels and with respect to those at THEMIS (panels (g) and (h)). This indicates that periodic modulations/injection fronts propagated from THEMIS toward LANL-97A. The high-latitude ground station KIAN, being closest to THEMIS's footpoint, recorded very

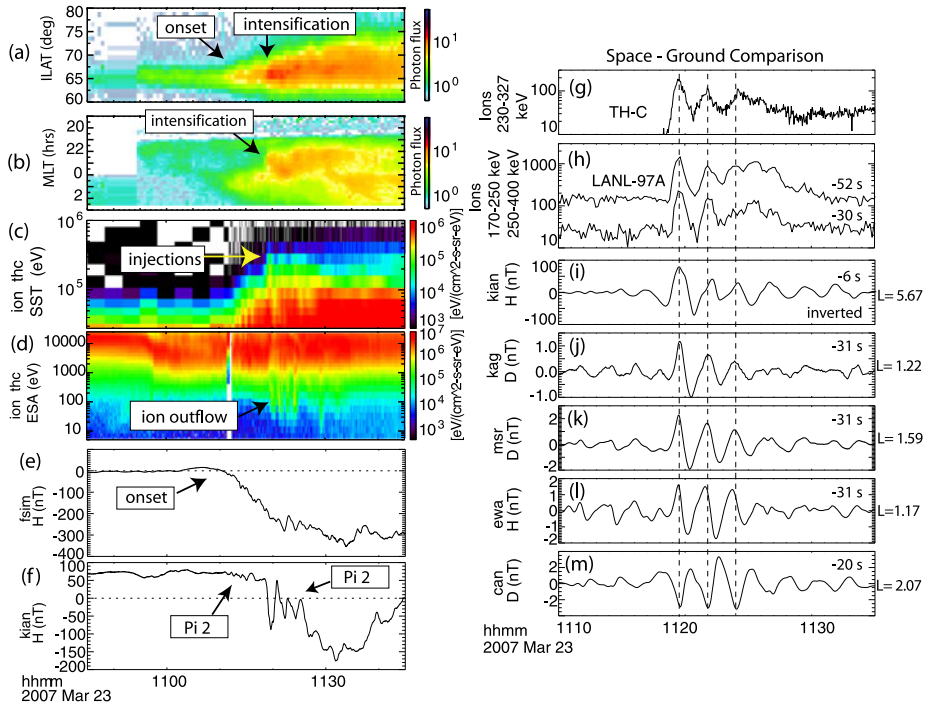

Fig. 36 (From Keiling et al. 2008b) THEMIS and LANL-97A data during a substorm on 23 March 2007. (*Left*) Auroral data (keograms), particle data (THEMIS), and unfiltered ground magnetometer data during a Pi2 event. (*Right*) Comparison of differential ion energy flux from THEMIS (located in the pre-midnight sector at 8.3 R_E), LANL-97A (geosynchronous), and filtered ground magnetometer data

large Pi2 with a 6-s time delay compared to the dispersionless ion injections at THEMIS. The correlated lower-latitude Pi2 pulsations had longer time delays (20–31 s). The authors speculated that a non-propagating, oscillatory plasma instability led to periodic disruptions of the current sheet followed by periodic particle injections. Because of the extreme Pi2 amplitude, it was further suggested that each Pi2 cycle was in fact a separate substorm intensification. The short time delay of 6 s between space and ground pulsations (which can only be achieved by energetic particles and not Alfvén waves), and the fact that only the most energetic particles (>100 keV) were correlated with the Pi2 (i.e., ruling out that simple boundary motion was involved) were taken as evidence against the TR mechanism for this Pi2 event. The coupling mechanism between the plasma injections and the high-latitude ground Pi2 could not be determined.

While in the previous scenario, the instability does not propagate, the next scenario, proposed for the small-amplitude Pi2 event by Keiling (2011), is based on the spatial properties of a drift ballooning mode. One reason for a different scenario was the lower energies of the oscillating particle fluxes that are compatible with plasma boundary motions and their drifting nature. In this scenario the spatial separation of wave ripples along an energized boundary at or near the transition region between dipolar-like and tail-like field lines, combined with a westward drift, directly map to the ground via upward and downward field-aligned currents (cf. Fig. 33). This ripple scenario is similar, or perhaps identical, to that mentioned by Roux et al. (1991) and Maynard et al. (1996). Each pair of downward and upward field-aligned currents causes perturbations in the ground magnetic fields. Figure 37

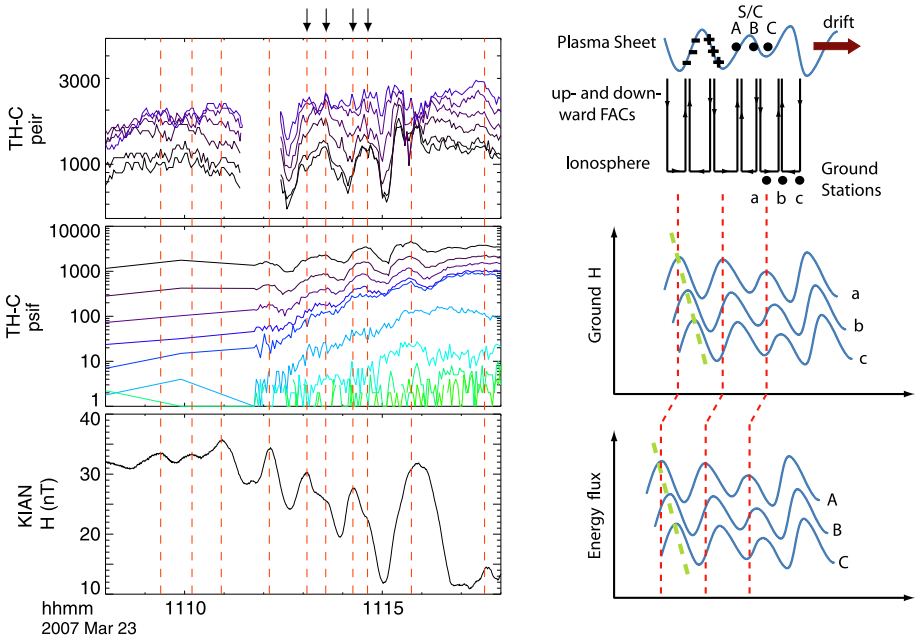

Fig. 37 (From Keiling 2011) (*Left*) Comparison of ion flux enhancements (energy range from ∼ keV to >300 keV) at the THEMIS spacecraft TH-C and Pi2 pulsation at ground station KIAN. Arrows point at finer-scale structures. (*Right*) (*Top*) Schematic of perturbations in the near-Earth plasma sheet and currents leading from the perturbations into the ionosphere. (*Middle*) Ground signature recorded at three longitudinally-separated ground stations. (*Bottom*) Plasma perturbations recorded in situ by three azimuthally-separated spacecraft

shows a one-to-one correlation between Pi2-like modulated particle fluxes and ground magnetic field with a period of ∼60 s. On the ground and in space, westward propagation of the Pi2 was recorded at azimuthally-separated ground stations and three THEMIS spacecraft. The spatial extent of the Pi2 was small in latitude and longitude on the ground. It is noted that Keiling (2011) reported a second Pi2 event further west with a different period, which was also correlated with plasma fluxes in a way similar to the other event. Hence, it can be concluded that at least two such instability regions, spatially separated, existed simultaneously in the plasma sheet with different oscillation frequency.

3.3 Bursty Bulk Flow

3.3.1 Model

Fast Earthward-moving plasma flows in the magnetotail have been associated with Pi2 pulsations (Yumoto et al. 1989; Nagai et al. 1998; Shiokawa et al. 1998), whereby deceleration of the flow in the near-Earth plasma sheet region launches a compressional pulse towards Earth. This broadband-frequency pulse, in turn, excites a cavity mode in the inner magnetosphere that establishes the Pi2 frequency, as described in Sect. 2, which can then be recorded on the ground. There is statistical evidence for a temporal relationship between the occurrences of flow bursts in the tail and ground Pi2 observations (Hsu and McPherron 2007; Kim et al. 2007). However, in this scenario the source of the Pi2 frequency (i.e., the Pi2

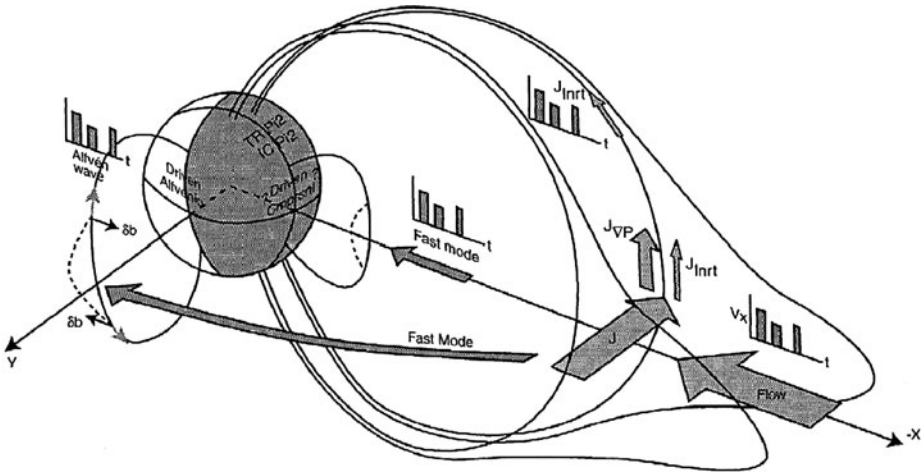

Fig. 38 (From Kepko et al. 2001) Illustration of different propagation paths of Pi2 pulsations driven by periodic flow bursts

source) is not the single flow burst but the cavity resonance; the flow burst only provides the energy for cavity excitation. An entirely different Pi2 generation scenario, reviewed in this section, is based on repetitive flow bursts in the magnetotail with a periodicity that matches that of ground Pi2 pulsations.

An early suggestion for a Pi2 source in the magnetotail came from Osaki et al. (1998). The authors presented energy budget calculations for a Pi2 in the plasmasphere and concluded that to maintain the Pi2 it would require a periodic driver external to the plasmasphere rather than a plasmaspheric cavity mode (see also Itonaga et al. 1997b). The driver could not be identified in this study, however. Later, Kepko and Kivelson (1999) reported such a possible driver in the magnetotail at distances up to 17 R_E in the form of oscillatory variations in the speed of Earthward-moving plasma flow. Allowing for travel time delays from the magnetotail to the ground, the flow variations were correlated one-to-one with the individual wave cycles of the ground Pi2. Hence, the authors suggested that these flows would determine the properties (such as duration, amplitude and period) of the correlated ground Pi2 pulsations. Kepko et al. (2001) described three separate paths for the Pi2 signal contained in the flows to propagate to the ground, as illustrated in Fig. 38. Two paths involve fast mode waves, generated by the decelerating flow bursts, that reach the flanks and the low-latitude nightside region; the third path involves field-aligned currents also generated by decelerating flow bursts.

The BBF-driven model has not addressed the issues of what mechanism generates the periodicity of the Pi2-like flow modulations, and what determines the number of individual flow bursts, which is related to the duration of Pi2 pulsations. Generally speaking, Earthward-moving fast flows have been attributed to either a reconnection process in the magnetotail or to some other plasma sheet instability (e.g., Sergeev et al. 1992). Kivelson (2006) mentioned several possibilities that could control periodicity but none of them has been confirmed yet. For example, compressional waves, launched at the reconnection site, reflect back either from a region near Earth or the magnetopause and act on the reconnection site by quenching the reconnection process temporarily; or a kinetic tearing mode instability may have a spatial structure that imposes a temporal structure on the flows when observed from a fixed point in space. Another scenario could be that an initially single, Earthward-

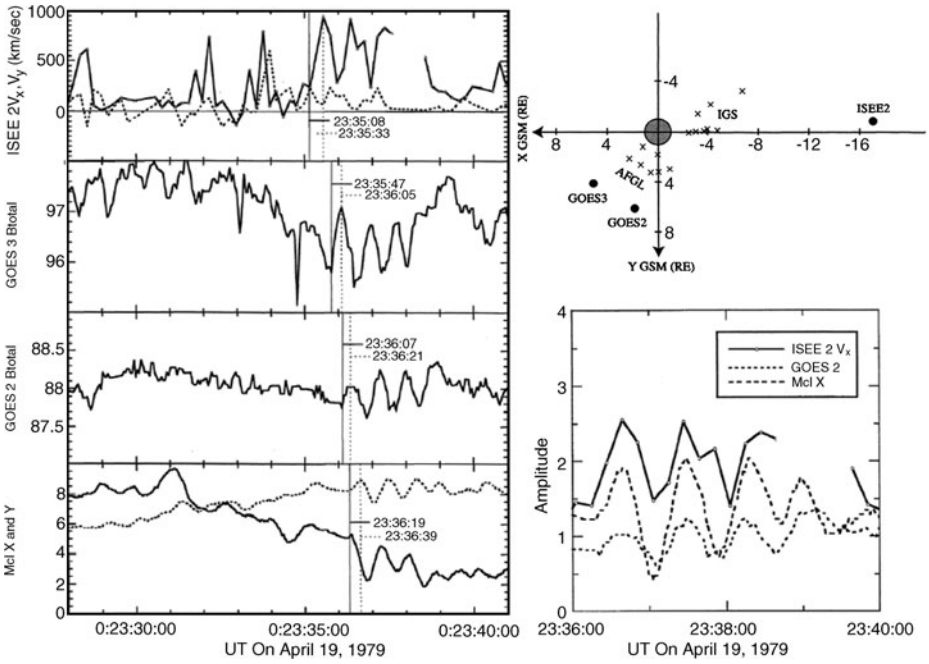

Fig. 39 (From Kepko and Kivelson 1999) Plasma flow and magnetic field data of Pi2 pulsations observed at various spacecraft and on the ground. Ground stations have been mapped to the GSM equatorial plane (*top right*). In the lower right, the data were time-shifted to compare waveforms of the various Pi2 signals

moving plasma flow breaks up into several individual flow bursts of 1-min or 2-min duration, in which case the BBF periodicity is generated only after the release of a single flow burst at the reconnection site. Such considerations show that, as of now, it is unclear as to what the actual Pi2 source (i.e., the location and mechanism that establish the Pi2 frequency) is. That is to say, the source is likely not the BBF itself. Instead, the BBF is likely only an intermediate carrier of the Pi2 signal that is created further down the magnetotail. Moreover, the BBF might only be one propagation path from that source and other paths are simultaneously taken. This idea is further fleshed out in Sect. 3.4.

Objections toward the BBF-driven model based on case studies have been put forward by a few authors (e.g., Yamaguchi et al. 2002; Murphy et al. 2006). These studies did not find the correlations reported by Kepko and Kivelson (1999). However, caution is in order because such case-based studies are not conclusive since they cannot rule out that flow bursts existed in narrow channels and were thus simply missed by the spacecraft.

3.3.2 Observations

Using spacecraft data located in the midtail region between 8 and 17 R_E, it was demonstrated for several events that the velocity variations in multiple Earthward-moving flow bursts qualitatively matched (i.e., amplitude peaks in flow velocity and ground magnetic field line up) the Pi2 waveforms on the ground at low latitudes on the flank, allowing for time delays of 60–90 s (Kepko and Kivelson 1999; Kepko et al. 2001). Figure 39 shows an example in which ISEE 2 recorded several flow bursts near $X = -17$ R_E and Mount

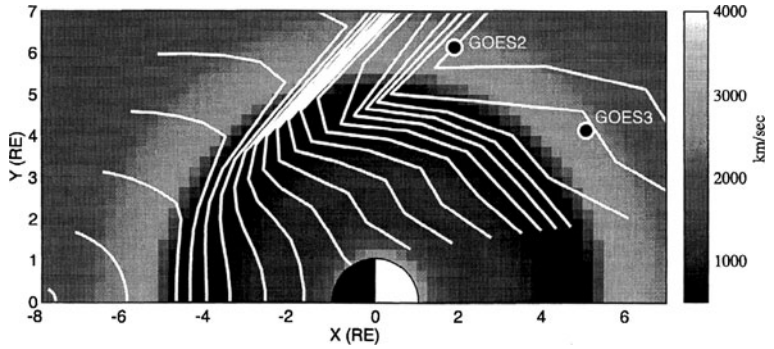

Fig. 40 (From Kepko and Kivelson 1999) Model calculations of compressional wave propagation through the inner magnetosphere from the nightside to the GOES 2 and 3 spacecraft

Clemens (Mcl) ground station recorded a Pi2. Mcl was located in the flank region. In addition, the two geosynchronous spacecraft GOES2 and GOES3, located outside the plasmasphere in the dayside, recorded Pi2 pulsations as a fast mode wave. The oscillations were time-delayed with regard to the oscillations at ISEE 2, namely, ∼40 s and ∼60 s later at GOES3 and GOES2, respectively, and ten seconds after reaching GOES2, the signal reached Mcl. Model calculations of compressional wave propagation through the inner magnetosphere were consistent with the observed time delays (Fig. 40). Thus, the authors proposed that periodic flow burst braking in the nightside region generated compressional pulses that propagated to the dayside flank (recorded by the GOES spacecraft), where they coupled to Alfvén waves (recorded at conjugate ground stations).

Later, Kepko et al. (2001) pointed out that in this scenario Pi2 pulsations should appear as odd-mode pulsations in the magnetic field: magnetometers in the opposite hemisphere would measure the X (or H) component in phase and the Y (or D) component out of phase. This was indeed observed for their events. However, this polarization is not unique for this scenario (cf. cavity resonance). It could further be asked whether the GOES observations of compressional Pi2 are consistent with the PVR model (Sect. 2.2), which allows for compressional power outside the plasmasphere in association with low-latitude Pi2 pulsations. However, the temporal sequence of events (GOES recorded the Pi2 earlier than on the ground) and the Kepko and Kivelson's model calculations are convincing evidence that PVR should be ruled out. Moreover, the peculiar temporal ordering of the Pi2 pulsations recorded by GOES2 and GOES3 was explained by their model calculations.

In addition to driving compressional waves, periodic flow bursts generate inertia currents during their deceleration in the near-Earth plasma sheet. As proposed by Kepko et al. (2001), these can be recorded as Pi2 pulsations at middle and high latitudes in the nightside. They further argued that for small ionospheric conductivity the Alfvén waves launched by each flow burst would not bounce back, as is the case in the TR model (Sect. 3.1). Therefore, the resulting ground Pi2 has the same period as the periodic flow bursts. This also requires that the larger SCW-associated Alfvén waves, if present, of the TR model do not bounce back, so that the smaller BBF-associated signal remains discernable. It was argued that the amplitude of the BBF-associated ground Pi2 riding on top of a magnetic bay would be a few nT and would not necessarily show a decaying trend, as it does for the TR model. This type of Pi2 is illustrated in Fig. 41, showing an event that occurred during a small auroral breakup. The perpendicular flow velocity measured by Geotail at ∼13 R_E qualitatively resembles the waveforms of the magnetic field from three ground stations in the nightside, covering a

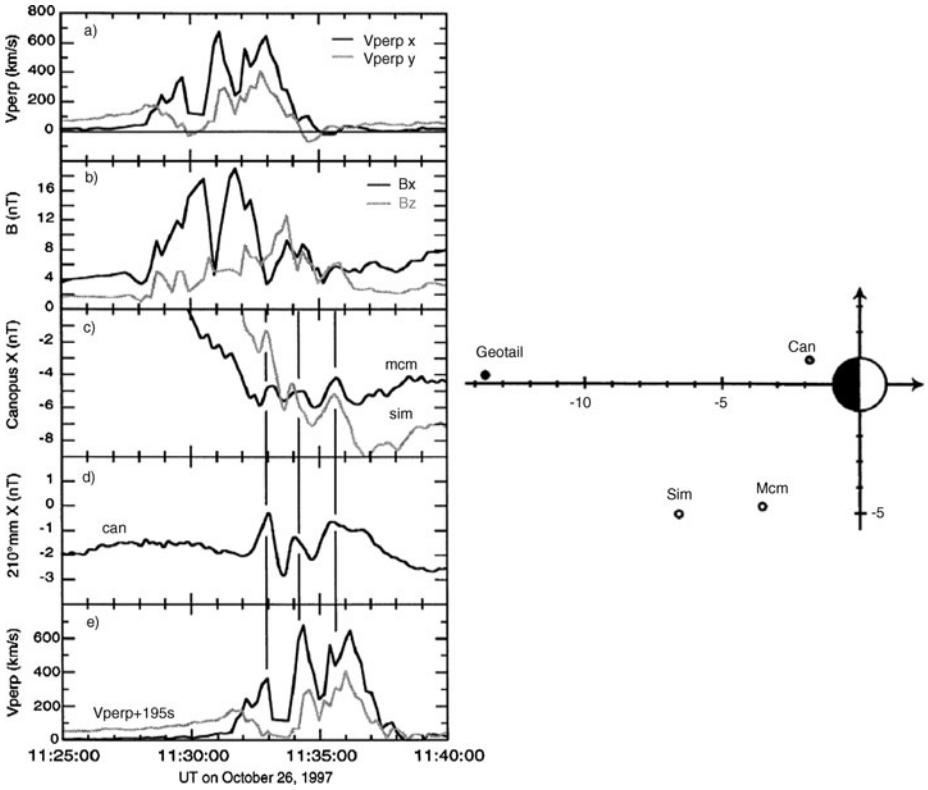

Fig. 41 (From Kepko et al. 2001) Plasma flow and magnetic field data of a Pi2 observed at the Geotail spacecraft and at ground stations. Ground stations have been mapped to the GSM equatorial plane (*right*). In the *bottom panel on the left*, the velocity data were time-shifted to emphasize correlations with the ground Pi2 signal

range of L values. The bottom panel shows the same Geotail data time-shifted by ∼3 min. It was suggested that the effect of the BBF-driven inertia currents caused the ground Pi2. Similar to the BBF-driven low-latitude, flank Pi2 pulsations, the Pi2 stops when the flows stop. Also note that the amplitude variations of the ground Pi2 are not damped in the way they are for the TR-Pi2.

There have been very few reports on observed correlations between periodic flow bursts and ground Pi2 pulsations. Some additional reports have given indirect evidence for the BBF-driven model without actually observing periodic flow bursts. We next review two such reports. Before the first observations of Pi2-related BBFs, Osaki et al. (1998) suggested that plasmaspheric Pi2 pulsations could be driven by an external (to the plasmasphere) source such as BBFs. In their study, two nightside Pi2 events covering a range from low to middle latitudes were correlated with two plasmaspheric Pi2 pulsations recorded by the Akenobo satellite. Using both magnetic and electric field measurements (left side of Fig. 42), each plasmaspheric Pi2 was found to be traveling Alfvén waves along magnetic fluxtubes for a duration of approximately 400 seconds (i.e., approximately four wave cycles). There was no indication of reflected waves, as inferred from the Poynting flux calculations (right side of Fig. 42). The authors calculated a strong ionospheric damping rate (ionospheric absorption) for Alfvén waves, consistent with the lack of reflected wave power (see also Fig. 50b and

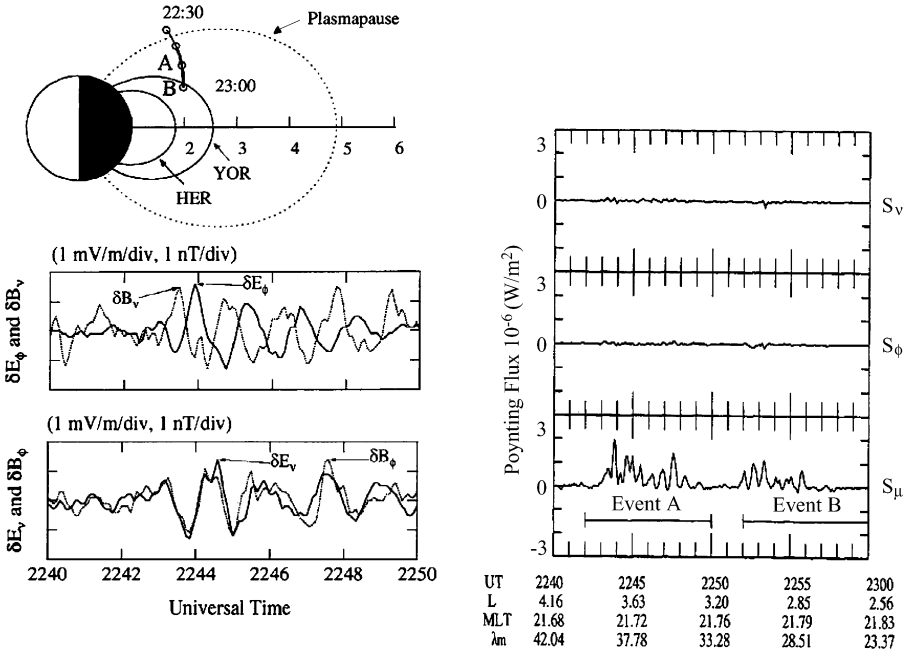

Fig. 42 (From Osaki et al. 1998) (*Top*) Partial orbit of the Akebono satellite on February 13, 1990, including two Pi2 events. The plasmapause ($L \sim 4.9$) is indicated with a *dashed line*. (*Bottom*) Comparison of the phase between the orthogonal components of the electric and magnetic fields of the plasmaspheric Pi2 pulsations. (*Right*) Poynting flux calculation for event A and event B, showing unidirectional energy flow (*last panel*)

further discussion in Sect. 4.1). Due to this energy leakage, it was argued from an energy budget calculation that a plasmaspheric cavity resonance would have been damped in a much shorter time than the duration of the observed Alfvén waves. Therefore, the authors concluded that a driver external to the plasmasphere was the more plausible explanation for both Pi2 events than a PCR/PVR mode.

A signature that might be expected for a ground Pi2 resulting from BBF-driven inertia currents is a polarization pattern as shown by Lester et al. (1983) (Fig. 26 in Sect. 3.1). Such a polarization pattern was shown for a Pi2 event suggested to be driven by periodic flow bursts. Kim et al. (2005a) reported a Pi2 event with identical waveforms and a common frequency of 11 mHz at low- to high-latitude ground stations. The Pi2 hodograms were almost linearly polarized and the major axes of the polarization ellipses were directed toward a common location, possibly the center of the Pi2 current system (Fig. 43). Although plasma flow data inside the plasma sheet were not available, the authors suggested that the source of the ground Pi2 might have been the field-aligned inertia current oscillation associated with periodic flow bursts, according to the scenario of Kepko et al. (2001). Using a global image of the plasmasphere from the IMAGE satellite, the plasmasphere was found to be small and strongly asymmetric in longitude (left in Fig. 43). Consequently, it was further argued, using additional model calculations, that the frequency of 11 mHz was too low for either the PCR (Sect. 2.1) or the PVR (Sect. 2.2) mode. The fact that the largest oscillations were observed at ground stations outside the plasmasphere is further evidence against the PCR/PVR mode.

Finally, it needs to be asked under what geomagnetic conditions BBF-driven Pi2 pulsations occur. While the events presented by Kepko et al. (2001; their Fig. 1) occurred during

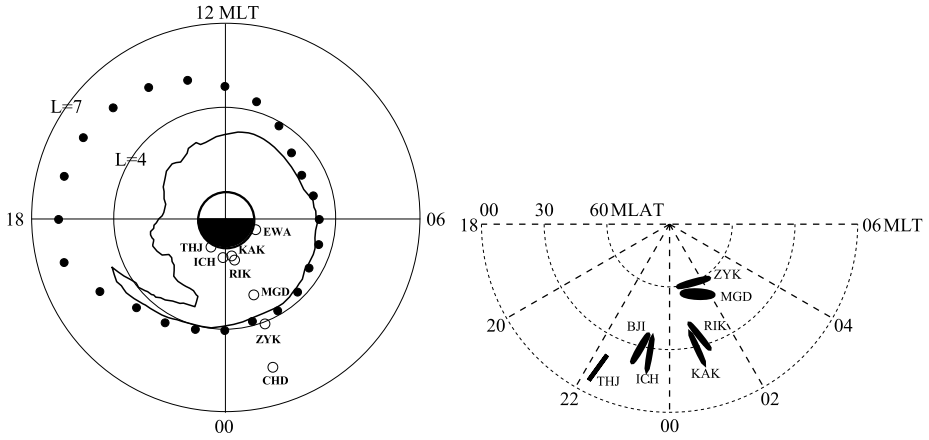

Fig. 43 (From Kim et al. 2005a) (*Left*) Plasmapause location in the L-MLT plane during the Pi2 event on 29 August 2000 (*solid curve*). The *solid circles* outside the plasmapause at each local time indicate the locations where the plasma density reaches a value typical of the plasmatrough. The locations of ground stations are indicated by open circles. (*Right*) Magnetic field hodograms incorporating both the azimuth and the ellipticity of the polarization ellipses of the Pi2 pulsation observed at middle and low latitudes

AE disturbances, they were not associated with the typical, sharp drop in *AL* of substorms. In contrast, the event reported by Kim et al. (2005a) occurred during a large drop in *AL* and the magnetosphere was very active. Currently, the small number of reported BBF-driven Pi2 events does not allow a more detailed analysis of the geomagnetic conditions.

3.4 Pulsed Reconnection

3.4.1 Model

The Pi2 model reviewed in this section was first based on an association of lobe Pi2 pulsations with another magnetic structure, called a TCR. TCRs are compressions in the lobe magnetic field with a characteristic bipolar B_z signatures, indicating a bulge-like appearance (Fig. 44). They are thought to be the remote signature of reconnection (Slavin et al. 1984, 2003; Sergeev et al. 1992; Taguchi et al. 1998). Although they often occur as a single compression event, TCRs can also occur as a series of compression events with temporal separation of less than 150 s (Slavin et al. 2005). Their temporal evolution has been modeled using a time-dependent Petschek-type model of reconnection (e.g., Semenov et al. 2005). Using the Pi2-like periodicity of multiple TCRs as an indicator of pulsed reconnection, it has been argued that reconnection itself is the frequency source of some ground Pi2 pulsations (Keiling et al. 2006).

It can be argued that especially high-latitude Pi2 pulsations are generated by this mechanism. There is also indication that it is associated with smaller substorms/pseudo-breakups and PBIs, rather than with more intense geomagnetic activities. PBIs are high-latitude phenomena that have been shown to be associated with Pi2 pulsations that are more localized and vary with latitude (Kim et al. 2005a). Kim et al. (2005a) speculated that PBI-Pi2 pulsations are generated by a source in the magnetotail, and Keiling et al. (2008a) provided observational evidence for pulsed reconnection.

Three propagation models for how the Pi2 signal at the reconnection site reaches the ground have been proposed (Fig. 45). TCRs have been associated with BBFs inside the cen-

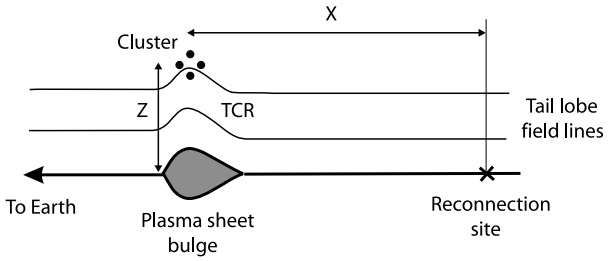

Fig. 44 (After Semenov et al. 2005) Cartoon illustrating TCR propagation and its encounter with the Cluster spacecraft

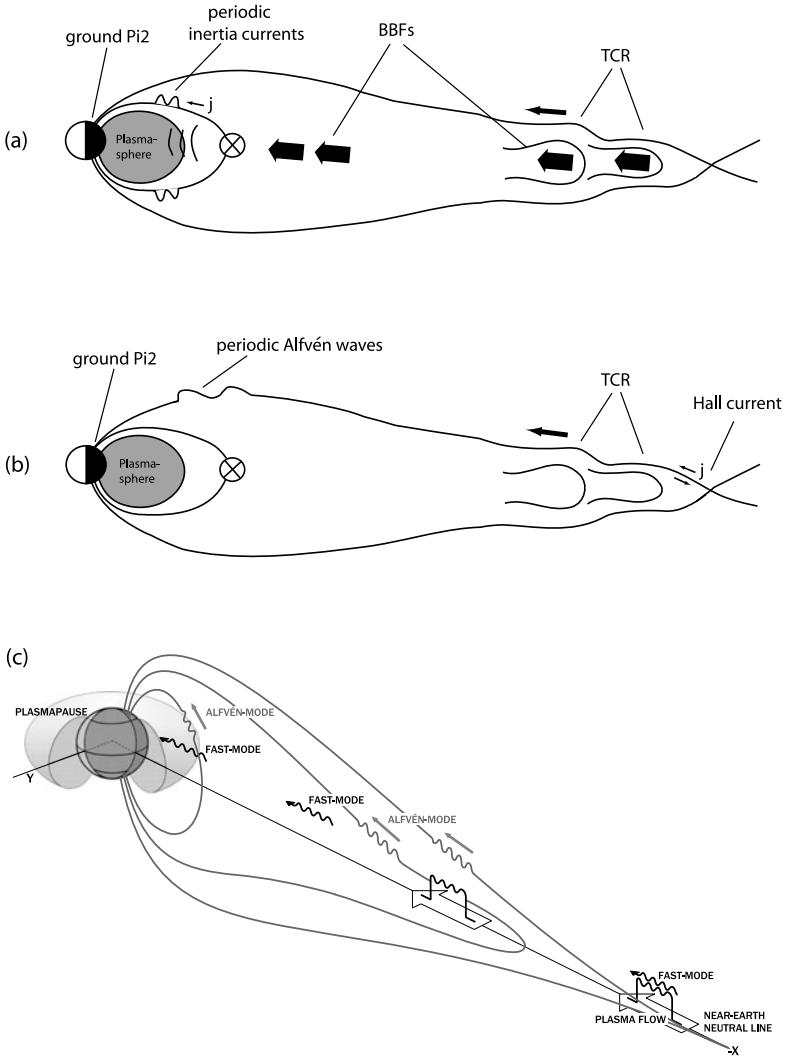

Fig. 45 Schematic showing three proposed propagation paths by which reconnection-driven Pi2 pulsations could reach ground. (**a**, **b**) After Keiling et al. (2006); (**c**) modified from Murphy et al. (2011)

tral plasma sheet (e.g., Slavin et al. 2003). Thus, those BBFs could cause ground Pi2 pulsations by the same sequence of events as described in the BBF-driven Pi2 model (Sect. 3.3). In another propagation model, the PSBL, which presumably maps closest to the reconnection site, is the primary transport layer of the Pi2 signal (Keiling et al. 2006). Transient Hall currents, connecting directly to the ionosphere from the reconnection region (e.g., Snekvik et al. 2009), propagate as Alfvén waves along PSBL field lines to the ground resulting in ground Pi2. The third propagation model is based on the Tamao travel time concept (Tamao 1964; Uozumi et al. 2000; Chi et al. 2001). It is assumed that pulsed reconnection launches periodic compressional disturbances which propagate along the magnetotail and couple to Alfvén waves on different L shells that in turn cause ground Pi2s (Murphy et al. 2011).

Currently, it is neither understood what triggers a reconnection pulse, nor what dictates the periodicity of reconnection pulses and their repetition number. These properties could be intrinsic to the reconnection phenomenon, but it is also conceivable that they are controlled away from the reconnection region (such as the magnetopause or a wave guide in the lobe region), in which case pulsed reconnection would only be an intermediate energy step and the actual frequency source for this model would lie outside the reconnection site.

3.4.2 Observations

Recorded by four Cluster spacecraft at 16 R_E in the tail lobe during a substorm, multiple Earthward-propagating (∼700 km/s) TCRs were one-to-one correlated with individual wave cycles of a ground Pi2 with a 90-s period (Fig. 46). Since the magnetic field of the TCRs resembled that of typical Pi2s in the inner magnetosphere, Keiling et al. (2006) coined them *lobe Pi2*. Location and propagation direction determined from multipoint measurements rule out that the lobe Pi2 was generated in the inner magnetosphere. Using analytical calculations, Semenov et al. (2005) argued in an independent study that the same TCRs were the result of multiple impulsive reconnection events from possibly a single X line, estimated to be located at about 30 R_E. This would imply that the time variation of transient reconnection (i.e., pulsed reconnection) actively controlled the Pi2 frequency as recorded on the ground (Keiling et al. 2006).

It was peculiar that the ground Pi2 was first recorded at high latitude followed by mid- and low-latitude Pi2 pulsations. One possible propagation scenario (Fig. 45a), discussed by Keiling et al. (2006), is that BBFs inside the central plasma sheet, which could have caused the TCR signatures in the lobe, caused the high-latitude Pi2 according to the scenario described in Sect. 3.3. However, it was noted that the time delay of the Pi2 signal from 16 R_E to the ground was only 30 s, which is difficult to reconcile with plasma flows in the central plasma sheet. Further, Keiling et al. (2006) showed that the high-latitude Pi2 occurred before the formation of the auroral electrojet intensification (the SCW), which also argues against the TR model (Sect. 3.1). Moreover, the magnetic field amplitude of the ground Pi2 was much larger than expected for BBF-driven Pi2 (Sect. 3.3).

In an alternative propagation path, proposed by Keiling et al. (2006), the Pi2 disturbance at the reconnection site travels possibly as an Alfvén wave through the PSBL (Fig. 45b). Arguments for this path are that the first and largest ground disturbances occurred near the polar cap boundary, and that simulation results show that the speed and amplitude of an Alfvénic structure is greater in the PSBL than in the central plasma sheet (Wright and Allan 2008; Lysak et al. 2009). In fact, during the substorm expansion phase large-amplitude Alfvén waves with estimated periods between 60 and 120 s have been reported in the PSBL

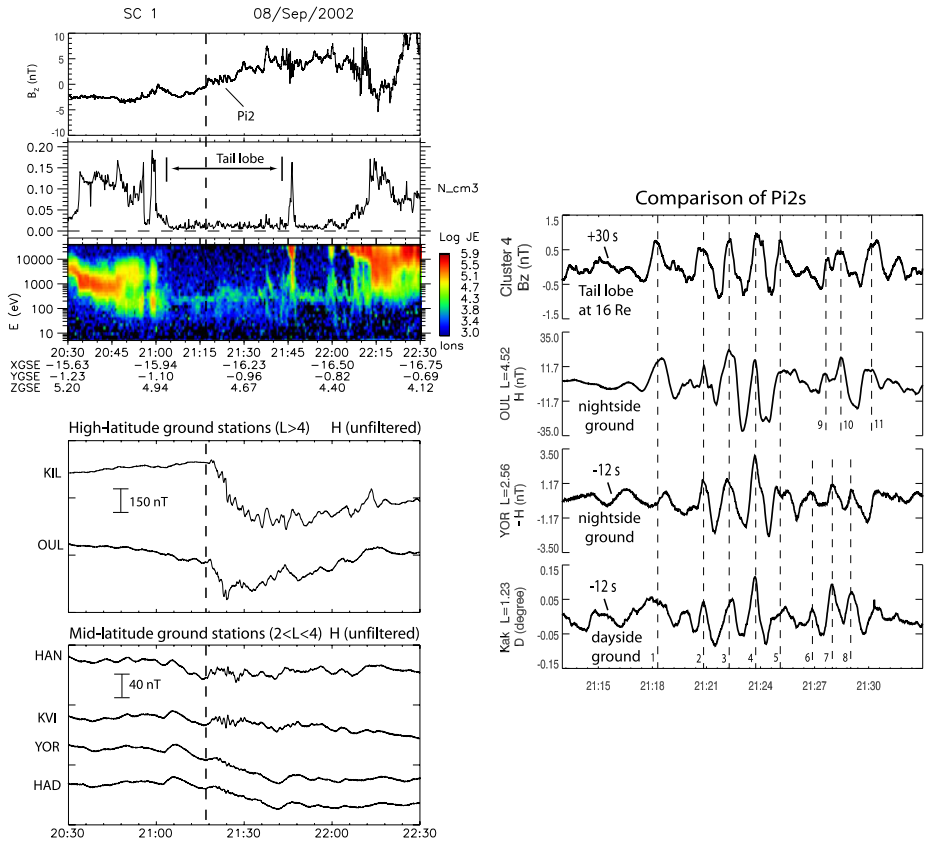

Fig. 46 (From Keiling et al. 2006) (*Left*) Satellite- and ground-based observations of the Pi2 event on 8 September 2002. The *vertical dashed line* marks the onset of the tail lobe Pi2 (first panel). (*Right*) Comparison of in-situ (Cluster), nightside and dayside ground data for the Pi2 event. The data were band-pass filtered (4 s, 150 s). Note the time shifts

before (Keiling et al. 2000). At the same time, these large waves are accompanied by smaller Pi2-like pulsations, often in the form of standing Alfvén waves in the tail lobe, which are one-to-one correlated with pulsations in the polar cap (Keiling et al. 2005). We also note the study by Volwerk et al. (2008) who reported Pi2-like oscillations in the tail lobe that traveled tailward, which are consistent with this propagation path, if they are interpreted as waves reflected off the ionosphere.

It is also mentioned that the reconnection site generates Hall currents of considerable intensity, and the field-aligned component of these currents is thought to directly link to the ionosphere (e.g., Snekvik et al. 2009). Furthermore, Keiling et al. (2006) investigated the polarization pattern of the ground Pi2, associated with the event in Fig. 46, and found it to be similar to that of Lester et al. (1983) (Fig. 26 in Sect. 3.1), namely, that the azimuths of the polarization ellipses pointed towards the center of the upward current. It was speculated that the Hall current in the PSBL created this polarization pattern.

In a second study, relating lobe Pi2 pulsations (TCRs) and ground Pi2 pulsations, Keiling et al. (2008a) reported three events at 18 R_E (using the Cluster spacecraft), all of which occurred in succession during a geomagnetically quiet, non-substorm period (Fig. 47). Each

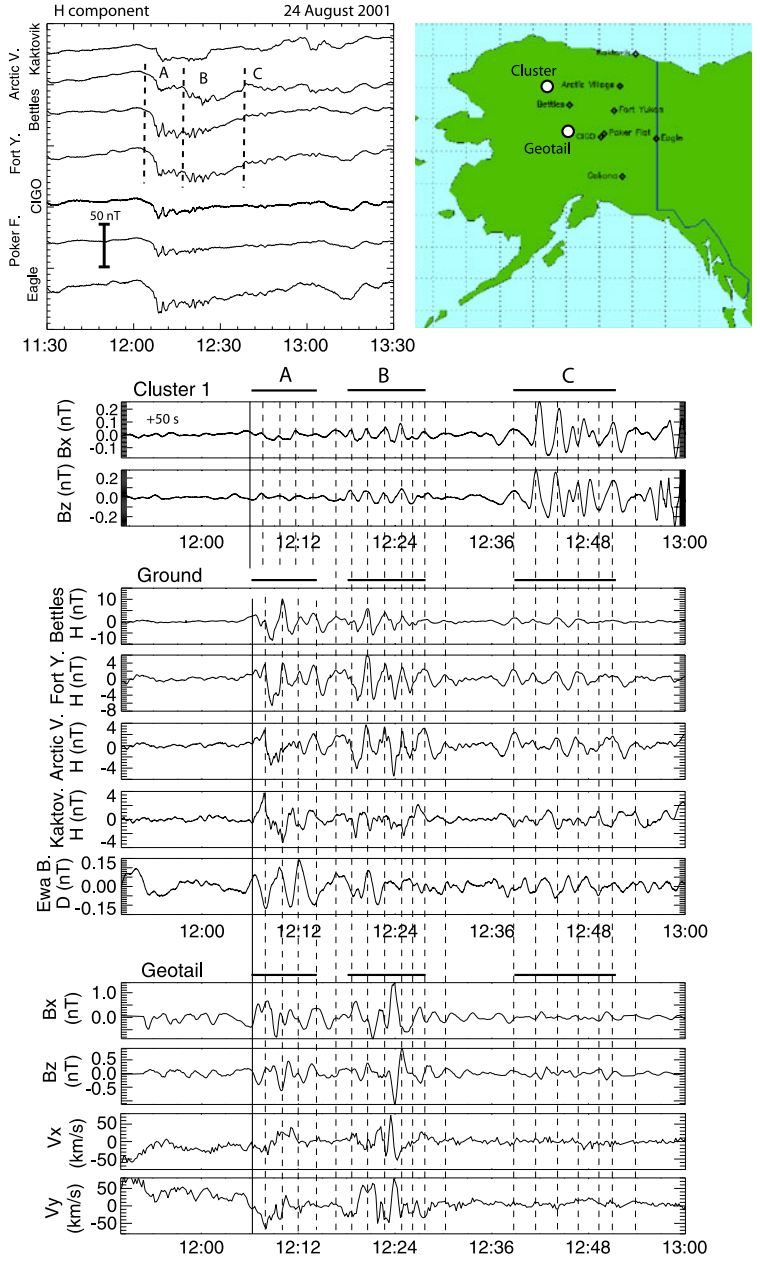

Fig. 47 (From Keiling et al. 2008a) *Top right*: Geographic map showing the GIMA ground stations and Cluster's and Geotail's footprints. *Top left*: Magnetometer data (24 August 2001) from GIMA ground stations. Labels A, B, and C indicate ground Pi2 events. The *dashed lines* mark the onsets of small bay-like deflections of the *H* component. *Bottom*: Comparison of Cluster, ground, and Geotail data during the events on 24 August 2001. All data were band-pass filtered (40 s, 150 s) except the flow data of Geotail (*last two panels*). The ground data are from GIMA stations: Bettles ($L = 6.35$), Fort Yukon ($L = 6.2$), Artic Village ($L = 6.47$), Kaktovik ($L = 7.5$), and the 210MM station: Ewa Beach ($L = 1.6$). Note that B_X of Cluster is shifted by 50 s

lobe event was associated with an interval of small H-bay-like ground disturbance (<40 nT). Such disturbances have been identified as poleward boundary intensifications (PBIs). The small H bays were superposed with Pi2 pulsations. Each lobe Pi2 showed one-to-one correlations with a ground Pi2 (Fig. 47). Pi2 pulsations associated with PBIs do not show as high a coherence among ground stations as substorm Pi2 pulsations (Kim et al. 2005a), as can be seen in this event. Using the Geotail satellite, which was located closer in at 9 R_E, it was shown that similar—but not identical—variations in **B** and flow velocities were only recorded closer to the outer edge of the plasma sheet. Together with the fact that the ground Pi2 pulsations were recorded at high latitude, this suggests that the Pi2 did indeed travel close to or at the outer edge of the plasma sheet, thus favoring scenario (b) in Fig. 45. It is also important to note that low-latitude Pi2 were observed during both studies (Keiling et al. 2006, 2008a), thus begging the question of how the Pi2 signal travelled from high latitude to low latitude.

In a very recent study, Murphy et al. (2011) used Geotail and ground-based data (Fig. 48) to examine the causality of the link between BBF flow bursts and Pi2 waveforms. The event occurred during a small magnetic bay (H component), typically associated with PBIs and pseudo-breakups. Geotail was located in the magnetotail at $\sim$13 R_E radial distance while recording four flow bursts (bottom panel). The flow burst resembled those that had been reported by Kepko et al. (2001), albeit with slower speed. Ground Pi2 pulsations were recorded on L shells covering low to high latitudes. Although the temporal structure of flow bursts and Pi2 pulsations were very similar (expressed in high correlation coefficients), some ground Pi2 pulsations (e.g., RABB) occurred prior to the flow bursts, ruling out that the flow bursts were the immediate source of the ground Pi2 pulsations, as suggested in the BBF-driven Pi2 model (Sect. 3.3). Instead, similar to Keiling et al. (2006), it was found more likely that both signals had a common source, possibly bursty, or pulsed, reconnection. Assuming that flow bursts and compressional disturbances were generated concurrently at the reconnection site, it was further suggested by Murphy et al. (2011) that along the way the Earthward-traveling compressional disturbances/waves coupled to the background magnetic field creating Alfvén waves that were, in turn, observed on the ground as Pi2 pulsations. Different propagation speeds of flow bursts and MHD waves in the plasma sheet could explain the various time delays observed at ground stations.

Finally, we mention several studies that reported ground ULF wave activity of long duration (one hour and longer) in the Pi2 frequency band. Such wave activity was found during substorm periods as well as quiet, non-substorm periods. In an early study, Singer et al. (1988) noted that for some events Pi2-band wave activity at middle latitudes was enhanced after substorm onset. In contrast, Grocott et al. (2003) and Sutcliffe (2010) showed wave activity at high and low latitude, respectively, during non-substorm intervals. Without available spacecraft evidence, the authors speculated that the wave activity was associated with reconnection events in either the near-Earth region during substorms or the distant tail reconnection during non-substorm periods. Two possible scenarios were proposed. Singer et al. (1988) suggested that Alfvén waves are continuously generated in the reconnection region and are then propagating towards ground middle latitudes. Sutcliffe (2010), on the other hand, speculated that the ground ULF waves are a consequence of the braking of reconnection-associated flow bursts, which, in turn, launch compressional waves that propagate to low latitudes. For either scenario, observations of corresponding wave activity in space were not reported. At this time, it is unclear whether these observations are related to the Pi2 pulsations reviewed here, because the Pi2-band wave activity shows different characteristics from "traditional" Pi2 pulsations. First, the wave activity does not have the typical short duration of only a few wave cycles, and second,

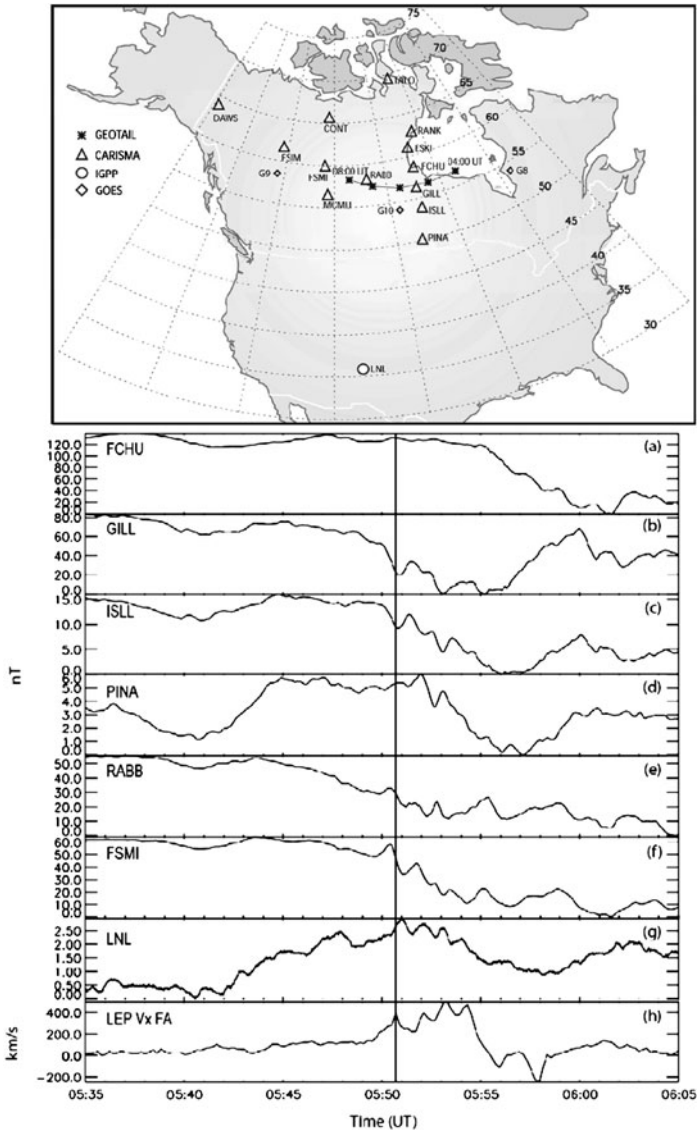

Fig. 48 (*Top*) Ground magnetic field trace of the conjunction between the Geotail spacecraft and CARISMA magnetometer array between 04:00 and 08:00 UT on 31 May 1998. The magnetic footprints of GOES-8, GOES-9 and GOES-10 are also shown. (*Bottom*) A stack plot of the H-component magnetic field for selected CARISMA magnetometers and the Los Alamos (LNL) magnetometer, and the $v_{\perp x}$ plasma flow observed by Geotail between 05:35–06:05 UT. The *vertical line* represents the time of maximum velocity of the first flow burst

the frequency changes more randomly throughout the interval. Perhaps related to these observations are the theoretical results of Horton et al. (2004), showing that ion pressure anisotropies $p_{\parallel} > p_{\perp}$ (firehose instability), possibly associated with the flow braking of magnetotail plasma, produce a wide spectrum of Alfvénic fluctuations in the Pi2 band.

3.5 Summary

In the past decade, Pi2 research saw a revival with the emergence of new Pi2 models, which have broken with the traditional belief that Pi2 pulsations are either generated in the inner magnetosphere or in association with the SCW. Instead, the outer magnetosphere has been explored as a Pi2 source region and surprising correlations of ground Pi2 pulsations with physical quantities—not limited to the magnetic field—in the central plasma sheet and the lobes have been found. Furthermore, the roles of Pi2 pulsations in association with dynamic magnetospheric modes other than substorms, including very quiet times, have been explored. These new data have shown a need for new Pi2 models, completely different from the existing ones.

The TR model is by definition associated with the formation of the SCW (albeit more modern viewpoints are not limited to the SCW). Several mechanisms of SCW initiation have been proposed and research continues to identify the responsible mechanism. This lack of knowledge does not affect the validity of the TR model because the bouncing frequency of Alfvén waves, which establishes the Pi2 frequency, is independent of what launches the waves. The evidence, mostly from the ground, that under these conditions high-latitude (auroral zone) Pi2 pulsations are caused by a westward-moving, transient current wedge is convincing. In contrast, the evidence that substorm-related, mid-latitude (sub-auroral) Pi2 are caused by the TR mechanism has been challenged in recent years. In simulations it has been found that the spatial variations of the Pi2 polarization pattern at middle latitudes, traditionally believed to be associated with the SCW, could also be generated by PCR/PVR. Consequently, two Pi2 models appear to be consistent with the observed mid-latitude polarization pattern, and further work is required to come to a conclusive answer.

While much work has been done on the ground/ionospheric signatures of TR-Pi2 pulsations, spacecraft observations are too few, yet they are required to better understand the magnetospheric portion of the current system and the extent of the Pi2 signal in the magnetosphere (Singer et al. 1985). For example, there are still no observations of bouncing Alfvén waves correlated with ground Pi2. Moreover, the coupling and the transport of MHD modes across magnetic field lines to connect the high-latitude Alfvén waves with the mid-latitude Pi2 (and possible low-latitude Pi2 as well) has not been verified with spacecraft observations for the TR model. Thus, it is advisable to search for such observational evidence, given that the current constellation of spacecraft is the most extensive ever. At the same time, the spacecraft observations should be combined with the ionospheric signatures to elicit the coupling of the magnetosphere and ionosphere, an area still poorly understood in association with TR-Pi2 pulsations.

Despite the dominant role the TR mechanism plays in generating high-latitude Pi2 pulsations, several studies have explained substorm-related, high-latitude Pi2 pulsations with models that discard the notion of Alfvén waves bouncing several times back and forth between ionospheres. Instead, it has been proposed that ground Pi2 pulsations indicate periodic launching of Alfvén wavelets or particle injections from the near-Earth plasma sheet, possibly associated with individual smaller or even larger substorm intensifications. Such periodic intensifications are thought to be caused by a non-propagating, oscillating plasma instability. Furthermore, it has been proposed that propagating, drift ballooning mode perturbations, forming ripples on the inner edge of the plasma sheet (or some energized boundary), could lead to ground Pi2. In this scenario, a diamagnetic drift combined with a system of downward and upward field-aligned currents mimics a temporal Pi2 signature on the ground. We emphasize that the observational evidence for such plasma-instability-driven models is however very limited and additional work is needed to critically evaluate the different scenarios.

To be confident that the plasma-instability-driven mechanism operates for a particular Pi2 event, simultaneous measurements closer to Earth and farther away from Earth are necessary to rule out Alfvén wave bouncing (TR model) or a Pi2 source in the outer magnetotail (BBF-driven or reconnection-driven models). Such comprehensive observations, however, need very fortuitous spacecraft constellations.

We also point out that although there is an extensive body of work on MHD plasma instabilities in the near-Earth plasma sheet associated with substorms, the theoretical understanding is far from conclusive. For decades it has proven difficult to observe the substorm instability in the near-Earth plasma region. This difficulty directly translates to the plasma-instability-driven Pi2 model as well, since it has its source in this instability region. While evidence is growing for ballooning modes with oscillations in the Pi2 frequency band, reports confirming their coupling to ground Pi2 pulsations is very limited. Consequently, it is difficult to characterize the ground signatures that would allow identifying this mechanism. It also remains a major challenge for the proposed plasma instability Pi2 model, as it is for substorm research, to confirm a propagation scenario for the initial Pi2 signal at the instability region to reach the ground.

One important realization in the last decade has been that Pi2 sources are not confined to the inner magnetosphere or the near-Earth plasma sheet but can be found in the extended magnetotail. Two models have been proposed based on different observations in the magnetotail. The BBF-driven model was proposed to explain surprising correlations between velocity-modulated flow bursts and ground Pi2 pulsations observed in the nightside region and on the flanks. The reconnection-driven model was proposed to explain surprising correlations between Earthward-propagating TCRs (lobe Pi2 pulsations) and ground Pi2 pulsations observed at low to high latitudes in the nightside region. Although the data are convincing for a few events, a paucity of reports, supporting either the BBF-driven or the reconnection-driven scenario, shows that both models are still speculative. Clearly, additional observations are necessary to critically evaluate them. In particular, it remains to be seen if both models truly describe two different Pi2 generation mechanisms, or whether they are simply different propagation models of one Pi2 mechanism. Indeed, there is some preliminary evidence that the reconnection-driven model encompasses the BBF-driven model as a subset of propagation paths.

A shortcoming of both models is that none of the two time constants (see Sect. 1) have been addressed so far: "how is the characteristic Pi2 frequency (repetition rate of individual flow bursts or reconnection bursts) established?", and "what determines the duration of the Pi2 pulsations (the length of the BBF train or the number of reconnection bursts)?" We note that the actual Pi2 source, as defined in Sect. 1, in the BBF-driven model remains unspecified. The Pi2-like flow bursts are only a consequence of an as-of-yet unknown Pi2 source mechanism which controls the periodicity. Therefore, the BBF-driven model is in fact only a *temporary* model, waiting to be replaced by a more fundamental model. For the reconnection-driven model, it is not understood yet how transient reconnection is controlled, so that it "turns on and off" at the Pi2 frequency during certain geomagnetic conditions. How such reconnection events are different from those that only show one reconnection "burst" is not understood, either. Hence, it is conceivable that the reconnection-driven model be replaced by a more fundamental Pi2 model, as well, if it turned out that the Pi2 period is established away from the reconnection site (e.g., the lobe region).

Another major challenge for both outer-magnetospheric models is the verification of the propagation paths. The BBF-driven model proposes various paths of the Pi2 signal from the flow braking region to different places on the ground. These paths, however, lack observational evidence in space. Similar, the various propagation paths of the initial Pi2 disturbance

at the reconnection site to the ground are speculative. Several other outstanding tasks remain for both models. A systematic description of the properties of the ground Pi2 pulsations needs to be done, including polarization analysis and spatial extent. Characterization of the BBF evolution along the magnetotail would be helpful in verifying this model. In particular, Kepko and Kivelson (1999) pointed out a potential difficulty in identifying additional events, owing to the possibility that individual flow bursts in the train of bursts might propagate with different speeds, so that no constant time shift can be applied to all individual flow bursts for comparison with the ground Pi2 pulsations.

4 Propagation Modes

The energy for all types of Pi2 pulsations comes from the Sun, enters the magnetosphere, and propagates along the magnetotail towards the ionosphere and the ground. In the previous two sections, we reviewed where and how the initial Pi2 signal is generated, according to different models. Once the characteristic Pi2 frequency has been generated, the Pi2 signal travels possibly via several propagation paths—while maintaining its periodicity—to the ground and other remote regions before it dissipates. Each path constitutes a sequence of energy transfer processes (mode conversion) from one propagation mode to another. In this section, we review mode conversion processes and propagation modes that have not been covered in the previous sections. We limit the review to processes that maintain the defining property of Pi2 pulsations, namely, the period (frequency). It is important to note that mode conversion does not constitute an independent Pi2 frequency source, since all it does is to pass the Pi2 frequency from one physical quantity onto the next. We also emphasize that these processes are not unique to a specific Pi2 model but could occur for several of them.

Our knowledge of mode conversion and propagation modes associated with Pi2 pulsations has benefited from the larger number of spacecraft that have become available in the last decade, allowing multipoint observations. An important tool has also come from computer simulations that allow us to fill in data gaps that exist in the vast space between observation points. Nevertheless, much work is needed to gain a better understanding of this aspect of Pi2 pulsations.

4.1 Coupling of Fast and Alfvén Modes

A fast mode wave in the magnetosphere can couple to standing Alfvén waves when the frequency (ω) and the parallel wavenumber (k_z) of the fast mode wave match those of a standing Alfvén wave. In this field line resonance (FLR) process, "resonance" means that the standing Alfvén wave resonates with the fast mode wave (driver wave). In the theoretical formulation of Chen and Hasegawa (1974a), ω and k_z of the driver wave were determined from the Kelvin-Helmholtz instability (KHI) condition under the constraint of field line tying at the ionosphere. In the inner magnetosphere the driver wave can be a PCR/PVR mode, which has a different frequency selection mechanism from the KHI. Nonetheless, the end result of the coupling is the same (Allan et al. 1986a; Lee and Lysak 1989; Zhu and Kivelson 1989; Samson et al. 1992): the Alfvén wave is sharply localized to resonant L shells.

Evidence of FLR associated with Pi2 pulsation has been presented. Fukunishi (1975) found a polarization reversal at $L \sim 4$ and attributed the observation to field line resonance occurring near the plasmapause. Keiling et al. (2001) combined ground and satellite (Polar) observations to obtain a detailed picture of Pi2-associated FLR. As shown in Fig. 49a, two

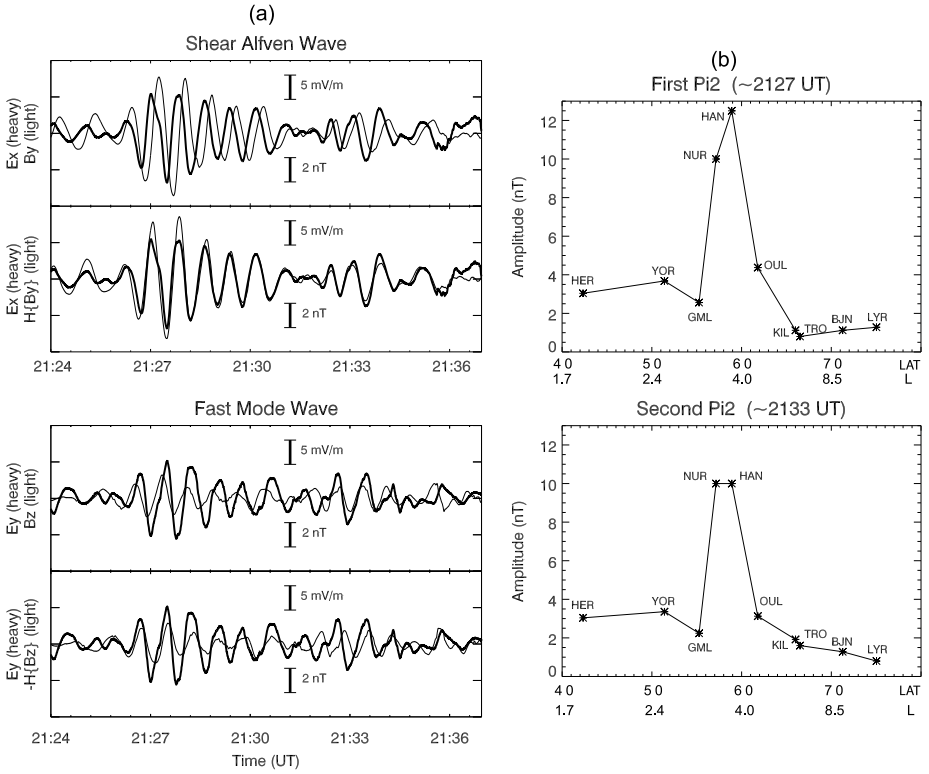

Fig. 49 (From Keiling et al. 2001) Two successive Pi2 pulsations observed by the Polar spacecraft and ground magnetometers. (**a**) Electric and magnetic field components of shear Alfvén and fast mode waves recorded by the Polar satellite. $H\{\}$ indicates the Hilbert transform, which phase-shifts all frequency component by 90°. (**b**) Latitudinal profile of the Pi2 amplitude constructed from the H component at several ground stations

Pi2 pulsations occurred in close succession as the satellite moved from $L = 4.3$ to 3.7. The first event was a trapped fast mode, while the second was propagating tailward as inferred from the phase relation between E_y and B_z (lower panel of Fig. 49a). On the ground, H showed a strong amplitude peak at $L \sim 4$ (Fig. 49b), while Polar detected toroidal standing Alfvén waves (Fig. 49a, upper panel). Keiling et al. (2001) argued that for the first Pi2 FLR coexisted with a cavity mode.

Collier et al. (2006) also reported standing Alfvén waves associated with compressional Pi2 pulsations. The standing nature of the Alfvén waves was deduced by calculating the field-aligned component of the Poynting flux. While three spacecraft (Cluster) were inside the plasmasphere, $L = 4.7, 4.5$, and 4.6, one was located at or just outside the plasmapause ($L = 6.6$). Interestingly, the event was clearly observed only on those spacecraft that were inside the plasmasphere. The study also provided evidence for the coupling of standing fast mode waves and FLR inside the plasmasphere. These observations are suggestive of a cavity resonance within the plasmasphere, and the relative phase between satellites located on either side of the geomagnetic equator indicates that the FLR was an odd harmonic (Collier et al. 2006).

In addition to standing Alfvén waves coupled with fast mode waves at a common frequency, cases have been reported in which toroidal Alfvén waves are impulsively ex-

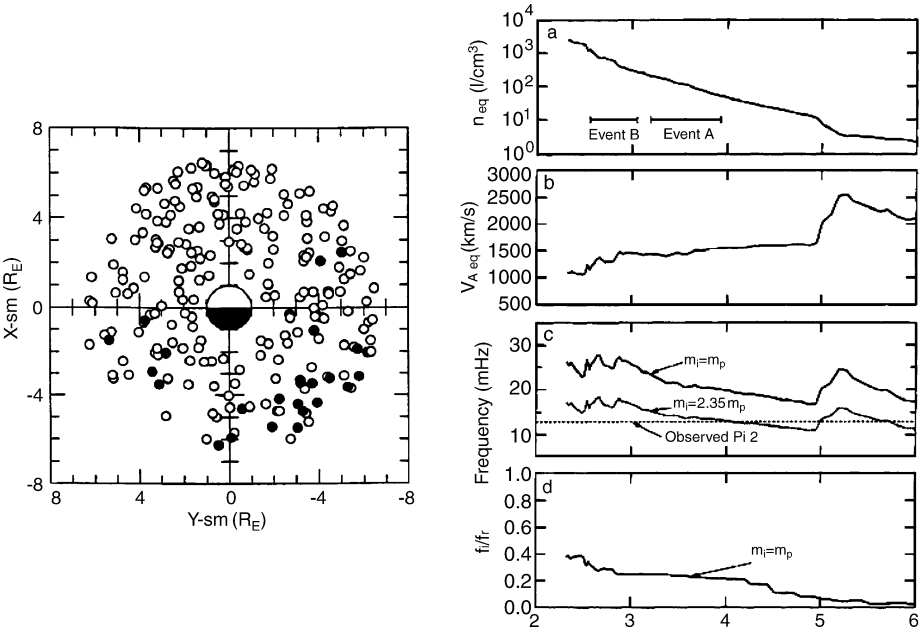

Fig. 50 (*Left*) (From Takahashi et al. 1996) *Circles* indicate the location of the AMPTE/CCE satellite at the time of ground Pi2 detected at Kakioka ($L \sim 1.3$) near midnight. A *solid circle* is used if the satellite detected a transient toroidal wave, and an *open circle* if it did not. (*Right*) (From Osaki et al. 1998) L profile of parameters associated with two Pi2 successive pulsations observed with the Akebono satellite in the plasmasphere. From top to bottom: Electron number density, equatorial Alfvén velocity, theoretical frequency of the fundamental toroidal wave for two assumed values (in proton mass m_p) of average ion mass m_i, and the normalized damping rate f_i/f_r for average for $m_i = m_p$, where f_i and f_r are the imaginary and real parts of the toroidal frequency. The damping comes from ionospheric Joule dissipation

cited near geosynchronous orbit and beyond with L-dependent frequency (e.g., Sakurai and McPherron 1983; Takahashi et al. 1988, 1996; Saka et al. 1996; Nosé et al. 1998; Keiling et al. 2003). This phenomenon is similar to dayside pulsation events triggered by solar wind dynamic pressure pulses (e.g., Petrinec et al. 1996). An impulsive disturbance occurring in the near-Earth magnetosphere in effect provides a broadband wave source for magnetic field lines to ring over a wide range of L (Hasegawa et al. 1983).

Excitation of standing Alfvén waves depends on the conductivity of the ionosphere at the footprint of the magnetic field lines, and not all field lines in the plasmasphere can participate in field line resonance. Specifically, deeper into the plasmasphere the ionospheric Pedersen conductivity becomes too low on the nightside to sustain long-lasting Alfvén waves. Takahashi et al. (1996) reported that substorm-triggered toroidal waves (transient toroidal waves) are rare inward of $L = 3$ (Fig. 50a) despite the fact that poloidal Pi2 pulsations are readily detected there (Takahashi et al. 1992 1995). A model calculation of the ionospheric damping rate for toroidal waves (Fig. 50b) indicates that the damping becomes stronger for smaller L and explains why transient toroidal waves do not occur at $L < 3$. The absence of field line resonance also explains why there is little phase variation with L for low-latitude Pi2 pulsations observed on the nightside (Shinohara et al. 1997). A field line resonance should introduce a rapid latitudinal phase shift around the latitude of the resonance (Chen and Hasegawa 1974a; Southwood 1974).

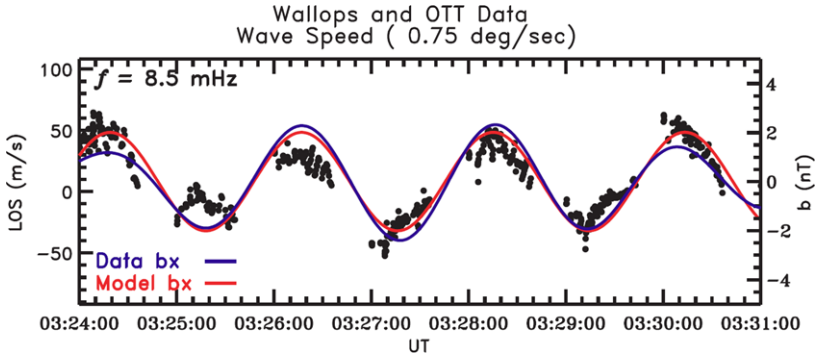

Fig. 51 (From Gjerloev et al. 2007) A Pi2 pulsation event at $L = 3.2$ observed with the SuperDarn radar

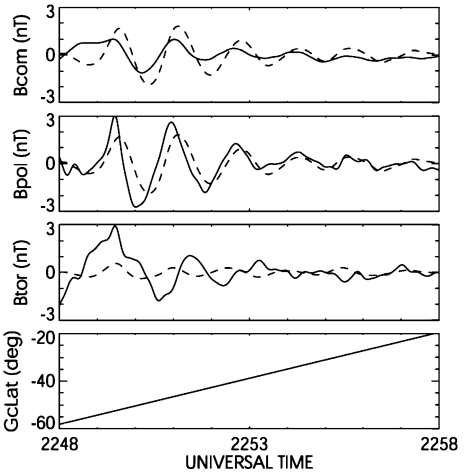

Fig. 52 (From Sutcliffe and Lühr 2003) A Pi2 pulsation observed by the CHAMP spacecraft (*solid* curve) in the southern hemisphere. The *dashed curves* are the magnetic field observed on the ground (the curves in the *top two panels* are the H component, and *the curve in the third panel* is the D component). For the satellite data B_{comp}, B_{pol}, and B_{tor} are the total field (B_z), transverse and inward ($-B_x$), and transverse and eastward (B_y) components, respectively

Alfvén waves driven by the PCR/PVR mode may strongly contribute to Pi2 signals detected on the ground. Figure 51 shows a Pi2 pulsation detected by the SuperDarn radar (Gjerloev et al. 2007). The observation was made at $L = 3.2$ and 2300 MLT, and the pulsation had $m = 2.3$. Model calculation of MHD wave propagation through the ionosphere (Sciffer et al. 2004) indicated a mixture of 99.8% shear Alfvén wave and 0.2% fast mode wave. This mixture, which is much biased toward the shear mode in light of LEO observations that indicate a strong compressional component (shown below in Fig. 52), warrants further investigation, ideally using observations made while a LEO satellite is in the field of view of the radar.

4.2 Propagation Through the Ionosphere

How the ionosphere modifies magnetospheric ULF waves is an important question in deducing the wave modes in the magnetosphere from ground observations. We refer the reader to the theoretical treatment of this topic by Southwood and Hughes (1983) and the references therein. An observational approach to this topic is to compare magnetic field perturbations below (on the ground) and above (with satellites on low-earth orbits) the ionosphere. This technique has been applied to Pi2 pulsations using magnetic field data from UARS

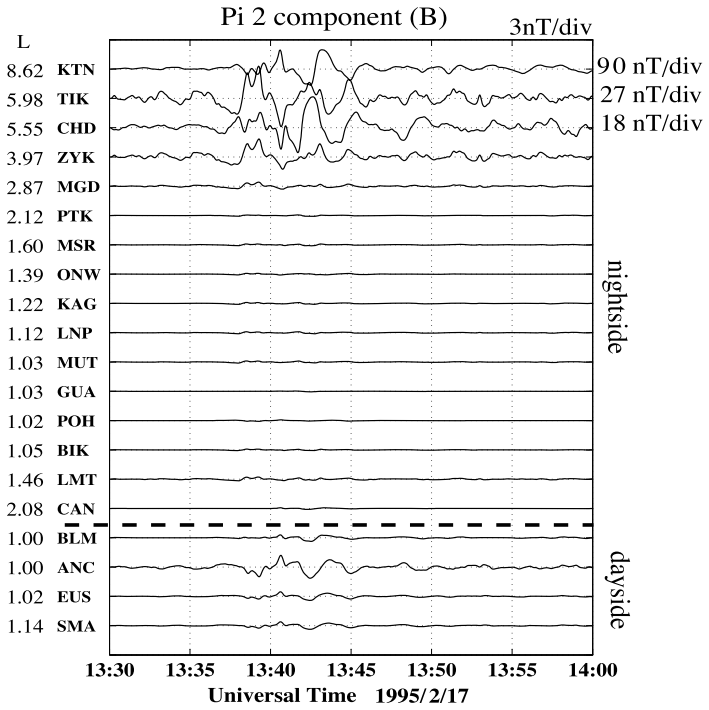

Fig. 53 (From Tokunaga et al. 2007) An example of independent component decomposition of Pi2 signals. The Pi2 oscillations are localized to the high-latitude region on the nightside but appear on the dayside at the equator in nearly identical waveform

(Takahashi et al. 1999), CHAMP (Sutcliffe and Lühr 2003), and Ørsted (Jadhav et al. 2001; Han et al. 2004).

As an example, an observation by the CHAMP satellite (altitude ~450 km) in the southern hemisphere is shown in Fig. 52. At the satellite $Bpol\ (= -B_x)$ and $Bcom\ (= B_z)$ oscillate in phase. The B_x and B_z oscillations are similar to the H oscillation detected on the ground near the satellite, and B_z and H are nearly in phase. The toroidal component B_y also has a substantial amplitude at the beginning of the event, but it diminishes rapidly compared to the poloidal components. In the Ørsted study (Han et al. 2004), in-phase oscillations of B_z and H were reported below the average plasmapause latitude and out-of-phase oscillation near the plasmapause. These features are the same as the equatorial observations represented by the field line displacement pattern in Fig. 15b (Takahashi et al. 1992, 1995, 2003a). The LEO observations support the theoretical view that the B_z component above the ionosphere directly maps to the H component on the ground (Kivelson and Southwood 1988; Allan et al. 1996). Finally, we note that the latitudinal dependence of the B_z phase found in the Ørsted study (Han et al. 2004) is related to the ~180° phase shift of the ground H component occurring at $L \sim 4$ (Björnsson et al. 1971; Yeoman and Orr 1989): it corresponds to the node of the B_z oscillation seen in the magnetosphere.

4.3 Ionospheric Waveguide

In most Pi2 propagation models ionospheric effects mean screening or reflection of magnetospheric MHD waves that are incident on the ionosphere. An exception is a model in

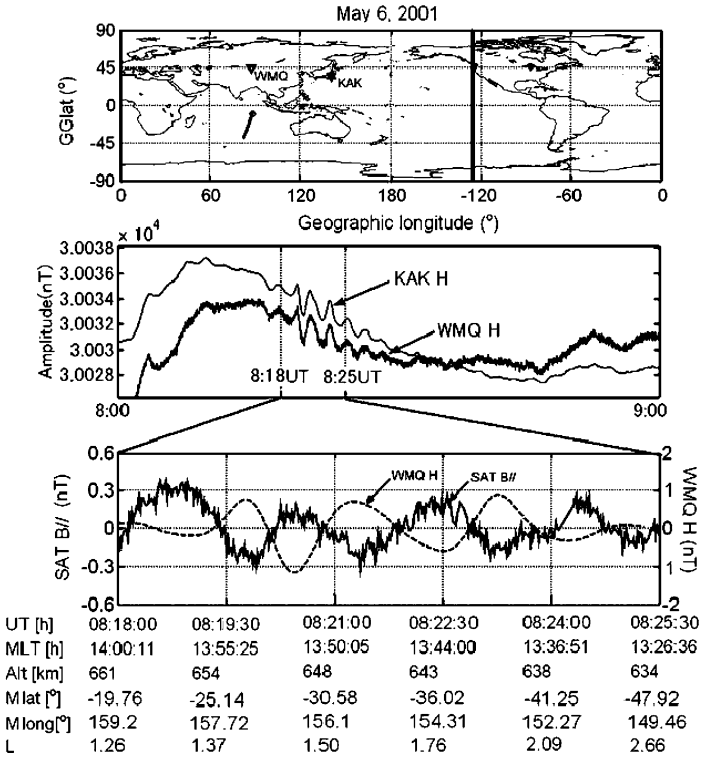

Fig. 54 (From Han et al. 2004) A dayside Pi2 pulsation observed simultaneously at the Ørsted satellite and at low latitude ground stations KAK ($L = 1.3$) and WMQ ($L = 1.7$). (*Top*) Location of the ground stations and the satellite track for the Pi2 event. (*Middle*) Ground H components showing a Pi2 pulsation. (*Bottom*) Comparison of the compressional component $B_{//}$ at the satellite and the H component on the ground

which Pi2 signals propagate horizontally as electromagnetic waves between the waveguide formed by the ionosphere and the conducting Earth. This model was initially developed to explain propagation of the preliminary reverse impulse and DP-2 magnetic field variations from the polar region to the equatorial region (Kikuchi and Araki 1979). Shinohara et al. (1997) suggested that the same mechanism explains a peculiarity of dayside Pi2 pulsations: at the equator the Pi2 amplitude is about ∼3 times as high and the phase is delayed by ∼30° relative to the pulsations observed at slightly higher latitudes (see Fig. 6) (Yanagihara and Shimizu 1966; Stuart and Barsczus 1980; Sastry et al. 1983; Shinohara et al. 1997). It is difficult to attribute these equatorial observations to MHD wave propagation in the magnetosphere since the magnetospheric plasma does not have known structures so tightly localized to the dip equator. However, if electric field Pi2 pulsations reach the dayside equatorial ionosphere, it is possible to drive a strong east-west current (thus a strong magnetic field perturbation) there because Cowling conductivity is high at the (dip) equator.

There is some evidence that Pi2 signals propagate from the nightside polar region to the dayside equatorial region. Tokunaga et al. (2007) applied the "independent component analysis" to pulsation data from multiple ground magnetometers covering both dayside and nightside. As shown in Fig. 53 the independent component that represents the long-period (∼130 s) portion of a Pi2 pulsation exhibited nearly identical waveforms without phase lag at nightside high latitude (KTN ground station) and at the dayside equator (ANC ground

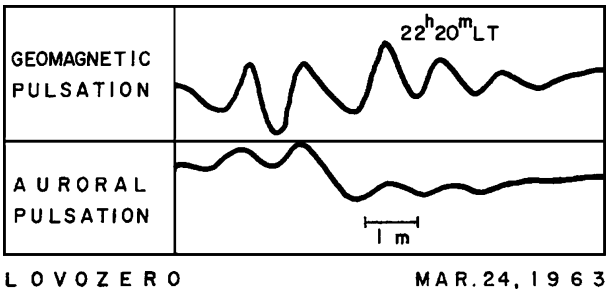

Fig. 55 (From Namgaladze et al. 1967) Simultaneous records of geomagnetic Pi2 pulsations and auroral pulsations

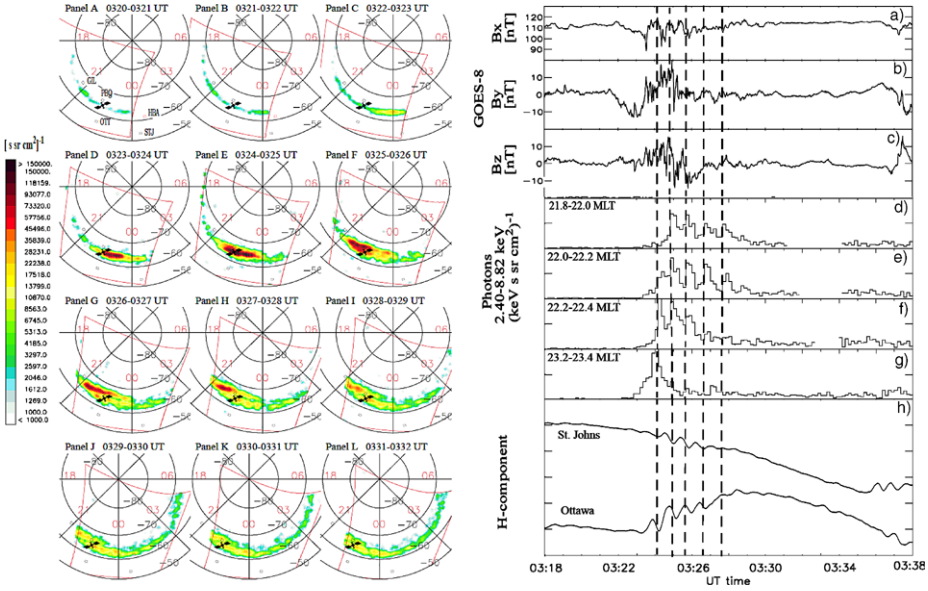

Fig. 56 (From Åsnes et al. 2004) (*Left*) PIXIE images from the Polar spacecraft from the substorm, 24 July 1998, with an energy range from 2.42–8.82 keV photons. (*Right*) Panels (**a**–**c**) show the magnetic field measured by GOES-8 in geosynchronous orbit converted into field-aligned coordinates. Panels (**d**–**f**) are X-ray fluxes integrated over selected MLT sectors from the PIXIE images. Panel (**g**) shows the *H* component of two Northern Hemisphere stations: Ottawa and St. Johns

station) while that component was missing on the nightside at $L < 3$. Thus it appears that there is a connection between nightside Pi2 at the polar region and dayside Pi2 at the equator.

The ionospheric-Earth waveguide model will be strengthened if we can measure current flowing in the Cowling channel. Conceptually, the current can be detected by simultaneously measuring magnetic field pulsations above and below the ionosphere at comparable vertical distances, using ground magnetometers and LEO satellites. If an oscillating East-West current flows in the ionosphere, it will produce a magnetic field perturbation in the North-South direction with opposite polarities between ground and satellite. In contrast, if fast mode waves propagating through the ionosphere are responsible for the dayside Pi2, the polarity will be the same. Such "sandwich" measurements have been conducted on nightside Pi2 pulsations, and the results indicate that the ionosphere is basically transparent (no ionospheric currents required) to incident poloidal (fast mode) waves (see Fig. 52).

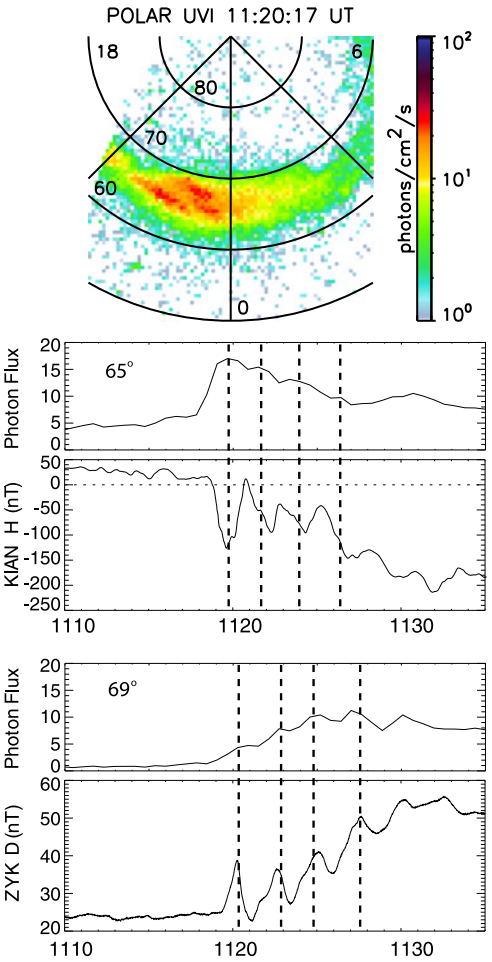

Fig. 57 (From Keiling et al. 2008c) (*Top*) UVI image from the Polar spacecraft, showing three auroral intensifications. (*Middle*, *bottom*) Temporal comparison of photon flux and ground magnetometer data. The photon flux was averaged at 65° and 69° latitude, spanning the sector 2100 to 0000 MLT, which covers the region of two auroral intensifications

Sandwich measurements of dayside Pi2 are sparse, and none have been reported at the equator (this is difficult because all LEO satellites flown so far that are useful for ULF wave measurements had a polar orbit, which means that the equatorial region is passed in less than one Pi2 period). However, Han et al. (2004) reported an interesting result on a dayside Pi2 pulsation detected away from the equator. As shown in Fig. 54, the pulsation was detected with the Ørsted satellite at an altitude of ∼650 km as it flew over two low-latitude ground stations located on the dayside. There is a 180° phase delay between the satellite $B_{//}$ ($\sim B_z$) component and the ground H component, implying that current flowing in the ionosphere produced the magnetic pulsation. The amplitude is larger on the ground, which is also consistent with the ionospheric current since the ground magnetometer was closer to the current (∼100 km altitude).

4.4 Auroral Modulation

In a few studies it has been shown that ground Pi2 pulsations are correlated with periodic modulations of auroral luminescence recorded by ground-based as well as spacecraft-based instruments, such as all-sky imagers and UVI/X-ray cameras. An early example is

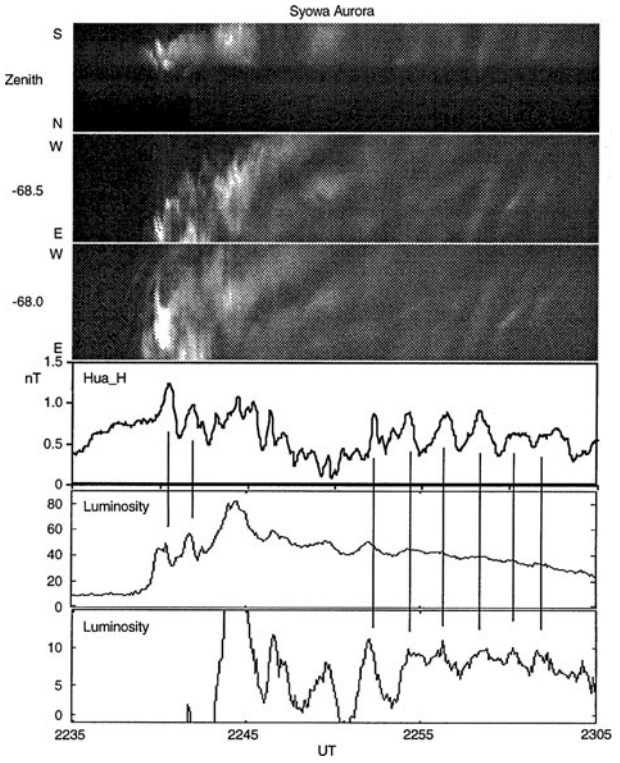

Fig. 58 (From Saka et al. 1999) The *first three panels* show meridian and east-west scans of an all-sky image from Syowa station, located in the Antarctica. The *fourth panel* shows magnetometer data from Huancayo ground station located at the dip equator. The *last two panels* show time series of luminosity integrated from the E-W scan crossing −68.5° latitude

shown in Fig. 55. This correspondence indicates the existence of periodic, energetic particles that excite/modulate the aurora (Saito 1969), and the different electromagnetic wavelengths are directly related to different particle energies. Although much is known about acceleration/modulation mechanisms in association with other ULF wave phenomena, it is largely unknown in association with Pi2 pulsations. In this section we review three studies demonstrating that Pi2-related auroral modulations occur in different wavelengths: optical, ultraviolet, and X-rays. None of the studies could conclusively identify where and how the transfer of the Pi2 signal onto the precipitating particles occurred.

Using X-ray images of the aurora (from the PIXIE instrument of the Polar spacecraft), Åsnes et al. (2004) showed that X-ray fluxes were well correlated with a Pi2 recorded at mid-latitude ground stations during a substorm. The left side of Fig. 56 shows a sequence of X-ray images; the right side shows time series of integrated X-ray fluxes for selected MLT sectors together with the magnetic field data from GOES-8 and ground stations. The X-rays are caused by highly energetic electrons and can at most only constitute a minor part of any field-aligned current that was potentially associated with a SCW. The electrons that carry the FAC of a SCW should only be of the order of hundreds of eV (Rothwell et al. 1986), ruling out Alfvénic acceleration. Åsnes et al. (2004) speculated that either the injections in the near-Earth plasma sheet were periodic or that the precipitation rate of an already injected electron population was modulated.

During a substorm, three auroral active regions were recorded in the ultra-violet light (Fig. 57). For two of them, Keiling et al. (2008b, 2008c) showed that associated auroral modulations were one-to-one correlated with high-latitude Pi2 pulsations (middle and bottom panels). In addition, spacecraft data from azimuthally-separated THEMIS spacecraft,

located at approximately 9 R_E and 11 R_E radial distance, confirmed one-to-one correlations with periodic, energetic (>100 keV) ion injections (see Fig. 36; same event). It was noted that the lower energetic particles (<50 keV) were not correlated with the auroral modulations. Thus, the authors suggested that the energetic ion injections were causally responsible for the auroral modulations, and plasma instability (Sect. 3.2) was proposed as a candidate mechanism.

A surprising result was reported by Saka et al. (1999), showing one-to-one correlations of a low-latitude Pi2 and high-latitude auroral modulation separated by several hours of local time (Fig. 58). The auroral modulation was in the visible spectrum and showed signs of FLR (see keograms). FLR can generate kinetic Alfvén waves with smaller perpendicular scales, which in turn can accelerate low-energetic, field-aligned electrons. The accelerated electrons are then energetic enough to cause visible auroras. While it is known that FLR-Pc5 pulsations can cause optical modulations (e.g., Lessard et al. 1999), it is not certain that it occurs in association with Pi2 pulsations and the evidence in Saka et al. (1999) is not conclusive.

5 Conclusions

Until today there appears to be a "false consensus" in some of the literature, namely, that high-latitude Pi2 pulsations are exclusively caused by the TR mechanism and low-latitude Pi2 pulsations are exclusively caused by a cavity-type resonance, while mid-latitude Pi2 pulsations have been associated with either model. In this review, we clearly demonstrated that the current understanding of the Pi2 phenomenon is far more complex. Observations, especially from the last decade, suggest that not all Pi2 pulsations are caused by only these two mechanisms. This has led to new Pi2 models (*new* in the sense that they have not appeared in the last review by Olson 1999). Adding to this complexity is (a) that a single model can account for Pi2 pulsations spanning many L values, and (b) that a Pi2 at a single L value has been explained by several Pi2 mechanisms, at least according to our current understanding. Figure 59 graphically illustrates this complexity. For example, corresponding to (b), both PCR/PVR-driven and BBF-driven models (among others) give explanations for low-latitude nightside Pi2 pulsations. Corresponding to (a), the PVR model can account for Pi2s on all latitudes (polar cap, low latitude, middle latitude, high latitude, and dayside). This complexity, which can be confusing to the non-expert, leads to controversy among the experts, and is one of the main obstacles to be overcome in Pi2 research.

This complexity raises the question of why pulsations caused by different mechanisms have the same periodicity, the Pi2 period. Is this just a coincidence? Or, is there actually only one Pi2 mechanism that generates Pi2 pulsations? With great confidence, we can say that there must be more than one mechanism, as outlined in this review. However, it is still uncertain, how many there are, and ongoing research will have to determine that. Importantly, despite being collectively called Pi2 pulsations, their properties (period, amplitude, etc.) displayed during different events can vary significantly, and therefore, the opening question of this paragraph is misleading, since it implies that there is no variation. The variation is, of course, the first indicator for the existence of several Pi2 mechanisms, and it allows us to distinguish between them. However, we would argue that the properties of the different Pi2 types are not yet well enough described (with a few exceptions) to allow such a distinction. To make further progress in Pi2 research a systematic approach to Pi2 characterization is necessary in order to be able to distinguish generation mechanisms from one another. Currently, however, for some proposed mechanisms there have simply been too few Pi2 events reported.

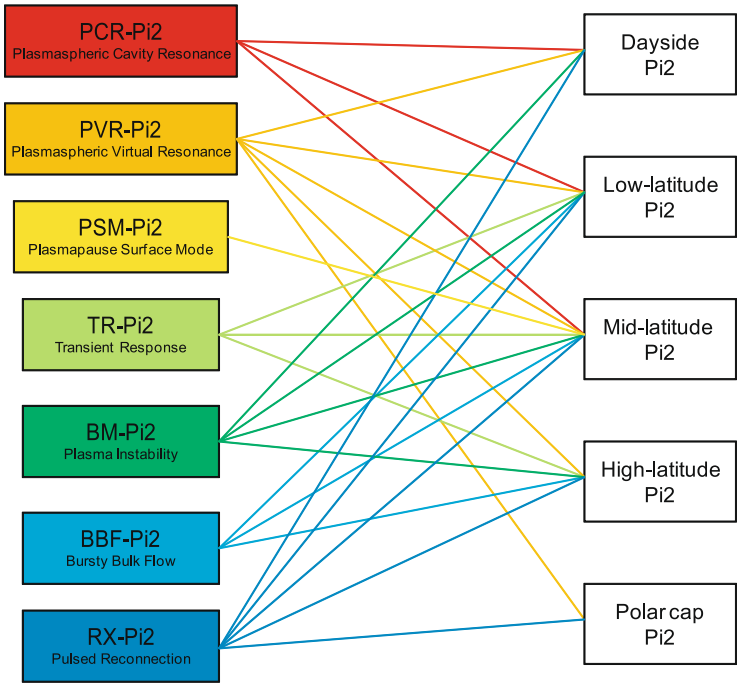

Fig. 59 Complexity of Pi2 research, showing that a single model can account for Pi2 pulsations spanning many latitudes, and also that a Pi2 at a single latitude range can be caused by several Pi2 mechanisms. Pi2 models are shown on the left and associated Pi2 pulsations at various latitudes are shown on the right (connected by *lines*)

It is well established that ground pulsations that fulfill the two basic Pi2 criteria (period and duration; see Sect. 1.1) do not only occur at substorm onset but also before onset and during other geomagnetic modes. While it is conceivable that we only call those Pi2 pulsations that occur at substorm onset *Pi2*, this restrictive usage cannot be found in the literature. It is also conceivable that only those pulsations generated by one mechanism, perhaps the TR model, be called Pi2. Instead, the current usage in the literature is to call all pulsations, regardless of the generation mechanism, *Pi2* as long as they satisfy the two basic criteria. However, a useful modification—in our opinion—is that each Pi2 type, thought to be generated by a different mechanism, be given a different name. We will next provide such a new nomenclature, drawing from existing acronyms and adding new ones. Although it is conceivable to go a step further by assigning names to Pi2 pulsations with different propagation paths, even if they have the same Pi2 source, we will not do so for such cases, partially because many of the propagation paths are very speculative—more speculative than the Pi2 source mechanisms themselves.

We now return to Fig. 2 of Sect. 1.1, whose description was postponed until after all Pi2 models have been reviewed. Each color marks the source region of a specific Pi2 model. In describing each color region, we go outward from close to Earth towards the reconnection site. The brown region refers to the plasmasphere which has been associated with a cavity-type resonance, either the PCR or the PVR mode (Sects. 2.1 and 2.2), respectively. Therefore, we suggest naming the associated Pi2 pulsations: PCR-Pi2 and PVR-Pi2. The orange line traces the plasmapause on which the surface mode (Sect. 2.3) presumably sup-

ports Pi2 pulsations, PSM-Pi2. Farther out is the green line, which indicates flux tubes that connect the ionosphere with the current generator region of the SCW. These flux tubes establish the TR-Pi2 pulsations (Sect. 3.1). The blue region represents Pi2 pulsations associated with plasma instabilities that occur in the near-Earth plasma sheet (Sect. 3.2). So far, only the ballooning mode/instability has been employed as a possible Pi2 source; thus BM-Pi2. Inside the yellow region reside BBFs, which have been proposed as drivers of ground Pi2; thus BBF-Pi2 (Sect. 3.3). We remind the reader that the mechanism and location of the flow burst periodicity inside the BBF is not known yet. Although it could be reconnection (i.e., the red region), it could also be inherent to the central plasma sheet, and therefore, we have included the yellow region as a potential source region. The red region is associated with reconnection-driven Pi2 pulsations; thus RX-Pi2 (Sect. 3.4). The "pulsation" mechanism of reconnection has not been determined yet. If the reconnection period is the result of, say, a wave guide eigenmode that forms in the tail lobes with the magnetopause as an outer boundary and that periodically quenches the reconnection site, then the source would be more appropriately associated with the tail lobes. Hence, we included a gray region as a potential Pi2 source region to pictorially remind us of this possibility.

Among the seven reviewed models, some are more developed than others. Progress has been made on the inner-magnetospheric PCR/PVR models in the past decade, owing to coordinated observations from the ground and space as well as numerical simulations. After decades of ground observations only, the radial amplitude and phase structure of the PCR model have been confirmed with spacecraft data. Not explained by the PCR model but by the PVR model are surprising observations of lobe Pi2 pulsations that are identical to low-latitude Pi2 pulsations. For another example, after decades of debate the secondary amplitude maximum of Pi2 pulsations has been shown to be caused by FLR that are driven by PCR/PVR. The third inner-magnetospheric Pi2 model, the PSM model, still lacks spacecraft-based and numerical evidence, and is thus the least likely to occur. In spite of the wide-spread acceptance of the TR mechanism as the source of substorm-related, high-latitude Pi2 pulsations, there are also some unresolved issues and contradicting observations, questioning the applicability of the TR model for mid-latitude Pi2 pulsations. A Pi2 candidate mechanism is a ballooning mode of some type. Its limited acceptance/confirmation is due to a paucity of coordinated ground-space conjunctions and the difficulty of observationally characterizing the ballooning modes themselves. Surprising results show a correspondence between ground Pi2 pulsations and non-magnetic-field quantities in the outer magnetosphere, which led to new Pi2 models, the BBF-driven model and the reconnection-driven model. Although both models provide no physical explanation for the two time constants associated with Pi2 pulsations (cf. Sect. 1.1), they are interesting new developments, giving explanations for Pi2 pulsations for which the other models do not provide an explanation.

It is important to note that several Pi2 models have proposed various propagation paths (i.e., propagation models) for the Pi2 signal to travel from the source to the ground, and it is unclear which of them occur. Each Pi2 propagation model represents a sequence of energy transfer processes. Most propagation models lack verification from multiple observation points in space, which led to much speculations; in particular for those associated with the outer-magnetospheric Pi2 models. Attempts to follow the path of the Pi2 signal via numerical simulations can only be successful in concert with observational confirmation. Given the very limited number of spacecraft simultaneously available in space, however, their verification remains a major challenge. Part of this challenge lies in describing the boundary condition at the plasma sheet inner edge, that is, our conceptual nightside boundary of the inner magnetosphere. On this boundary and beyond there are a variety of phenomena occurring in the Pi2 band (auroral zone Alfvén waves, periodic BBFs, reconnection, and balloon-

ing mode/instability) and knowing the physical property of these will be essential to build a complete model of Pi2 propagation to the inner magnetosphere.

In conclusion, we find that the outer-magnetospheric models have advanced the field of Pi2 research the most in the last decade, and we believe that these new developments will assure that Pi2 research will remain active in this decade and beyond. We also hope that our review will help the Pi2 community to be guided in their research to resolve the outstanding problems of the Pi2 phenomenon.

Acknowledgements Andreas Keiling was supported by NASA grants NAS5-02099 and NNX08AF29G, and Kazue Takahashi was supported by NSF grants ATM-0646055 and ATM-0750689. Both authors prepared parts of this manuscript while visiting Dong-Hun Lee at Kyung Hee University under the support of the WCU grant (R31-10016) and KRF-2008-313-C00375.

References

W. Allan, S.P. White, E.M. Poulter, Impulse-excited hydromagnetic cavity and field-line resonances in the magnetosphere. Planet. Space Sci. **34**(4), 371–385 (1986a)

W. Allan, E.M. Poulter, S.P. White, Hydromagnetic wave coupling in the magnetosphere-plasmapause effects on impulse-excited resonances. Planet. Space Sci. **34**(12), 1189–1220 (1986b)

W. Allan, F.W. Menk, B.J. Fraser, Y. Li, S.P. White, Are low-latitude Pi2 pulsations cavity/waveguide modes? Geophys. Res. Lett. **23**(7), 765–768 (1996)

R.L. Arnoldy, Fine structure and pitch angle dependence of synchronous orbit electron injections. J. Geophys. Res. **91**, 13411–13421 (1986)

A. Åsnes et al., Pi2-pulsations observed in energetic electron precipitation and magnetic field in association with a substorm surge. Ann. Geophys. **22**, 2097–2105 (2004)

L.N. Baranskiy, P.A. Vinogradov, O.M. Raspopov, Polarization of geomagnetic pulsations of the Pi2 type. Geomagn. Aeron. **10**, 743–745 (1970)

L.N. Baranskiy, V.A. Troitskaya, I.V. Sterlikova, M.B. Gokhberg, N.A. Ivanov, I.P. Khartchenko, J.W. Munch, K. Wilhelm, The analysis of simultaneous observations of nighttime Pi pulsations on an east-west profile. J. Geophys. **48**, 1 (1980)

W. Baumjohann, K.-H. Glassmeier, The transient response mechanism and Pi2 pulsations at substorm onset: Review and outlook. Planet. Space Sci. **32**, 1361–1370 (1984)

T.M. Bauer, W. Baumjohann, R.A. Treumann, Neutral sheet oscillations at substorm onset. J. Geophys. Res. **100**, 23737–23742 (1995). doi:10.1029/95JA02448

F.T. Berkey, Y. Kamide, On the distribution of global auroras during intervals of magnetospheric quiet. J. Geophys. Res. **81**, 4701–4714 (1976)

A. Bhattacharjee, Z.W. Ma, X. Wang, Ballooning instability of a thin current sheet in the high-Lundquist-number magnetotail. Geophys. Res. Lett. **25**, 861–864 (1998). doi:10.1029/98GL00412

J.M. Birn et al., Flow braking and the substorm current wedge. J. Geophys. Res. **104**, 19895 (1999)

A. Björnsson, O. Hillebrand, H. Voelker, First observational results of geomagnetic Pi2 and Pc5 pulsations on a north–south profile through Europe. Z. Geophys. **37**, 1031–1042 (1971)

D.L. Carpenter, R.R. Anderson, An ISEE/whistler model of equatorial electron density in the magnetosphere. J. Geophys. Res. **97**(A2), 1097–1108 (1992)

C.R. Chappell, K.K. Harris, G.W. Sharp, A study of the influence of magnetic activity on the location of the plasmapause as measured by OGO 5. J. Geophys. Res. **75**(1), 50–56 (1970)

L. Chen, A. Hasegawa, A theory of long-period magnetic pulsations. 1. Steady state excitation of field line resonance. J. Geophys. Res. **79**(7), 1024–1032 (1974a)

L. Chen, A. Hasegawa, A theory of long-period magnetic pulsations. 2. Impulsive excitation of surface eigenmode. J. Geophys. Res. **79**(7), 1033–1037 (1974b)

C.C. Cheng, J.K. Chao, K. Yumoto, Spectral power of low-latitude Pi2 pulsations at the 210° magnetic meridian stations and plasmaspheric cavity resonances. Earth Planets Space **52**, 615–627 (2000)

C.Z. Cheng, A kinetic-magnetohydrodynamic model for low frequency phenomena. J. Geophys. Res. **96**, 21159–21171 (1991). doi:10.1029/91JA01981

C.Z. Cheng, A.T.Y. Lui, Kinetic ballooning instability for substorm onset and current disruption observed by AMPTE/CCE. Geophys. Res. Lett. **25**, 4091–4094 (1998). doi:10.1029/1998GL900093

P.J. Chi et al., Propagation of the preliminary reverse impulse of sudden commencements to low latitudes. J. Geophys. Res. **106**, 18857–18864 (2001)

C.R. Clauer, R.L. McPherron, Mapping the local universal time development of magnetospheric substorms using mid-latitude magnetic observatories. J. Geophys. Res. **79**, 2811 (1974)
A.B. Collier, A.R.W. Hughes, L.G. Blomberg, P.R. Sutcliffe, Evidence of standing waves during a Pi2 pulsation event observed on Cluster. Ann. Geophys. **24**, 2719–2733 (2006)
C. Crabtree, W. Horton, H.V. Wong, J.W. Van Dam, Bounce-averaged stability of compressional modes in geotail flux tubes. J. Geophys. Res. **108**(A2), 1084 (2003). doi:10.1029/2002JA009555
R.E. Denton, D.H. Lee, K. Takahashi, J. Goldstein, R. Anderson, Quantitative test of the cavity resonance explanation of plasmaspheric Pi2 frequencies. J. Geophys. Res. **107**(A7) (2002). doi:10.1029/2001JA00272
R.E. Denton, J. Goldstein, D.H. Lee, R.A. King, Z.C. Dent, D. Berube, D.L. Gallagher, K. Takahashi, Realistic magnetospheric mass density model for 29 August 2000. J. Atmos. Sol.-Terr. Phys. **68**, 625 (2006)
D.W. Dungey, Electrodynamics of the outer atmosphere. Pennsylvania State University Science Report, No. 69, 1954
R.C. Elphic, M.F. Thomsen, J.E. Borovsky, D.J. McComas, Inner edge of the electron plasma sheet: Empirical models of boundary location. J. Geophys. Res. **104**(A10), 22679–22693 (1999)
G.M. Erickson, N.C. Maynard, W.J. Burke, G.R. Wilson, M.A. Heinemann, Electromagnetics of substorm onsets in the near-geosynchronous plasma sheet. J. Geophys. Res. **105**(A11), 25265–25290 (2000). doi:10.1029/1999JA000424
B.J. Fraser, J.L. Horwitz, J.A. Slavin, Z.C. Dent, I.R. Mann, Heavy ion mass loading of the geomagnetic field near the plasmapause and ULF wave implications. Geophys. Res. Lett. **32**, L04102 (2005). doi:10.1029/2004GL021315
S. Fujita, M. Itonaga, A plasmaspheric cavity resonance in a longitudinally non-uniform plasmasphere. Earth Planets Space **55**, 219–222 (2003)
S. Fujita, V.L. Patel, Eigenmode analysis of coupled magnetohydrodynamic oscillations in the magnetosphere. J. Geophys. Res. **97**(A9), 13777–13788 (1992)
S. Fujita, M. Itonaga, H. Nakata, Relationship between the Pi2 pulsations and the localized impulsive current associated with the current disruption in the magnetosphere. Earth Planets Space **52**, 267–281 (2000)
S. Fujita, T. Mizuta, M. Itonaga, A. Yoshikawa, H. Nakata, Propagation property of transient MHD impulses in the magnetosphere-ionosphere system: The 2D model of the Pi2 pulsation. Geophys. Res. Lett. **28**, 2161–2164 (2001)
S. Fujita, H. Nakata, M. Itonaga, A. Yoshikawa, T. Mizuta, A numerical simulation of the Pi2 pulsations associated with the substorm current wedge. J. Geophys. Res. **107**(A3) (2002). doi:10.1209/2001JA900137
H. Fukunishi, Polarization changes of geomagnetic Pi2 pulsations associated with the plasmapause. J. Geophys. Res. **80**(1), 98–110 (1975)
C.W. Gelpi et al., Mid-latitude Pi2 polarization pattern and synchronous orbit magnetic activity. J. Geophys. Res. **90**, 6451–6458 (1985)
C.W. Gelpi et al., A comparison of magnetic signatures and DMSP auroral images at substorm onset: Three case studies. J. Geophys. Res. **92**, 2447–2460 (1987)
V. Genot et al., Alfvén wave interaction with inhomogeneous plasmas: acceleration and energy cascade towards small-scales. Ann. Geophys. **22**(6), 2081–2096 (2004)
J.W. Gjerloev, R.A. Greenwald, C.L. Waters, K. Takahashi, D. Sibeck, K. Oksavik, R. Barnes, J. Baker, J.M. Ruohoniemi, Observations of Pi2 pulsations by the Wallops HF radar in association with substorm expansion. Geophys. Res. Lett. **34**, L20103 (2007). doi:10.1029/2007GL030492
J. Goldstein, M. Spasojević, P.H. Reiff, B.R. Sandel, W.T. Forrester, D.L. Gallagher, B.W. Reinisch, Identifying the plasmapause in IMAGE EUV data using IMAGE RPI in situ steep density gradients. J. Geophys. Res. **108**(A4), 1147 (2003)
A. Grocott, S.W.H. Cowley, J.B. Sigwarth, Ionospheric flows and magnetic disturbance during extended intervals of northward but By-dominated IMF. Ann. Geophys. **21**, 509–538 (2003)
E. Hameiri et al., The ballooning instability in space plasmas. J. Geophys. Res. **96**, 1513–1526 (1991)
D.S. Han, T. Iyemori, M. Nosé, H. McCreadie, Y. Gao, F. Yang, S. Yamashita, P. Stauning, A comparative analysis of low-latitude Pi2 pulsations observed by Ørsted and ground stations. J. Geophys. Res. **109**, A10209 (2004). doi:10.1029/2004JA010576
D. Han, T. Iyemori, Y. Gao, Y. Sano, F. Yang, W. Li, M. Nosé, Local time dependence of the frequency of Pi2 waves simultaneously observed at 5 low-latitude stations. Earth Planets Space **55**, 601–612 (2003)
A. Hasegawa, K.H. Tsui, A.S. Assis, A theory of long-period magnetic pulsations. 3. Local field line oscillations. Geophys. Res. Lett. **10**(8), 765–767 (1983)
B. Heilig, H. Luhr, M. Rother, Comprehensive study of ULF upstream waves observed in the topside ionosphere by CHAMP and on the ground. Ann. Geophys. **25**, 737–754 (2007)
M.G. Henderson et al., Substorms during the 10–11 August 2000 sawtooth event. J. Geophys. Res. **111**, A06206 (2006). doi:10.1029/2005JA011366

E.W. Hones, Transient phenomena in the magnetotail and their relation to substorms. Space Sci. Rev. **23**, 393–410 (1979)
W. Horton et al., Stability properties of high-pressure Geotail flux tubes. J. Geophys. Res. **106**, 18803–18822 (2001)
W. Horton, B.-Y. Xu, H.V. Wong, Firehose driven magnetic fluctuations in the magnetosphere. Geophys. Res. Lett. **31**, L06807 (2004). doi:10.1029/2003GL018309
T.-S. Hsu, R.L. McPherron, A statistical study of the relation of Pi2 and plasma flows in the tail. J. Geophys. Res. **112**, A05209 (2007). doi:10.1029/2006JA011782
W.J. Hughes, H.J. Singer, Mid-latitude Pi 2 pulsations, geosynchronous substorm onset signatures and auroral zone currents on March 22, 1979: CDAW 6. J. Geophys. Res. **90**(A2), 1297–1304 (1985). doi:10.1029/JA090iA02p01297
M. Itonaga, T.-I. Kitamura, O. Saka, H. Tachihara, M. Shinohara, A. Yoshikawa, Discrete spectral structure of low-latitude and equatorial Pi2 pulsation. J. Geomagn. Geoelectr. **44**, 253–259 (1992)
M. Itonaga, A. Yoshikawa, K. Yumoto, One-dimensional transient response of the inner magnetosphere at the magnetic equator. 1. Transfer function and poles. J. Geomagn. Geoelectr. **49**, 21–48 (1997a)
M. Itonaga, A. Yoshikawa, K. Yumoto, One-dimensional transient response of the inner magnetosphere at the magnetic equator. 2. Analysis of waveforms. J. Geomagn. Geoelectr. **49**, 49–68 (1997b)
J.A. Jacobs, K. Sinno, World-wide characteristics of geomagnetic micropulsations. J. Geophys. Res. **3**, 333–352 (1960)
G. Jadhav, M. Rajaram, R. Rajaram, Modification of daytime compressional waves by the ionosphere: First results from OERSTED. Geophys. Res. Lett. **28**(1), 103–106 (2001)
A. Keiling et al., Large Alfvén wave power in the plasma sheet boundary layer during the expansion phase of substorms. Geophys. Res. Lett. **27**, 3169 (2000)
A. Keiling, J.R. Wygant, C. Cattell, K.H. Kim, C.T. Russell, D.K. Milling, M. Temerin, F.S. Mozer, C.A. Kletzing, Pi2 pulsations observed with the polar satellite and ground stations: Coupling of trapped and propagating mode waves to a midlatitude field line resonance. J. Geophys. Res. **106**, 25891–25904 (2001)
A. Keiling, K.-H. Kim, J.R. Wygant, C. Cattell, C.T. Russell, C.A. Kletzing, Electrodynamics of a substorm-related field line resonance observed by the Polar satellite in comparison with ground Pi2 pulsations. J. Geophys. Res. **108**(A7), 1275 (2003). doi:10.1029/2002JA009340
A. Keiling, G.K. Parks, J.R. Wygant, J. Dombeck, F.S. Mozer, C.T. Russell, A.V. Streltsov, W. Lotko, Some properties of Alfvén waves: Observations in the tail lobes and the plasma sheet boundary layer. J. Geophys. Res. **110**, A10S11 (2005). doi:10.1029/2004JA010907
A. Keiling et al., Association of Pi2 pulsations and pulsed reconnection: ground and Cluster observations in the tail lobe at 16RE. Ann. Geophys. **24**, 3433–3449 (2006)
A. Keiling et al., Periodic traveling compression regions during quiet geomagnetic conditions and their association with ground Pi2. Ann. Geophys. **26**, 3341–3354 (2008a)
A. Keiling et al., Correlation of substorm injections, auroral modulations, and ground Pi2. Geophys. Res. Lett. **35**, L17S22 (2008b) doi:10.1029/2008GL033969
A. Keiling et al., Multiple intensifications inside the auroral bulge and their association with plasma sheet activities. J. Geophys. Res. **113**, A12216 (2008c). doi:10.1029/2008JA013383
A. Keiling, Pi2 pulsations driven by ballooning instability (2011, submitted)
L. Kepko, M. Kivelson, Generation of Pi2 pulsations by bursty bulk flows. J. Geophys. Res. **104**(A11), 25021–25034 (1999)
L. Kepko, M.G. Kivelson, K. Yumoto, Flow bursts, braking, and Pi2 pulsations. J. Geophys. Res. **106**(A2), 1903–1915 (2001)
T. Kikuchi, T. Araki, Horizontal transmission of the polar electric field to the equator. J. Atmos. Sol.-Terr. Phys. **41**, 927–936 (1979)
K.-H. Kim, K. Takahashi, D.H. Lee, P. Sutcliffe, K. Yumoto, Pi2 pulsations associated with poleward boundary intensifications during the absence of substorms. J. Geophys. Res. **110**, A01217 (2005a). doi:10.1029/2004JA010780
K.-H. Kim, D.-H. Lee, R.E. Denton, K. Takahashi, J. Goldstein, Y.-J. Moon, K. Yumoto, Y.S. Pyo, A. Keiling, Pi2 pulsations in a small and strongly asymmetric plasmasphere. J. Geophys. Res. **110**, A10201 (2005b). doi:10.1029/2005JA011179
K.-H. Kim, D.-H. Lee, K. Takahashi, C.T. Russell, Y.-J. Moon, K. Yumto, Pi2 pulsations observed from the Polar satellite outside the plasmasphere. Geophys. Res. Lett. **32**, L18102 (2005c). doi:10.1029/2005GL023872
K.-H. Kim, K. Takahashi, S. Ohtani, S.-K. Sung, Statistical analysis of the relationship between earthward flow bursts in the magnetotail and low-latitude Pi2 pulsations. J. Geophys. Res. **112**, A10211 (2007). doi:10.1029/2007JA012521

K.-H. Kim et al., Substorm and pseudo-substorm Pi2 pulsations observed during the interval of quasi-periodic magnetotail flow bursts: A case study. Earth Planets Space **62**, 413 (2010)
T. Kitamura, O. Saka, M. Shimoizumi, H. Tachihara, T. Oguti, T. Araki, N. Sato, M. Ishituka, O. Veliz, J.B. Nyobe, Global mode of Pi2 waves in the equatorial region-Difference of Pi2 mode between high and equatorial latitudes. J. Geomagn. Geoelectr. **40**, 621–634 (1988)
K. Kitamura, H. Kawano, S. Ohtani, A. Yoshikawa, K. Yumoto, Local time distribution of low and middle latitude ground magnetic disturbances at sawtooth injections of 18–19 April 2002. J. Geophys. Res. **110**, A07208 (2005). doi:10.1029/2004JA010734
M.G. Kivelson, ULF waves from the ionosphere to the outer planets, in *AGU Geophysical Monograph*, ed. by Takahashi et al. (2006)
M.G. Kivelson, D.J. Southwood, Hydromagnetic waves and the ionosphere. Geophys. Res. Lett. **15**(11), 1271–1274 (1988)
M.G. Kivelson, J. Etcheto, J.G. Trotignon, Global compressional oscillations of the terrestrial magnetosphere: The evidence and a model. J. Geophys. Res. **89**(A11), 9851–9856 (1984)
K. Kosaka et al., Local time dependence of the dominant frequency of Pi2 pulsations at mid- and low-latitudes. Earth Planets Space **54**, 771–781 (2002)
H. Laakso, R. Pfaff, P. Janhunen, Polar observations of electron density distribution in the Earth's magnetosphere. 2. Density profiles. Ann. Geophys. **20**, 1725–1735 (2002)
L.J. Lanzerotti, L.V. Medford, Local night, impulsive (Pi2-type) hydromagnetic wave polarization at low latitudes. Planet. Space Sci. **32**, 135–142 (1984)
D.H. Lee, Dynamics of MHD wave propagation in the low-latitude magnetosphere. J. Geophys. Res. **101**(A7), 15371–15386 (1996)
D.H. Lee, On the generation mechanism of Pi2 pulsations in the magnetosphere. Geophys. Res. Lett. **25**(5), 583–586 (1998)
D.H. Lee, K. Kim, Compressional MHD waves in the magnetosphere: A new approach. J. Geophys. Res. **104**(A6), 12379–12385 (1999)
D.H. Lee, R.L. Lysak, ULF wave coupling in the dipole model: the impulsive excitation. J. Geophys. Res. **94**, 17097–17103 (1989)
D.H. Lee, R.L. Lysak, Monochromatic ULF wave excitation in the dipole magnetosphere. J. Geophys. Res. **96**(A4), 5811–5817 (1991)
D.H. Lee, R.L. Lysak, MHD waves in a three-dimensional dipolar magnetic field: A search for Pi2 pulsations. J. Geophys. Res. **104**(A12), 28691–28699 (1999)
D.-H. Lee, K. Takahashi, MHD eigenmodes in the inner magnetosphere, in *Magnetospheric ULF Waves: Synthesis and New Directions*. Geophysical Monograph Series, vol. 169, ed. by T. Takahashi et al. (AGU, Washington, 2006), pp. 73–90
D.-H. Lee, K.-H. Kim, R.E. Denton, K. Takahashi, Effects of ionospheric damping on MHD wave mode structure. Earth Planets Space **56**, e33–e36 (2004)
M.R. Lessard et al., Simultaneous satellite and ground-based observations of a discretely driven field line resonance. J. Geophys. Res. **104**, 12361–12371 (1999)
M. Lester, D. Orr, Correlations between ground observations of Pi2 geomagnetic pulsations and satellite plasma density observations. Planet. Space Sci. **31**, 143–160 (1983)
M. Lester, W.J. Hughes, H.J. Singer, Polarization patterns of Pi2 magnetic pulsations and the substorm current wedge. J. Geophys. Res. **88**(A10), 7958–7966 (1983)
M. Lester, W.J. Hughes, H.J. Singer, Longitudinal structure in Pi2 pulsations and the substorm current wedge. J. Geophys. Res. **89**, 5489–5494 (1984)
M. Lester, K.H. Glassmeier, J. Behrens, Pi2 pulsations and the eastward electrojet: a case study. Planet. Space Sci. **33**, 351–364 (1985)
Y. Li, B.J. Fraser, F.W. Menk, D.J. Webster, K. Yumoto, Properties and sources of low and very low latitude Pi2 pulsations. J. Geophys. Res. **103**, 2343–2358 (1998)
Y. Li, K. Yumoto, M. Itonaga, M. Shinohara, T.I. Kitamura, S.K.Y. Kokubun, Equatorial Pi2 pulsations as indicators of substorms and the relation between dayside and nightside Pi2 pulsations, in *Substorms-4: International Conference on Substorms-4*, Lake Hamana, Japan, 9–13 March 1998, ed. by S. Kokubun, Y. Kamide. Astrophysics and Space Science Library, vol. 238 (Springer, Berlin, 1999), pp. 555–558
J. Liang, W.W. Liu, E.F. Donovan, E. Spanswick, In-situ observation of ULF wave activities associated with substorm expansion phase onset and current disruption. Ann. Geophys. **27**, 2191–2204 (2009)
C.C. Lin, J.L.J. Cahill, Pi2 pulsations in the magnetosphere. Planet. Space Sci. **23**, 693–711 (1975)
C.A. Lin, L.C. Lee, Y.J. Sun, Observations of Pi2 pulsations at a very low latitude ($L = 1.06$) station and magnetospheric cavity resonances. J. Geophys. Res. **96**(A12), 21105–21113 (1991)
K. Liou, C.I. Meng, P.T. Newell, K. Takahashi, S.I. Ohtani, A.T.Y. Lui, M. Brittnacher, G. Parks, Evaluation of low-latitude Pi2 pulsations as indicators of substorm onset using Polar ultraviolet imagery. J. Geophys. Res. **105**, 2495–2505 (2000)

A.T.Y. Lui, Current disruption in the Earth's magnetosphere: Observations and models. J. Geophys. Res. **101**, 13067 (1996)
A.T.Y. Lui, A.H. Najmi, Time-frequency decomposition of signals in a current disruption event. Geophys. Res. Lett. **24**(24), 3157–3160 (1997). doi:10.1029/97GL03229
A.T.Y. Lui, C.-L. Chang, A. Mankofsky, H.-K. Wong, D. Winske, A cross-field current instability for substorm expansions. J. Geophys. Res. **96**(A7), 11389–11401 (1991). doi:10.1029/91JA00892
A.T.Y. Lui, R.E. Lopez, B.J. Anderson, K. Takahashi, L.J. Zanetti, R.W. McEntire, Current disruptions in the near-Earth neutral sheet region. J. Geophys. Res. **97**, 1461–1480 (1992)
L.R. Lyons, T. Nagai, G.T. Blanchard et al., Associations between Geotail plasma flows and auroral poleward boundary intensifications observed by CANOPUS photometers. J. Geophys. Res. **104**, 4485–4500 (1999)
R.L. Lysak et al., Propagation of Alfvén waves in the magnetotail during substorms. Ann. Geophys. **27**, 2237 (2009)
A.J. Mallinckrodt, C.W. Carlson, Relations between transverse electric fields and field-aligned currents. J. Geophys. Res. **83**, 1426–1432 (1978)
N.C. Maynard et al., Dynamics of the inner magnetosphere near times of substorm onset. J. Geophys. Res. **101**, 7705 (1996)
R.L. McPherron, Physical processes producing magnetospheric substorms and magnetic storms. Geomagnetism **4**, 593–739 (1991)
R.L. McPherron et al., Response of the Earth's magnetosphere to changes in the solar wind. J. Atmos. Sol.-Terr. Phys. **70**, 303–315 (2008)
S.B. Mende, C.W. Carlson, H.U. Frey, L.M. Peticolas, N. Østgaard, FAST and IMAGE-FUV observations of a substorm onset. J. Geophys. Res. **108**(A9), 1344 (2003). doi:10.1029/2002JA009787
A. Miura, Validity of the fluid description of critical β and Alfvén time scale of ballooning instability onset in the near-Earth collisionless high-β plasma. J. Geophys. Res. **109**, A02211 (2004). doi:10.1029/2003JA009924
A. Miura, S. Ohtani, T. Tamao, Ballooning instability and structure of diamagnetic hydromagnetic waves in a model magnetosphere. J. Geophys. Res. **94**, 15231–15242 (1989). doi:10.1029/JA094iA11p15231
K.R. Murphy, A. Kale, I.J. Rae, I.R. Mann, Z.C. Dent, Pi2 pulsation periodicity and variations in magnetotail flows, in *Proceedings of the Eighth International Conference on Substorms (ICS-8)*, ed. by M. Syrja Suo, E. Donovan (Univ. of Calgary, Calgary, 2006), pp. 191–196
K.R. Murphy et al., The dependence of Pi2 waveforms on periodic velocity enhancements within bursty bulk flows. Ann. Geophys. **29**, 493–509 (2011)
A.N. Namgaladze, O.M. Raspopov, V.K. Roldugin, Relationship between Pi2 pulsations of the geomagnetic field and pulsations in the intensity of auroral luminescence. Geomagn. Aeron. **7**, 302–304 (1967)
T. Nagai, M. Fujimoto, Y. Saito, S. Machida, T. Terasawa, R. Nakamura, T. Yamamoto, T. Mukai, A. Nishida, S. Kokubun, Structure and dynamics of magnetic reconnection for substorm onsets with Geotail observations. J. Geophys. Res. **103**(A3), 4419–4440 (1998). doi:10.1029/97JA02190
R.S. Newton, D.J. Southwood, W.J. Hughes, Damping of geomagnetic pulsations by the ionosphere. Planet. Space Sci. **26**, 201–209 (1978)
A. Nishida, Formation of plasmapause, or magnetospheric plasma knee, by the combined action of magnetospheric convection and plasma escape from the tail. J. Geophys. Res. **71**(23), 5669–5679 (1966)
M. Nosé, Automated detection of Pi2 pulsations using wavelet analysis: 2. An application for dayside Pi2 pulsations study. Earth Planets Space **51**, 23–32 (1999)
M. Nosé, T. Iyemori, S. Nakabe, T. Nagai, H. Matsumoto, T. Goka, ULF pulsations observed by the ETS-VI satellite: Substorm associated azimuthal Pc4 pulsations on the nightside. Earth Planets Space **50**, 63–80 (1998)
M. Nosé, K. Takahashi, T. Uozumi, K. Yumoto, Y. Miyoshi, A. Morioka, D.K. Milling, P.R. Sutcliffe, H. Matsumoto, T. Goka, Multipoint observations of a Pi2 pulsation on morning side: The September 20, 1995, event. J. Geophys. Res. **108**(A5), 1219 (2003). doi:10.1029/2003JA009847
M. Nosé, K. Liou, P.R. Sutcliffe, Longitudinal dependence of characteristics of low-latitude Pi2 pulsations observed at Kakioka and Hermanus. Earth Planets Space **58**, 775–783 (2006)
T.P. O'Brien, M.B. Moldwin, Empirical plasmapause models from magnetic indices. Geophys. Res. Lett. **30**(4), 1152 (2003). doi:10.1029/2002GL016007
S. Ohtani, Substorm trigger processes in the magnetotail: Recent observations and outstanding issues. Space Sci. Rev. **95**, 347–359 (2001)
S. Ohtani, T. Tamao, Does the ballooning instability trigger substorms in the near-Earth magnetotail? J. Geophys. Res. **98**, 19369–19379 (1993). doi:10.1029/93JA01746
S. Ohtani, K. Takahashi, L.J. Zanetti, T.A. Potemra, R.W. McEntire, T. Iijima, Initial signatures of magnetic field and energetic particle fluxes at tail reconfiguration: Explosive growth phase. J. Geophys. Res. **97**(A12), 19311–19324 (1992). doi:10.1029/92JA01832

J.V. Olson, Pi2 pulsations and substorm onsets: A review. J. Geophys. Res. **104**, 17499–17520 (1999)
J.V. Olson, G. Rostoker, Pi2 pulsations and the auroral electrojet. Planet. Space Sci. **23**, 1129–1139 (1975)
H. Osaki, K. Yumoto, K. Fukao, K. Shiokawa, F.W. Menk, B.J. Fraser, The 210° MM Magnetic Observation Group, The 210° characteristics of low-latitude Pi2 pulsations along the 210° magnetic meridian. J. Geomagn. Geoelectr. **48**, 1421–1430 (1996)
H. Osaki, K. Takahashi, H. Fukunishi, T. Nagatsuma, H. Oya, A. Matsuoka, D.K. Milling, Pi2 pulsations observed from the Akebono satellite in the plasmasphere. J. Geophys. Res. **103**, 17605–17615 (1998)
A.B. Pashin, O.M. Raspopov, A.G. Iakhnin et al., Pi2 magnetic pulsations, auroral break-ups and the substorm current wedge: A case study. J. Geophys. Res. **51**, 223–233 (1982)
S.M. Petrinec, K. Yumoto, H. Lühr, D. Orr, D.K. Milling, H. Hayashi, S. Kokubun, T. Araki, The CME event of February 21, 1994: Response of the magnetic field at the Earth's surface. J. Geomagn. Geoelectr. **48**, 1341–1379 (1996)
H. Pekrides, A.D.M. Walker, P.R. Sutcliffe, Global modeling of Pi2 pulsations. J. Geophys. Res. **102**, 14341–14343 (1997)
V. Pilipenko, N. Mazur, E. Fedorov, T. Uozumi, K. Yumoto, Excitation of Alfvén impulse by the anomalous resistance onset on the auroral field lines. Ann. Geophys. **23**, 1455–1465 (2005)
S.V. Polyakov, V.O. Rapoport, The ionospheric Alfvén resonator. Geomagn. Aeron. **21**, 816 (1981)
H.R. Radoski, Highly asymmetric MHD resonances: the guided poloidal mode. J. Geophys. Res. **72**(15), 4026–4027 (1967)
G. Rostoker, The frequency spectrum of Pi2 micropulsation activity and its relationship to planetary magnetic activity. J. Geophys. Res. **72**, 2032–2039 (1967)
G. Rostoker, J.C. Samson, Polarization characteristics of Pi2 pulsations and implications for their source mechanisms: location of source regions with respect to the auroral electrojets. Planet. Space Sci. **29**, 225–247 (1981)
G. Rostoker, S.-I. Akasofu, J. Foster, R.A. Greenwald, Y. Kamide, K. Kawasaki, A.T.Y. Lui, R.L. Mcpherron, C.T. Russell, Magnetospheric substorms—Definition and signatures. J. Geophys. Res. **85**, 1663–1668 (1980)
P.L. Rothwell, M.B. Silevitch, L.P. Block, Pi2 pulsations and the westward traveling surge. J. Geophys. Res. **91**, 6921–6928 (1986)
A. Roux, S. Perraut, P. Robert, A. Morane, A. Pedersen, A. Korth, G. Kremser, B. Aparicio, D. Rodgers, R. Pellinen, Plasma sheet instability related to the westward traveling surge. J. Geophys. Res. **96**, 17697–17714 (1991). doi:10.1029/91JA01106
T. Saito, Oscillation of geomagnetic field with the progress of pt-type pulsations. Tohoku Geophys. J. **13**, 53 (1961)
T. Saito, Geomagnetic pulsations. Space Sci. Rev. **10**, 319–412 (1969)
T. Saito, S. Matsushita, Solar cycle effects on geomagnetic Pi2 pulsations. J. Geophys. Res. **73**, 267 (1968)
T. Saito, K. Yumoto, Y. Koyama, Magnetic pulsation Pi2 as a sensitive indicator of magnetospheric substorm. Planet. Space Sci. **24**, 1025 (1976)
M.H. Saito, Y. Miyashita, M. Fujimoto, I. Shinohara, Y. Saito, K. Liou, T. Mukai, Ballooning mode waves prior to substorm-associated dipolarizations: Geotail observations. Geophys. Res. Lett. **35**, L07103 (2008). doi:10.1029/2008GL033269
O. Saka et al., Ground-satellite correlation of low-latitude Pi2 pulsations: A quasi-periodic field line oscillation in the magnetosphere. J. Geophys. Res. **101**, 15433–44015 (1996)
O. Saka et al., Pi2-associated particle flux and magnetic field modulations in geosynchronous altitudes. J. Geophys. Res. **102**, 11363–11373 (1997)
O. Saka et al., A slow mode wave as a possible source of Pi2 and associated particle precipitation: A case study. Ann. Geophys. **17**, 674 (1999)
O. Saka, H. Akaki, D.N. Baker, A satellite magnetometer observation of dusk-to-dawn current in the midnight magnetosphere at low latitude Pi2 onset. Earth Planets Space **54**, e1–e4 (2002)
O. Saka et al., A Pi2-associated dusk-to-dawn current in the midnight sector as observed at $L = 6.6$ during multiple Pi2 onsets. Earth Planets Space **56**, 663–668 (2004)
T. Sakurai, R.L. McPherron, Satellite observations of Pi2 activity at synchronous orbit. J. Geophys. Res. **88**(A9), 7015–7027 (1983)
J.C. Samson, Pi2 pulsations: High latitude results. Planet. Space Sci. **30**, 1239 (1982)
J.C. Samson, Large-scale studies of Pi2's associated with auroral breakups. J. Geophys. Res. **56**, 133–145 (1985)
J.C. Samson, B.G. Harrold, Maps of the polarizations of high latitude Pi2 pulsations. J. Geophys. Res. **88**, 5736 (1983)
J.C. Samson, G. Rostoker, Polarization characteristic of Pi2 pulsations and implications for their source mechanisms: Influence of the westward traveling surge. Planet. Space Sci. **31**, 435–458 (1983)

J.C. Samson, J. Jacobs, G. Rostoker, Latitude-dependent characteristics of long-period geomagnetic micropulsations. J. Geophys. Res. **76**(16), 3675–3683 (1971)
J.C. Samson, B.G. Harrold, K.L. Yeung, Characteristic time constants and velocities of midlatitude Pi2's. J. Geophys. Res. **90**, 3448–3456 (1985)
J.C. Samson, B.G. Harrold, J.M. Ruohoniemi, R.A. Greenwald, A.D.M. Walker, Field line resonance associated with MHD waveguides in the magnetosphere. Geophys. Res. Lett. **19**, 441–444 (1992)
B.R. Sandel, J. Goldstein, D.L. Gallagher, M. Spasojevic, Extreme Ultraviolet Imager observations of the structure and dynamics of the plasmasphere. Space Sci. Rev. **109**, 25–46 (2003)
T.S. Sastry, Y.S. Sarma, S.V.S. Sarma, P.V.S. Narayan, Day-time Pi pulsations at equatorial latitudes. J. Atmos. Terr. Phys. **45**, 733–741 (1983)
V.S. Semenov, T. Penz, V.V. Ivanova, V.A. Sergeev, H.K. Biernat, R. Nakamura, M.F. Heyn, I.V. Kubyshkin, I.B. Ivanov, Reconstruction of the reconnection rate from Cluster measurements: First results. J. Geophys. Res. **110**, A11217 (2005). doi:10.1029/2005JA011181
V.A. Sergeev, R.C. Elphic, F.S. Mozer et al., A two-satellite study of nightside flux transfer events in the plasma sheet. Planet. Space Sci. **40**, 1551–1572 (1992)
C.E. Seyler, A mathematical model of the structure and evolution of small-scale discrete auroral arcs. J. Geophys. Res. **95**, 17199–17215 (1990)
K. Shiokawa, W. Baumjohann, G. Haerendel, Braking of high-speed flows in the near-Earth tail. Geophys. Res. Lett. **24**, 1179–1182 (1997)
K. Shiokawa, G. Haerendel, W. Baumjohann, Azimuthal pressure gradient as driving force of substorm currents. Geophys. Res. Lett. **25**, 959–962 (1998)
M. Shinohara, K. Yumoto, A. Yoshikawa, O. Saka, S.I. Solovyev, E.F. Vershinin, N.B. Trivedi, J.M. Da Costa, M.M.M.O.G. The 210° Wave characteristics of daytime and nighttime Pi2 pulsations at the equatorial and low latitudes. Geophys. Res. Lett. **24**(18), 2279–2282 (1997)
M.D. Sciffer, C.L. Waters, F.W. Menk, Propagation of ULF waves through the ionosphere: Inductive effect for oblique magnetic fields. Ann. Geophys. **22**, 1155–1169 (2004)
K. Sigsbee, C.A. Cattell, D. Fairfield, K. Tsuruda, S. Kokubun, Geotail observations of low-frequency waves and high-speed earthward flows during substorm onsets in the near magnetotail from 10 to 13 RE. J. Geophys. Res. **107**(A7), 1141 (2002)
H.J. Singer et al., The localization of Pi2 pulsations: Ground satellite observations. J. Geophys. Res. **88**, 7029–7036 (1983)
H.J. Singer, W.J. Hughes, C. Gelpi, B.G. Ledley, Magnetic disturbances in the vicinity of synchronous orbit and the substorm current wedge: a case study. J. Geophys. Res. **90**, 9583 (1985)
H.J. Singer, E.W. Hones Jr., T.J. Rosenberg, Multipoint measurements from substorm onset to recovery: The relation between magnetic pulsations and plasma sheet thickening. Adv. Space Res. **8**(9–10), 443–446 (1988)
N. Singh, G. Khazanov, A. Mukhter, Electrostatic wave generation and transverse ion acceleration by Alfvénic wave components of broadband extremely low frequency turbulence. J. Geophys. Res. **112**, A06210 (2007). doi:10.1029/2006JA011933
J.A. Slavin, I.E.J. Smith, B.T. Tsurutani et al., Substorm associated traveling compression regions in the distant tail: ISEE-3 geotail observations. Geophys. Res. Lett. **11**, 657–660 (1984)
J.A. Slavin, R.P. Lepping, J. Gjerloev et al., Geotail observations of magnetic flux ropes in the plasma sheet. J. Geophys. Res. **108**(A1), 1015 (2003). doi:10.1029/2002JA009557
J.A. Slavin, E.I. Tanskanen, M. Hesse et al., Cluster observations of traveling compression regions in the near-tail. J. Geophys. Res. **110**, A06207 (2005). doi:10.1029/2004JA010878
K. Snekvik, L. Juusola, N. Østgaard, O. Amm, Reconnection Hall current system observed in the magnetotail and in the ionosphere. Geophys. Res. Lett. **36**, L08104 (2009). doi:10.1029/2009GL037239
S.I. Solovyev et al., Pi2 magnetic pulsation as response on spatio-temporal oscillations of auroral arc current system. Geophys. Res. Lett. **27**, 1839–1842 (2000)
D.J. Southwood, Some features of field line resonances in the magnetosphere. Planet. Space Sci. **22**, 483–491 (1974)
D.J. Southwood, W.J. Hughes, Theory of hydromagnetic waves in the magnetosphere. Space Sci. Rev. **35**, 301–366 (1983)
A.V. Streltsov, W. Lotko, Multiscale electrodynamics of the ionosphere-magnetosphere system. J. Geophys. Res. **109**, A09214 (2004). doi:10.1029/2004JA010457
W.F. Stuart, A mechanism of selective enhancement of Pi2's by the plasmasphere. J. Atmos. Sol.-Terr. Phys. **36**, 851–859 (1974)
W.F. Stuart, H.G. Barsczus, Pi's observed in the daylight hemisphere at low latitudes. J. Atmos. Sol.-Terr. Phys. **42**, 487–497 (1980)
W.F. Stuart, P.M. Brett, T.J. Harris, Mid-latitude secondary resonance in Pi2's. J. Atmos. Sol.-Terr. Phys. **41**, 65–75 (1979)

P.R. Sutcliffe, The association of harmonics in Pi2 power spectra with the plasmapause. Planet. Space Sci. **23**, 1581 (1975)
P.R. Sutcliffe, Ellipticity variations in Pi2 pulsations at low latitudes. Geophys. Res. Lett. **8**, 91 (1981)
P.R. Sutcliffe, Observations of Pi2 pulsations in a near ground state magnetosphere. Geophys. Res. Lett. **25**, 4067–4070 (1998)
P.R. Sutcliffe, Pi2 band activity at low latitudes during non-substorm intervals. Geophys. Res. Lett. **37**, L05101 (2010). doi:10.1029/2009GL041661
P.R. Sutcliffe, H. Lühr, A comparison of Pi2 pulsations observed by CHAMP in low Earth orbit and on the ground at low latitudes. Geophys. Res. Lett. **30**(21) (2003). doi:10.1029/2003GL018270
P.R. Sutcliffe, L.R. Lyons, Association between quiettime Pi2 pulsations, poleward boundary intensification, and plasma sheet particle fluxes. Geophys. Res. Lett. **29**, 4067–4070 (2002). doi:10.1029/2001GL014430
P.R. Sutcliffe, E. Nielsen, STARE observations of Pi2 pulsations. Geophys. Res. Lett. **17**(5), 603–606 (1990)
P.R. Sutcliffe, E. Nielsen, The ionospheric signature of Pi2 pulsations observed by STARE. J. Geophys. Res. **97**(A7), 10621–10636 (1992)
P.R. Sutcliffe, K. Yumoto, Dayside Pi2 pulsations at low latitudes. Geophys. Res. Lett. **16**, 887–890 (1989)
P.R. Sutcliffe, K. Yumoto, On the cavity mode nature of low-latitude Pi2 pulsations. J. Geophys. Res. **96**(A2), 1543–1551 (1991)
S. Taguchi, J.A. Slavin, M. Kiyohara et al., Temporal relationship between midtail traveling compression regions and substorm onset: Evidence for near-Earth neutral line formation in the late growth phase. J. Geophys. Res. **103**(A11), 26607–26612 (1998)
K. Takahashi, K. Liou, Longitudinal structure of low-latitude Pi2 pulsations and its dependence on aurora. J. Geophys. Res. **109**, A12206 (2004). doi:10.1029/2004JA010580
K. Takahashi, L.J. Zanetti, R.E. Lopez, R.W. McEntire, T.A. Potemra, K. Yumoto, Disruption of the magnetotail current sheet observed by AMPTE/CCE. Geophys. Res. Lett. **14**(10), 1019–1022 (1987). doi:10.1029/GL014i010p01019
K. Takahashi, S. Kokubun, T. Sakurai, R.W. McEntire, T.A. Potemra, R.E. Lopez, AMPTE/CCE observations of substorm associated standing Alfvén waves in the midnight sector. Geophys. Res. Lett. **15**(11), 1287–1290 (1988). doi:10.1029/GL015i011p01287
K. Takahashi, S. Ohtani, K. Yumoto, AMPTE CCE observations of Pi2 pulsations in the inner magnetosphere. Geophys. Res. Lett. **19**, 1447–1450 (1992)
K. Takahashi, S. Ohtani, B.J. Anderson, Statistical Analysis of Pi2 Pulsations Observed by the AMPTE CCE Spacecraft in the Inner Magnetosphere. J. Geophys. Res. **100**, 21929–21941 (1995)
K. Takahashi, B.J. Anderson, S. Ohtani, Multisatellite study of nightside transient toroidal waves. J. Geophys. Res. **101**, 24815–24826 (1996)
K. Takahashi, B.J. Anderson, K. Yumoto, Upper atmosphere research satellite observation of a Pi2 pulsation. J. Geophys. Res. **104**(A11), 25035–25045 (1999)
K. Takahashi, D.H. Lee, M. Nosé, R.R. Anderson, W.J. Hughes, CRRES electric field study of the radial mode structure of Pi2 pulsations. J. Geophys. Res. **108**(A5), 1210 (2003a). doi:10.1029/2002JA009761
K. Takahashi, R.R. Anderson, W.J. Hughes, Pi2 pulsations with second harmonic: CRRES observations in the plasmasphere. J. Geophys. Res. **108**(A5), 1242 (2003b). doi:10.1029/2002JA009747
K. Takahashi, R.E. Denton, R.R. Anderson, W.J. Hughes, Frequencies of standing Alfvén wave harmonics and their implication for plasma mass distribution along geomagnetic field lines: Statistical analysis of CRRES data. J. Geophys. Res. **109**, A08202 (2004). doi:10.1029/2003JA010345
K. Takahashi, K. Liou, K. Yumoto, K. Kitamura, M. Nosé, F. Honary, Source of Pc4 pulsations observed on the nightside. J. Geophys. Res. **110**, A12207 (2005). doi:10.1029/2005JA011093
K. Takahashi, D. Berube, D.-H. Lee, J. Goldstein, H.J. Singer, F. Honary, Possible evidence of virtual resonance in the dayside magnetosphere. J. Geophys. Res. **114**, A05206 (2009). doi:10.1029/2008JA013898
T. Tamao, The structure of three-dimensional hydromagnetic waves in a uniform cold plasma. J. Geomagn. Geoelectr. **18**, 89–114 (1964)
M. Teramoto, M. Nosé, P.R. Sutcliffe, Statistical analysis of Pi2 pulsations inside and outside the plasmasphere observed by the polar orbiting DE-1 satellite. J. Geophys. Res. **113**, A07203 (2008). doi:10.1029/2007JA012740
T. Tokunaga, H. Kohta, A. Yoshikawa, T. Uozumi, K. Yumoto, Global features of Pi2 pulsations obtained by independent component analysis. Geophys. Res. Lett. **34**, L14106 (2007). doi:10.1029/2007GL030174
T. Uozumi, K. Yumoto, H. Kawano et al., Characteristics of energy transfer of Pi2 magnetic pulsations: Latitudinal dependence. Geophys. Res. Lett. **27**, 1619–1622 (2000)
T. Uozumi, K. Yumoto, H. Kawano et al., Propagation characteristic of Pi2 magnetic pulsations observed at ground high latitudes. J. Geophys. Res. **109**(A8) (2004). doi:10.1029/2003JA009898
M. Volwerk, R. Nakamura, W. Baumjohann, T. Uozumi, K. Yumoto, A. Balogh, Tailward propagation of Pi2 waves in the Earth's magnetotaillobe. Ann. Geophys. **26**, 4023–4030 (2008). doi:10.5194/angeo-26-4023-2008

I. Voronkov, R. Rankin, P. Frycz, V.T. Tikhonchuk, J.C. Samson, Coupling of shear flow and pressure gradient instabilities. J. Geophys. Res. **102**(A5), 9639–9650 (1997). doi:10.1029/97JA00386

I.O. Voronkov, E.F. Donovan, J.C. Samson, Observations of the phases of the substorm. J. Geophys. Res. **108**(A2), 1073 (2003). doi:10.1029/2002JA009314

C.L. Waters, F.W. Menk, B.J. Fraser, The resonance structure of low latitude Pc3 geomagnetic pulsations. Geophys. Res. Lett. **18**(12), 2293–2296 (1991)

D.J. Webster, J.C. Samson, G. Rostoker, Eastward propagation of transient field-aligned currents and Pi2 pulsations at auroral latitudes. J. Geophys. Res. **94**, 3619–3630 (1989)

A.N. Wright, W. Allan, Simulations of Alfvén waves in the geomagnetic tail and their auroral signatures. J. Geophys. Res. **113**, A02206 (2008). doi:10.1029/2007JA012464

R. Yamaguchi et al., The timing relationship between bursty bulk flows and Pi2s at the geosynchronous orbit. Geophys. Res. Lett. **29**(6), 1092 (2002). doi:10.1029/2001GL013783

K. Yanagihara, N. Shimizu, Equatorial enhancement of micropulsations Pi2. Mem. Kakioka Magn. Obs. **12**, 57–63 (1966)

T.K. Yeoman, D. Orr, Phase and spectral power of mid-latitude Pi2 pulsations: Evidence for a plasmaspheric cavity resonance. Planet. Space Sci. **37**(11), 1367–1383 (1989)

T.K. Yeoman et al., A comparison of midlatitude Pi2 pulsations and geostationary orbit particle injections as substorm indicators. J. Geophys. Res. **99**, 4085–4093 (1994)

K. Yumoto, Generation and propagation mechanisms of low-latitude magnetic pulsations—A review. J. Geophys. **60**, 79–105 (1986)

K. Yumoto, K. Takahashi, T. Sato, F.W. Menk, B.J. Frazer, T.A. Potemra, L.J. Zanetti, Some aspects of the relation between Pi 1-2 magnetic pulsations observed at $L = 1.3$–2.1 on the ground and substorm-associated magnetic field variations in the near-Earth magnetotail observed by AMPTE CCE. J. Geophys. Res. **94**, 3611–3618 (1989)

K. Yumoto et al., Multiple ground-based and satellite observations of global Pi2 magnetic pulsations. J. Geophys. Res. **95**, 15175–15184 (1990)

K. Yumoto, R. Yamaguchi, H. Kawano, Circumpan Pacific Magnetometer Network Group, Role of Pi2 pulsations in substorm process. Abstract Eu-024, 2001 Japan Earth and Planetary Science Joint Meeting (95th Meeting of the Geodetic Society of Japan), Tokyo, 4–8 June 2001

X. Zhu, M.G. Kivelson, Global mode ULF pulsations in a magnetosphere with a nonmonotonic Alfvén velocity profile. J. Geophys. Res. **94**(A2), 1479–1485 (1989)

P. Zhu, J. Raeder, K. Germaschewski, C.C. Hegna, Initiation of ballooning instability in the near-Earth plasma sheet prior to the 23 March 2007 THEMIS substorm expansion onset. Ann. Geophys. **27**, 1129–1138 (2009)